

Ecological Modelling of Lake Erie: Sensitivity Analysis and Simulation of Nutrient, Phytoplankton and Zooplankton Dynamics

by

Erin L. Jones

A thesis
presented to the University of Waterloo
in fulfillment of the
thesis requirement for the degree of
Master of Science
in
Biology and Civil Engineering

Waterloo, Ontario, Canada, 2011

©Erin L. Jones 2011

Author's Declaration

I hereby declare that I am the sole author of this thesis. This is a true copy of the thesis, including any required final revisions, as accepted by my examiners.

I understand that my thesis may be made electronically available to the public.

Abstract

Lake Erie has undergone a substantial amount of ecosystem changes over the past century; including cultural eutrophication and several invasions by industrious exotic species. Simple mass balance models for phosphorus have been useful in guiding policy decisions that led to reduced eutrophication, but new, confounding threats to the ecological health of Lake Erie continue to appear and lake managers continue to need useful tools to better understand the lake. As more complex ecological questions are asked to guide future management decisions, more complex ecological models are developed in an effort to provide some clues.

The walleye fishery in Lake Erie is economically very important. Walleye recruitment has been highly variable from year to year since the 1990s. Modelling zooplankton is desired as a diagnostic tool for elucidating the quality of habitat – spatially and temporally – that is available to walleye in their vulnerable larval state. ELCOM-CAEDYM (or ELCD) is a 3-dimensional, coupled hydrodynamic and ecological model, which has been successfully applied to Lake Erie to model the nutrients and phytoplankton. The objectives of this study were to better understand the ELCOM-CAEDYM model of Lake Erie through a sensitivity analysis (SA), which has not been done before, and to explicitly simulate zooplankton in this model.

An SA is important for determining which of the uncertain parameters have the greatest impact on the output variables. Due to the complexity of the CAEDYM model and the highly interdependent functions and variables modelled, a local SA (comparing changes in output by perturbing parameters one-at-a-time from some baseline configuration) was not desirable. Local SA's ignore the possibility of a parameter's effects being correlated to the status of other parameters. However, quantitative global methods are enormously computationally expensive for a complex model.

The Lake Erie ELCD model simulates temperature, mixing, nutrient cycles, and phytoplankton dynamics. Phytoplankton are represented by 5 functional groups. With the explicit inclusion of 2 functional groups of zooplankton (copepods and cladocerans), the model uses over 300 function parameters in addition to requiring meteorological data and river inflow characteristics throughout the simulation. The model is set up with a 2-km grid over 40 layers with a 5-minute timestep from April 11 to September 1. This full simulation takes 6 days to complete. A quantitative global method to evaluate all parameters potentially significant to zooplankton would be impossible. The Morris method was selected for its streamlined global sampling procedure combined with the manageable computational demands of a one-at-a-time analysis. This method provides the relative sensitivity of diagnostic outputs to perturbed parameters.

Ninety-one parameters were selected to be evaluated in 3680 simulations for the Morris SA. The selection of which parameters to evaluate and their assigned ranges are critical components in any SA. The ranges for parameters that represent a measurable quantity were assessed based on observed values in Lake Erie and other relevant studies. For some parameters, a measured realistic range was unknown. In these cases, values from relevant published models or judgements based on experience with the ELCD-Erie model were used to choose a suitable range. To assess the sensitivity of CAEDYM variables to parameters, DYRESM was substituted for ELCOM to vastly decrease the computation time of a single run. DYRESM is not suitable to model the entire lake due to the large

size and irregular shape of the entire lake. Therefore, only the West Basin was modelled and analysed using DYCD. The West Basin was of special interest for a sensitivity analysis of CAEDYM parameters with respect to zooplankton because it is an important area for walleye larval development. DYCD output profiles for temperature, total chlorophyll a (TChla as a surrogate for total phytoplankton concentration) were similar in magnitudes and seasonal dynamics compared to ELCD outputs in deep West Basin stations.

The sensitivity of zooplankton, TChla and TP to each parameter was assessed using two single value diagnostics: the simulated seasonal maximum and the simulated day on which peak maximum was reached. Zooplankton were sensitive to almost all of the zooplankton parameters perturbed in the analysis. This may indicate that modelling zooplankton is extremely complex, relying on many dynamic processes, or that evaluated ranges were not constrained well enough. An example of sensitivity to a poorly known parameter is the messy feeding coefficient. Reducing the uncertainty of this parameter would improve the confidence in the zooplankton assimilation submodel. Other parameters that stood out for being especially significant to zooplankton were: the respiration rate, mortality rate, internal phosphorus to carbon ratio, the temperature multiplier and standard temperature for feeding dynamics, and the half saturation constant. Most of these are easily explained as they directly aid or impede growth or they directly affect zooplankton losses.

The most significant phytoplankton parameters on TChla and zooplankton outputs were, not surprisingly, the maximum growth rate and the mortality and respiration coefficient. Some particulate matter parameters proved to be important to outputs as well.

More than 2500 of the 3680 parameter configurations resulted in unrealistic zooplankton simulations: peak values that did not much exceed initial conditions on the first day of the simulation. The SA exercise pinpointed a few configurations that resulted in reasonable peak zooplankton values and timing; these runs were used as a starting point for calibrating the ELCD model. Parameters were further manually adjusted by quickly checking their impacts on DYCD before applying them to ELCD. Post SA and minor calibration, the modelled zooplankton results were dramatically better than initial modelling attempts prior to the SA. Zooplankton concentrations throughout the lake were close to measured ranges and in some parts of the lake seasonal patterns were also similar to measured patterns. Modelled zooplankton results were least consistent with observations in the south west area of the lake: zooplankton were overestimated in late June-early July and they subsequently crashed and were underestimated in late July-August. It is supposed that this is due to higher grazing pressure from fish larvae in that area of the lake, which is not explicitly modelled.

Although it is not anticipated that the south west seasonal zooplankton patterns will improve through parameter calibration (since predator effects are uniformly characterized throughout the lake by the same mortality factor), further calibration is needed to improve results in the rest of the lake since copepods are generally overestimated and cladocerans generally underestimated. Phytoplankton groups must also be calibrated simultaneously to ensure that they are still operating within reasonable concentrations given more successful zooplankton simulations.

Acknowledgements

I would like to thank my advisors, Ralph Smith and James Craig, for their patience, financial support, and guidance throughout this long project. Their contributions have made me a better scientist and writer. I also thank my committee members – Bryan Tolson, David Barton, and Yingming Zhao – for taking the time to review and critique my thesis and for their valuable guidance in the early stages. I am especially grateful to Yingming for his boundless enthusiasm, for providing me with MNR zooplankton data, and for his critical DYRESM debugging skills. Thank you to Luis Leon, Serghei Bocaniov, and Emilija Cvetanovska for their assistance with ELCOM-CAEDYM and for sharing essential files with me. I would also like to thank Jeff Tyson, Tom MacDougal, and Tim Johnson from the Ohio Department of Natural Resources who shared with me extensive measured data from the Lake Erie Plankton Abundance Study.

I thank Shawn Mattot for his encouragement and for inspiring me to realise how to accomplish my analysis; he shared and provided support for his OSTRICH tool that was very helpful in organizing and running my simulations. I greatly appreciate the attentive ears, helpful scientific advice, and encouragement from my labmates and friends, especially Jennifer Hood and Joel Harrison. Finally, I thank my partner, Ryan O'Connor, for his unconditional support and confidence in me.

Dedication

My mom, who was “going to be so happy when I finished this thing” did not get to see it finished and presented, but she was nevertheless happy to see me work towards my master’s and, more importantly, happy to enjoy the flexibility I had to spend quality time with her in her last few months. Now complete, this thesis is dedicated to her.

Table of Contents

Author’s Declaration	ii
Abstract.....	iii
Acknowledgements	v
Dedication.....	vi
Table of Contents.....	vii
List of Figures.....	ix
List of Tables.....	xi
Chapter 1 Introduction.....	1
1.1 Rationale.....	1
1.2 Objectives	2
Chapter 2 Background	3
2.1 Lake Erie.....	3
2.1.1 Phosphorus.....	3
2.1.2 Zooplankton Distribution and implications for Fish.....	4
2.2 Ecological Lake Models	5
2.3 Calibration and sensitivity analysis in ecological models	8
Chapter 3 Description of Lake Erie Models.....	10
3.1 Hydrodynamic drivers: ELCOM and DYRESM.....	10
3.1.1 ELCOM Model of Lake Erie.....	11
3.2 Ecological model: CAEDYM.....	12
3.3 CAEDYM Model of Lake Erie.....	13
3.4 CAEDYM with Zooplankton in Lake Erie.....	15
3.5 DYRESM-CAEDYM in West Basin of Lake Erie.....	15
Chapter 4 Sensitivity Analysis	20
4.1 Morris Sensitivity screening method	20
4.1.1 Implementing the Morris screening method.....	20
4.1.2 Improved sampling algorithm.....	23
4.2 Application of the Morris method to DYRESM-CAEDYM model	24
4.2.1 Software used for processing.....	24

4.2.2 Initial experiments to test code.....	24
4.2.3 Selection of sampling experimental design.....	26
4.2.4 Selection of parameters and ranges.....	27
4.3 Results.....	33
4.3.1 Sensitivity of zooplankton.....	34
4.3.2 Sensitivity of total phytoplankton and phosphorus.....	40
4.4 Discussion.....	43
Chapter 5 Calibration of ELCOM-CAEDYM.....	47
5.1 Zooplankton data available for comparison.....	47
5.2 Modelled zooplankton in the ELCD Lake Erie model.....	48
5.2.1 The zooplankton set-up in the existing ELCD Lake Erie model.....	48
5.2.2 Sensitivity screening results applied to initial calibration efforts.....	49
5.3 Current calibration results: spatial distribution of zooplankton.....	53
5.3.1 Last week in May.....	53
5.3.2 Last week in June.....	54
5.3.3 Last week in July.....	55
5.3.4 Last week in August.....	56
5.4 Current calibration results: temporal distribution of zooplankton.....	57
5.4.1 West Basin (NW and SW).....	57
5.4.2 Central Basin (NWC, SWC and SC).....	59
5.4.3 East Basin (NE).....	61
5.5 Discussion.....	61
Chapter 6 Conclusions and Recommendations.....	64
Bibilography.....	68

Appendices

Appendix A CAEDYM Equations for Phytoplankton and Zooplankton Dynamics.....	73
Appendix B Matlab Code for Modified Morris Selection Matrix.....	78
Appendix C CAEDYM Parameters File for Chapter 5 Simulation.....	82

List of Figures

Figure 2-1 Lake Erie (from http://www.ngdc.noaa.gov/mgg/greatlakes/erie.html).	3
Figure 3-1 Lake Erie ELCOM grid and layer set-up (Leon et al. 2005).	11
3-2 Schematic of CAEDYM state variables.....	14
Figure 3-3 Comparison of modelled seasonal temperature profiles. Top: ELCD-modelled temperature at a site in the middle of the West Basin. Bottom: basin-averaged DYCD-modelled temperature.....	17
Figure 3-4 Comparison of modelled seasonal total phosphorus (left) and total chlorophyll a (right) profiles. Top: ELCD-modelled variables at a site in the middle of the West Basin. Bottom: basin-averaged DYCD-modelled TChla and TP.....	18
Figure 3-5 Comparison of modelled seasonal cladoceran ("Zoop 1", left) and copepods ("Zoop 2", right) profiles. Top: ELCD-modelled variables at a site in the middle of the West Basin. Bottom: basin-averaged DYCD-modelled zooplankton.....	19
4-1 Morris sensitivity results for seasonal average value of Zooplankton 1, cladocerans, evaluating only 8 zooplankton parameters (4 each for Z1 and Z2) and 2 phytoplankton parameters that were expected to be irrelevant.....	26
Figure 4-2 Frequency of 3680 computed zooplankton 1 (top) and zooplankton 2 (bottom) outputs for seasonal maximum (left) and the day of seasonal maximum (right). The maximum dates are between 101=April 1 and 243=Sept 1. Due to the large proportion of simulations with early and/or very low peaks the scale is logarithmic. The 90th percentile of computed results is shown in each plot by the dashed line.	35
Figure 4-3 Parameter effects on seasonal maxima of [a,b] zooplankton 1 (cladocerans) and [c,d] zooplankton 2 (copepods). [a,c] absolute average and [b,d] average versus standard deviation of parameter effects on output.	38
Figure 4-4 Parameter effects on the day at which [a,b] zooplankton 1 (cladocerans) and [c,d] zooplankton 2 (copepods) reach their seasonal maxima. [a,c] absolute average and [b,d] average versus standard deviation of parameter effects on output.	39
Figure 4-5 Absolute average (a and c) and average effects (b and d) of parameters on predicted seasonal maximum of total chlorophyll (a and b) and total phosphorus (c and d).	41
Figure 4-6 Absolute average (a and c) and average effects (b and d) of parameters on the predicted day of the seasonal maximum of total chlorophyll (a and b) and total phosphorus (c and d).	42
Figure 5-1 Location of sites at which zooplankton surveys were conducted between 1997 and 2006 via the LEPAS or LEB sampling programs. Zones are delineated for the purpose of comparison between data sets and modelled results. The size of the dots is an indication of how many times a particular site was sampled for cladocerans and copepods.	47
Figure 5-2 Spatial distributions of measured cladocerans and copepods (top left and right) and computed cladocerans and copepods (bottom left and right) grouped by zone during the last week of May. Concentrations are in $\mu\text{gC}/\text{m}^3$	54
Figure 5-3 Spatial distributions of measured cladocerans and copepods (top left and right) and computed cladocerans and copepods (bottom left and right) grouped by zone during the last week of June. Concentrations are in $\mu\text{gC}/\text{m}^3$	55

Figure 5-4 Spatial distributions of measured cladocerans and copepods (top left and right) and computed cladocerans and copepods (bottom left and right) grouped by zone during the last week of July. Concentrations are in $\mu\text{gC}/\text{m}^3$ 56

Figure 5-5 Spatial distributions of measured cladocerans and copepods (top left and right) and computed cladocerans and copepods (bottom left and right) grouped by zone during the last week of August. Concentrations are in $\mu\text{gC}/\text{m}^3$ 57

Figure 5-6 Computed cladoceran (left) and copepod (right) concentrations (grey lines, $\mu\text{gC}/\text{m}^3$) throughout the simulated season at sites within a specified zone in the West Basin. Top: North end of the West basin; Bottom: South end of the West Basin. Grey boxes: 25th to 50th and 50th to 75th percentile of measured data available in the given zone. Dots: measurements from 2002..... 58

Figure 5-7 Computed cladoceran (left) and copepod (right) concentrations (grey lines, $\mu\text{gC}/\text{m}^3$) throughout the simulated season at sites within a specified zone in the Central Basin. Top: North West end of the central basin; Middle: South West zone; Bottom: South shore zone. Grey boxes: 25th to 50th and 50th to 75th percentile of measured data available in the given zone. Dots: measurements from 2002. 60

List of Tables

Table 4-1 Description of variables used to generate Morris method orientation matrices and elementary effects distributions for all parameters. Variables denoted with an asterisk are randomly generated. Other variables are either selected or computed.	21
Table 4-2 Parameters that are included in the sensitivity analysis and describe phytoplankton processes. The ID # represents a given parameter in the plots in section 4.4. P4, P5, P6 represent the "others", "flagellates", and "late diatoms" groups respectively. Lower and upper are the bounds of the range evaluated for each parameter. The numbered literature sources are given in Table 4-3.	29
Table 4-3 List of references for tables 4-2, 4-4 and 4-5.	31
Table 4-4 Parameters describing zooplankton processes included in the sensitivity analysis. The ID # corresponds to the plots in section 4.3. Z1 and Z2 represent the cladocerans and copepods respectively. Lower and upper are the bounds of the range evaluated for each parameter.	32
Table 4-5 Parameters describing some other processes relating to particulate matter that were considered in the sensitivity analysis. The ID # represents a given parameter in the plots in section 4.3. Lower and upper are the bounds of the range evaluated for each parameter.	33
Table 4-6 Simulated zooplankton statistics from the Morris experiment for runs that were not symptomatic of a lack of growth.	36
Table 4-7 Summary of total chlorophyll a and total phosphorus output results from the full set of 3680 runs.	40
Table 4-8 Parameters showing significance (relative to clustered parameters) in any of the sensitivity diagnostics. "Both" in a variable's column indicates that the parameter was significant for both the seasonal maximum and day of seasonal maximum. For brevity, zooplankton parameters are labelled as Zx- to include either zooplankton 1 or 2 (zooplankton parameters significantly impacted only their respective zooplankton groups; where they were significant to TChla 'x' indicates which zooplankton group parameter was significant).....	44
5-1 Phytoplankton parameter values used in the semi-calibrated model simulation presented in this chapter. ID numbers are those used in the sensitivity analysis presented in Chapter 4. "SA" value indicates the initial parameter configuration used from the best sensitivity analysis run and "Final Value" indicates which parameters were manually altered in calibration.	50
5-2 Zooplankton parameter values used in the semi-calibrated model simulation. Initial parameter configuration used from the best sensitivity analysis run are shown in "SA value" and "Final Value" indicates which parameters were manually altered in calibration.	52
5-3 Other parameter values used in the semi-calibrated model simulation. Initial parameter configuration used from the best sensitivity analysis run are shown in "SA value" and "Final Value" indicates which parameters were manually altered in calibration.	53
Table A-1: Selected functions, fractions, and mass balance equations for variables not including phytoplankton and zooplankton.	73
Table A-2: Phytoplankton (A) functions (see Table A-3 for notation).	74
Table A-3: Parameter definitions for phytoplankton characteristics and processes.	75
Table A-4: Zooplankton processes (see Table A5 for parameter notation).	76
Table A-5: Parameter definitions for zooplankton characteristics and processes.	77

Chapter 1

Introduction

Ecological lake modelling is a promising but daunting process. The modeller struggles to balance complex ecological realism with enough generality to be numerically meaningful and verifiable. The structure and complexity of a model should be carefully considered to achieve the desired goals. These goals may include interpreting and understanding data and working theories; testing hypotheses with numerical experiments instead of mounting labour-intensive or impossible sampling experiments; informing the management of lakes; and, if a model is robust enough, it could be used as a predictive tool.

This thesis describes the application of a three-dimensional physical model (ELCOM) coupled with an ecological model (CAEDYM) in Lake Erie to simulate the lower food web (phytoplankton and zooplankton). In addition, a one-dimensional model that includes all of the biological and ecological processes (DYRESM-CAEDYM) was used to simulate the West basin of Lake Erie. The one-dimensional model allowed vastly faster computations so that a thorough sensitivity analysis of the ecological parameters that are most pertinent to the Lake Erie model could be carried out.

Chapter 1 and 2 present the rationale, objectives and background for the work. Descriptions of ELCOM, DYRESM, and CAEDYM as applied in Lake Erie are given in Chapter 3. The results of a sensitivity screening analysis on CAEDYM parameters using DYRESM-CAEDYM in the West Basin of Lake Erie are discussed in Chapter 4. Preliminary calibration results in the ELCOM-CAEDYM model for Lake Erie are presented in Chapter 5.

1.1 Rationale

Lake Erie has undergone a substantial amount of ecosystem changes over the past century. Simple mass balance models for phosphorus have proven useful in guiding policy decisions for the reduction of phosphorus loading in the past. Significant improvement in lake quality was achieved, but new, confounding threats to the ecological health of Lake Erie have appeared and lake managers continue to grapple with challenging problems. As more complex ecological questions are asked to guide future management decisions, more complex ecological models are developed in an effort to provide some clues.

Questions of variable fish recruitment, hypolimnetic hypoxia, and impacts of invasive dreissenid mussels, for example, require an understanding of the interactions between physical, chemical, and biological processes through space and time. In particular, a key motivator of this thesis was the presence of open questions about the year-to-year variability of walleye recruitment (Zhao et al. 2009), necessitating the development of a complex model which can provide insight into key processes controlling this variability. The walleye fishery in Lake Erie is extremely important economically as well as ecologically.

An effective hydrodynamic model, ELCOM, has been set up in Lake Erie and a detailed ecological model, CAEDYM, which includes nutrient cycles and phytoplankton groups, has been coupled to it (Leon et al. 2005). This Lake Erie application of the model has not previously included a

representation of zooplankton, critical for modelling the conditions of walleye larvae, which consume the zooplankton. A rigorous sensitivity screening analysis to aid in the set-up, calibration, and interpretation of the zooplankton submodel is detailed in this thesis.

1.2 Objectives

The purpose of this thesis is to realistically incorporate a zooplankton submodel in an existing Lake Erie ecological model to provide more insight into the variability of habitat quality for walleye larvae. To this end, two main objectives are addressed in this thesis:

1. Better understand the influence of CAEDYM submodels and parameters on zooplankton outputs. This is to be accomplished via a sensitivity screening analysis of all parameters considered relevant to zooplankton. A sensitivity analysis of the Lake Erie CAEDYM model has not previously been done. To facilitate a thorough analysis, DYRESM-CAEDYM is used as a proxy for the West Basin of the ELCOM-CAEDYM model. The sensitivity of the model results to changes in parameters is assessed for four modelled variables: total chlorophyll (phytoplankton), total phosphorus, and two zooplankton groups. Due to the complex non-linearity of CAEDYM, the analysis must sample many parameters simultaneously to investigate the parameter space. Some questions the analysis seeks to answer are:
 - Which parameters are the output variables most sensitive to?
 - Are there submodels that are more important than previously realised?
 - Which parameters cause little or no impact on output?
2. Incorporate a reasonable representation of zooplankton into behaviour and abundance into the Lake Erie CAEDYM model. Based on the sensitivity analysis results (objective 1) with respect to the zooplankton variables, parameter choices are to be refined so that the zooplankton model captures the spatial and seasonal trends in zooplankton distribution.

The first objective is primarily discussed in Chapter 4; the second in Chapter 5.

Chapter 2 Background

2.1 Lake Erie

Lake Erie is the smallest of the Laurentian Great Lakes by volume and depth, but it is the most biologically productive and diverse (Barbiero 2001, USEPA 2006) and accounts for 80% of the total value of the Great Lakes fisheries (OMNR, 2010). Its watershed is also home to over 12 million residents in Canada and the United States (GLERL, 2004).

The lake (Figure 2-1) has three naturally distinct basins. The mean depth of Lake Erie is 19m with a maximum depth of 64 m (GLERL, 2004) in the east basin. The west basin is the shallowest with a mean depth of 7m (Hartig, 2008); it is generally well mixed, turbid and does not develop thermal stratification in the summer. The west basin is mesotrophic, whereas the central and east basins are classified as oligotrophic (Hartig, 2008). Both Central and East basins develop stable thermal stratification in the summer.

There are several rivers that flow into Lake Erie. The Detroit River with its water from Lake St. Clair (and the upper Great Lakes upstream of Lake St. Clair) contributes the majority of the inflow to Lake Erie at the northwest end near Detroit. Another significant inflow is the Maumee River, which is high in nutrients and sediment as it carries water from a watershed dominated by agriculture, in the southwest end of the West Basin.

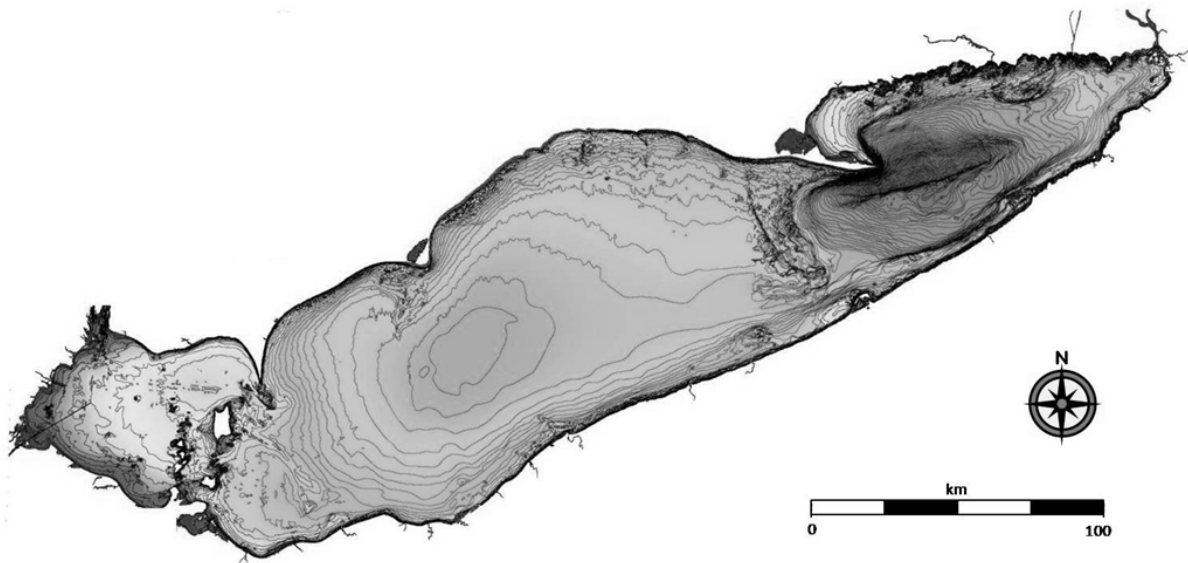


Figure 2-1 Lake Erie (from <http://www.ngdc.noaa.gov/mgg/greatlakes/erie.html>).

2.1.1 Phosphorus

Among the Great Lakes, Lake Erie is exposed to the greatest stress from urbanization, agriculture, and industrialization, particularly in light of the lake's shallow depth. In the 1960s, due to excessive phosphorus loading from these stresses, Lake Erie was replete with algae, but declared "dead" by the

media (Hartig, 2008). Lake Erie was a prime example of “cultural eutrophication”: the overproduction of phytoplankton biomass thanks to a significant increase in nutrients from anthropogenic sources (Dolan and McGunagle, 2005). The nutrient enrichment had effected a shift in the algal composition of Lake Erie to a higher abundance of undesirable cyanobacteria, decreased dissolved oxygen in the hypolimnion of the central basin, caused fish kills and disruptions to many native organisms, produced stinky mats of *Cladophora* on beaches, created taste and odour issues in drinking water, and was generally unfit for recreation (USEPA, 2006).

There has been a concerted response from communities and agencies in Canada and the United States to solve these problems. Both countries signed the Great Lakes Water Quality Agreement (GLWQA) in 1972 (IJC, 2010). A major outcome of the GLWQA was the objective to reduce phosphorus loadings to Lake Erie to control the nuisance algae growth and reduce hypoxia in the central basin throughout the year. Mass balance models were consulted for guidance on setting phosphorus loading targets into the Great Lakes. The widespread efforts in reducing phosphorus were successful in meeting the recommended targets (Hartig et al. 2008, Dolan and McGunagle 2005, Hecky et al. 2004). A marked decline in the abundance of algae, especially nuisance species, was observed in the 1980’s compared to 1970, which is well correlated with decreased phosphorus concentration (Makarewicz, 1993a). Encouragingly, numerous native organisms have since returned (Dolan and McGunagle 2005).

Despite effective phosphorus loading controls, symptoms of eutrophication have been on the rise since the mid 1990’s (Hartig 2008, Conroy et al. 2005, Hecky et al. 2005). For example, cyanobacteria biomass has been increasing; there is an abundance of the benthic filamentous algae, *Cladophora*; and oxygen depletion in the hypolimnion continues to worry managers. In recent years, Conroy et al. (2005) found a poor relationship between external phosphorus loading and total phytoplankton despite the robust relationship established in the past. They suggest internal phosphorus mechanisms, as opposed to external phosphorus loadings, are causing the discrepancy. Internal phosphorus is released from sediments during anoxic events and through biotic activity. Hecky et al. (2004) blame the dreissenids – the prolific benthic invaders that arrived in the late 1980s – for re-engineering the nutrient cycling in the nearshore zone. In addition to the effects of dreissenids, Vanderploeg et al. (2009) suggest intense summer thermal stratification associated with warmer summers, low water levels and increased non-point loading of nutrients may also contribute to the low hypolimnetic oxygen observed. Hartig et al. (2008) note that non-point source pollution is increasing due to population growth, transportation expansion, and unrelenting land development for suburbanisation. They further note that concentration of soluble reactive phosphorus (the most easily available phosphorus to phytoplankton) has been on the rise in the Maumee River over the last 10 years.

2.1.2 Zooplankton Distribution and implications for Fish

In a study of zooplankton abundance in Lake Erie between 1983 and 1987, Makarawicz (1993b) found the biggest contributors to biomass in the zooplankton community to be Cladocera (30.6%), Cyclopoida (19.0%), and Calanoida (18.5%). Calanoids are better adapted for oligotrophic conditions, whereas the other two are better adapted for eutrophic water. The eutrophic Lake Erie of

the 1950s and 60s saw a decreased dominance by Calanoids, and the expanded range of warm-water eutrophic species, but since then some of those trends appear to be reversing (Barbiero et al 2001).

Barbiero et al. (2001) reported on an extensive 1998 plankton survey in the Great Lakes. They found that Lake Erie had the greatest abundance, diversity, and variation in zooplankton. During the spring, zooplankton abundance varied from 19 individuals per m³ in an East Basin station to over 6000 individuals per m³ in a West Basin station. The 1998 study also shows the early dominance of copepod biomass in the springtime followed by cladocerans becoming increasingly important during the summer. Zooplankton density is much higher in the summer. There is a substantial degree of heterogeneity in Lake Erie zooplankton communities most notably along an east-west axis. This is not surprising due to the morphometric and trophic differences in the basins. There is a strong correlation between the abundance of zooplankton and temperature (Stockwell and Sprules 1995, Barbiero et al. 2001). Temperature explains a lot of the inter-basin variability, while chlorophyll a is more associated with intra-basin variability (Barbiero et al. 2001).

This extreme variation zooplankton abundance is particularly difficult to model. It would be unrealistic to expect a good fit between measured and modelled zooplankton abundance given the temporal and spatial scarcity and variation in measurements, however, a successful model should capture general temporal and spatial trends in abundance and dominance of major groups (cladocerans and calanoid copepods in this thesis). It is also desirable for a successful zooplankton model to reproduce the shift in dominance from copepods to cladocerans as Western waters become more eutrophic with increased temperatures.

The variability in zooplankton abundance is of interest as it pertains to the success of walleye recruitment. Walleye in Lake Erie are economically very important. The walleye population was considered to be in crisis in 1978 due to overfishing and pollution. Since then, after a fishing ban and subsequent fishing quotas, the lake has seen a revival of the fish community. Despite a very strong year in 2005, the walleye population has shown considerable year-to-year variability since the early 1990's (Hartig, 2008). The modelling of walleye larvae is not included in this study, but zooplankton are added to the existing ELCD Lake Erie model with an eye to making estimates of the suitability of habitat for good walleye recruitment.

Roseman et al. (1996) discussed the importance of egg survival to walleye recruitment. Walleye egg survival is directly related to fluctuations in water temperature during incubation time. The larval stage of walleye is another critical period contributing to variation in fish recruitment. According to Cushing's (1990) "match-mismatch" theory a close overlap between fish larvae and their food (zooplankton) in time and space results in greater larval growth and survival than if larvae do not find themselves amidst abundant food. This match or mismatch will affect year class strength accordingly.

2.2 Ecological Lake Models

Early models in lake ecology were simple: defined using empirical relationships between nutrients in a lake and a biological response to nutrient concentrations (Dillon and Rigler, 1974, Jones and Bachmann, 1976, Cannfield and Bachmann, 1981). Many early models estimate the concentration of total phosphorus in the lake based on phosphorus loading, lake flushing rates, and lake morphology

using some form of Vollenweider's equation, which was proposed in his 1969 German paper, as cited by Canfield and Bachmann (1981):

$$TP = \frac{L}{z(\sigma + \rho)}$$

where L is the areal phosphorus loading per year, z is the mean depth, σ is the water flushing rate of the lake, and ρ is the phosphorus sedimentation coefficient which is empirically derived in various studies. This equation continues to be useful in both theoretical and applied limnology as it helps describe why some lakes are oligotrophic and others are eutrophic (Kalf, 2002). The phosphorus loading rate includes inputs from wastewater as well as from the surface runoff in the catchment area of a given lake. Greater phosphorus loading rates, shallower mean depths, and long flushing times each contribute to making a lake more eutrophic.

Other empirical models have been historically used to describe key relationships between lake variables. For example, many regression models have been developed to characterize the relationship between chlorophyll a and the total phosphorus in the lake (Dillon and Rigler, 1974). Chlorophyll a (chl_a) is typically measured and modelled as a surrogate for algal abundance as it makes up approximately 0.5% of phytoplankton biomass (Kasprzak, 2008). These simple regression models assume a basin or compartment is well-mixed and that the variable of interest is in steady state (Riley, 1965; Dillon and Rigler, 1974, Jones and Bachmann, 1976, Chapra and Sonzogni, 1979). Dillon and Rigler (1974) presented a straightforward approach for managers to use in their estimates of appropriate regulations for phosphorus loadings to achieve a desired level of eutrophication mitigation. Based on their literature review and work on 19 lakes in Southern Ontario, a very strong relationship between measured phosphorus concentration during spring turnover and the average summer phytoplankton (represented as chlorophyll or chlorophyll a (chl_a)) was quantified. Dillon and Rigler suggested that the Vollenweider equation for phosphorus estimation could be coupled with this TP-chl_a regression equation and from this the acceptable phosphorus loadings can be calculated.

Lesht et al. (1991) prepared a post audit analysis on a mass balance empirical model of phosphorus in the Great Lakes by Chapra and Sonzogni (1979). The model was highly spatially aggregated, representing the five lakes as a series of eleven well-mixed basins. It does not attempt to provide any detailed description of mixing, circulation, atmosphere exchange, or any within basin physical processes. It achieves its goal – the approximation of phosphorus concentration in the lakes - without this complexity. The post-audit showed that model predictions were consistent with observed decline in the total phosphorus concentrations in the Great Lakes between the 1970s and 80s.

Although relationships between phosphorus and chlorophyll have been deemed useful in many different lakes, such empirical models are not always appropriate. Furthermore, these models do not describe or imply any of the processes that affect the ecology of a lake nor do they provide any information on the seasonal succession and or peak abundance of algae. More complex ecological models have been developed to address questions of ecological mechanisms, causality, and interactions between environmental variables.

“Process-oriented models” are an alternative to empirical “data-oriented models”. These are more explicitly mechanistic and they include chemical/biological interactions that are not usually accounted

for by basic mass balance models (Arhonditsis, 2005). Some early efforts to capture seasonal dynamics of phytoplankton communities (i.e. non steady-state) include Steele in 1958 (as cited in Riley 1965), Lehman et al. (1975), Park et al. (1974) and several others (Park et al. 1974). These process-oriented models have become increasingly complex as computational technology has improved.

With increasing complexity in ecological modelling came an increased need for more detailed physical modelling of circulation patterns in the lake, exchanges between sediment and water, and air and water, and the seasonal temperature stratification of lakes. Some spatial variation on a basin or sub-basin scale is often incorporated in Great Lakes models (e.g. Bierman & Dolan 1981, Lam et al. 1987). For all but the most general predictions, the ability to resolve spatial variability is essential because of the importance of the complex hydrodynamics in large lakes (Rao & Schwab 2007). Many of the models applied in lakes use simplified descriptions of transport and mixing and compartment sizes that are large compared to the scale of the key processes. The interactions between physical and chemical/biological processes are significant especially with the onset and collapse of summer stratification. It is for this reason that modern models, such as ELCOM- (or DYRESM-) CAEDYM typically incorporate vertical variability. For example, the Nine-box model, described by Lam et al. (1987), is a one-dimensional mixing model with 3 vertical compartments (epilimnion, mesolimnion, and hypolimnion) for each of Lake Erie's three basins. Because it accounts for thermal stratification and changes in hypolimnion thickness, the 9-box model (even without much lateral discretization) was able to highlight some of the key physical factors (forcing functions based on weather and phosphorus loading) that contribute to the development of hypoxia in the central basin.

The one-dimensional mixing models preceded by the work of Lam et al. (1987) have seen quite a bit of use in ecological process modelling due to their computational expediency. Examples of one dimensional process-based physical models coupled with ecological models include DYRESM (Schladow & Hamilton, 1997), the Lake Zurich model presented by Omlin et al. (2001), and the Princeton Ocean Model (POM) modified for Lake Michigan by Chen et al. (2002). In a one-dimensional model, parameters and variables are horizontally averaged. This type of model can effectively represent temperature and dissolved oxygen profiles, and presumably other ecological variables, in small lakes that are not very long and narrow nor very broad and shallow (Hamilton and Schladow, 1997). Lake Erie is a very large lake and it has three distinct basins. Therefore, for many applications, one-dimensional models for all of Lake Erie are considered overly simple.

The numerous models developed in the last several decades vary a great deal in complexity, spatial and temporal structure, state variables, and the ordering of the submodels used to compute those variables. At least some kind of nutrient and primary producer is required in a mechanistic ecological lake model, but other variables and processes (such as a zooplankton submodel) are optional depending on the purpose of the model and the data available for forcing functions and comparisons to output. Models also vary a great deal in the number of nutrients, solids or other compounds included and the degree of detail in the partitioning of those compounds. The models used for the present work, DYRESM, ELCOM, and CAEDYM are described in greater detail in Chapter 3.

2.3 Calibration and sensitivity analysis in ecological models

As computational power has improved, ecological models have become increasingly ambitious. Complex hydrodynamic-ecological models, such as the ones used in this study, have a large number of input parameters that impact results in an interactive and non-linear fashion. Some of these parameters may be well-described in the literature, some may be directly measured in the field, and some parameters can only be estimated through the calibration of the model. Calibration involves adjusting parameters within physically reasonable ranges until model output agrees reasonably well with measured data. While calibration is an obvious step in model development, a sensitivity analysis is also an important step that is sometimes overlooked. A sensitivity analysis interrogates a model through many iterations to analyze the effects that model parameters have on output variables. This information is useful to the calibration efforts, improves our understanding of a complex model, and can identify which parameters weigh most heavily on the conclusions derived from the modelling effort. This may point out strengths or weaknesses in the model.

Complex ecological models are often criticized for being difficult to analyze and for having numerous parameters relative to data availability. Beck (1987) states that over-parameterized models violate the parsimony principle - that is, they don't use the least complex method to describe an observation. However, over-parameterized models can be useful for suggesting system dynamics beyond the conditions for which the model was calibrated (Arhonditsis et al. 2005). The calibration of an 'over-parameterized' model can lead to estimates for parameters that cannot easily be determined experimentally.

A well-designed sensitivity analysis (SA) can help address some of the concerns about complex models. SA is important for determining which of the uncertain parameters have the greatest impact on the output variables. This knowledge enables the modeller to focus on reducing the uncertainty of the most significant parameters to reduce the variance of the output and also expedites the calibration process by narrowing the scope of parameter adjustments to only those parameters with significant impacts upon results.

The choice of which method is used to carry out the SA depends on the type and complexity of the model and the goal of the analysis. SAs are often referred to as "local" or "global" depending on the method of sampling the parameters for the analysis of their effects on output variables.

Many studies use local methods to evaluate their aquatic models (eg. Bierman and Dolan 1981, Omlin et al. 2001, Schladow & Hamilton 1999, Bruce et al. 2006). A local analysis involves examining the effect on model output from changing factors one at a time while keeping all others constant. A factor can be a parameter involved in a submodel, a boundary condition, an initial value for a variable, or a temporal loading rate for an environmental characteristic. A common local SA approach is to perturb parameters one at a time by 10% or 50% from an initial base case (Jorgensen & Bendoricchio, 2001). The advantage to this approach is that it is computationally inexpensive (compared to global methods) and, because parameters are modelled one-at-a-time, changes in output can clearly be attributed to changes in that parameter. Also, since all changes are compared to the same base case, it is easy to compare the impacts of each parameter. However, a local analysis samples only a few points in a parameter distribution and cannot account for the effects of correlated parameters. Furthermore, the results are biased by the selection of the parameter configuration in the

base case which is used for comparison to each individual parameter perturbation. A very different SA outcome might be found if a different base case was used. In a local analysis, a variable's sensitivity, S , to a given parameter change is a common way of presenting results. Jorgensen & Bendoricchio (2001) define sensitivity, S , according to the equation

$$S = \frac{\delta x / x}{\delta P / P}$$

where P and x are the values for the parameter and output variable respectively in the base model run. δP is the difference between perturbed parameter value and the base value and δx is the resulting change in output for the variable of interest.

A local analysis may be suitable for relatively simple models where complex interactions between factors is not expected to be significant. The local SA's presented by Schladow and Hamilton (1997) on DYRESM-WQ (a precursor to CAEDYM) and Bruce et al. (2006) on an ELCOM-CAEDYM application in Lake Kinneret model provided a limited picture of model sensitivity. The Bruce et al. analysis only compares local output results averaged across the entire season, which does not provide much information for a dynamic, three-dimensional model. Furthermore, the analysis arbitrarily perturbs every parameter by 10% regardless of its degree of uncertainty so the relative S values have limited use, although these studies provide a starting point for the selection of parameter value ranges in the present study. The sensitivity analysis on the Kinneret model by Makler Pick et al. (in press) is much more thorough, as it uses global screening methods to isolate important parameters with some consideration of the effect of the choices of other parameters.

A global SA samples the entire interval of definition for each factor. Monte Carlo (MC) methods are commonly used in global SAs (Saltelli et al. 2004) of models for which there are no exact solutions. In an MC approach, a distribution of possible values for each factor examined in the analysis is chosen. All factors are concurrently randomly sampled from their distributions thousands of times to thoroughly explore the parameter space. Parameter space is the breadth of possible combinations of factors given their possible distributions. For a large model with long run times and numerous parameters, such as ELCOM-CAEDYM, it is impractical, if not impossible, to run hundreds of thousands of simulations for testing the entire parameter space.

Campolongo et al. (2007) present a global screening method – their modified method of Morris – for environmental models with many functions and parameters. The method is a compromise between the less useful local sensitivity analyses and much more computationally expensive Monte Carlo sampling methods. A randomized sampling method is employed to change one parameter at a time in a variety of different configurations of the other parameters. The magnitude of the average effects of a given parameter on a chosen diagnostic output is an indication of the parameter's importance. The method of Morris, as modified by Campolongo et al. (2007) is used in the present study. The method is explained in greater detail in Chapter 4.

Chapter 3

Description of Lake Erie Models

3.1 Hydrodynamic drivers: ELCOM and DYRESM

The Estuary, Lake and Coastal Ocean Model (ELCOM) is a three-dimensional hydrodynamic model that can be coupled with the Computational Aquatic Ecosystem Dynamics Model (CAEDYM) (Hipsey et al., 2004) to provide a sophisticated representation of a lake's physical-chemical-biological processes. ELCOM is an effective model for describing transport and mixing in lakes, estuaries and oceans.

The ELCOM model accounts for baroclinic and barotropic responses, rotational effects, tidal forcing, wind stresses, surface thermal forcing, inflows, outflows, and transport of salt, heat, and passive scalars. Standard bulk transfer models compute the heat transfer across the water's surface; non-penetrative components (longwave radiation, sensible and latent heat) apply only to the surface mixed layer, while penetrative (shortwave) radiation may be distributed to one or more vertical grid layers using Beer's law (Hodges & Dallimore, 2007). Further details regarding governing equations and numerical methods used in ELCOM are available on the Centre for Water Research (CWR) website (CWR, 2006a).

The Dynamic Reservoir Simulation Model (DYRESM) is a one-dimensional hydrodynamic model that can also be coupled with CAEDYM to model biological processes (eg. Bruce et al. 2006.). Whereas ELCOM can predict horizontal transport and mixing, DYRESM only predicts the temperature and salinity of water with depth. The development of vertical stratification is captured and will affect the vertical mixing of salinity and CAEDYM variables. The lake is modelled as a vertical profile of horizontally-averaged layers. Layer thicknesses change as inflow, outflow, and evaporation affect the stored volume in the simulated basin. DYRESM uses the same bulk heat transfer models as ELCOM to compute the temperature profile. Further details regarding the DYRESM model calculations are available in the DYRESM user and scientific manuals (CWR, 2008).

The one-dimensional model works on the assumption that vertical mixing effects are more important than horizontal mixing. It best applies to lakes that are not too shallow or long. Hence, DYRESM is not recommended for modelling Lake Erie, however, it is used to model the West Basin in this study, which is more suitable. Section 3.5 presents the support for this approach to facilitate the use of a global sensitivity screening analysis.

Both DYRESM and ELCOM are process-based models, rather than empirical, and do not require calibration (Hamilton and Schladow, 1997, Hipsey et al. 2004, CWR 2006a, CWR 2008). Both models have been coupled to CAEDYM for a variety of studies around the world such as ELCOM-CAEDYM in Lake Burragong and Prospect Reservoir, Australia (Schladow & Hamilton 1997, Romero & Imberger 2003, Romero et al. 2004) and DYRESM-CAEDYM in Lake Kinneret, Israel (Bruce et al. 2006, Makler-Pick et al. in press). CWR provides a list of studies that have used these models on their website.

3.1.1 ELCOM Model of Lake Erie

The bathymetry of the lake was described as a 2km grid through 40 layers of dept (Figure 3-1). Typically, the ELCOM-CAEDYM model is run at a 5-minute timestep to reduce numerical diffusion, however, a 15-minute timestep was considered suitable in this study to speed up the simulation. The meteorological data - air temperatures, wind speed and direction, solar radiation, relative humidity, and cloud cover - for 2002 were taken from the archives of the National Water Research Institute (NWRI) and the NOAA National Data Buoy Center (Leon et al. in press). Three sets of forcing data were applied to the lake; one for each of the three basins. Details on the performance of ELCOM compared to measured temperature profiles are discussed in Leon et al. (in press) and Leon et al. (2005).

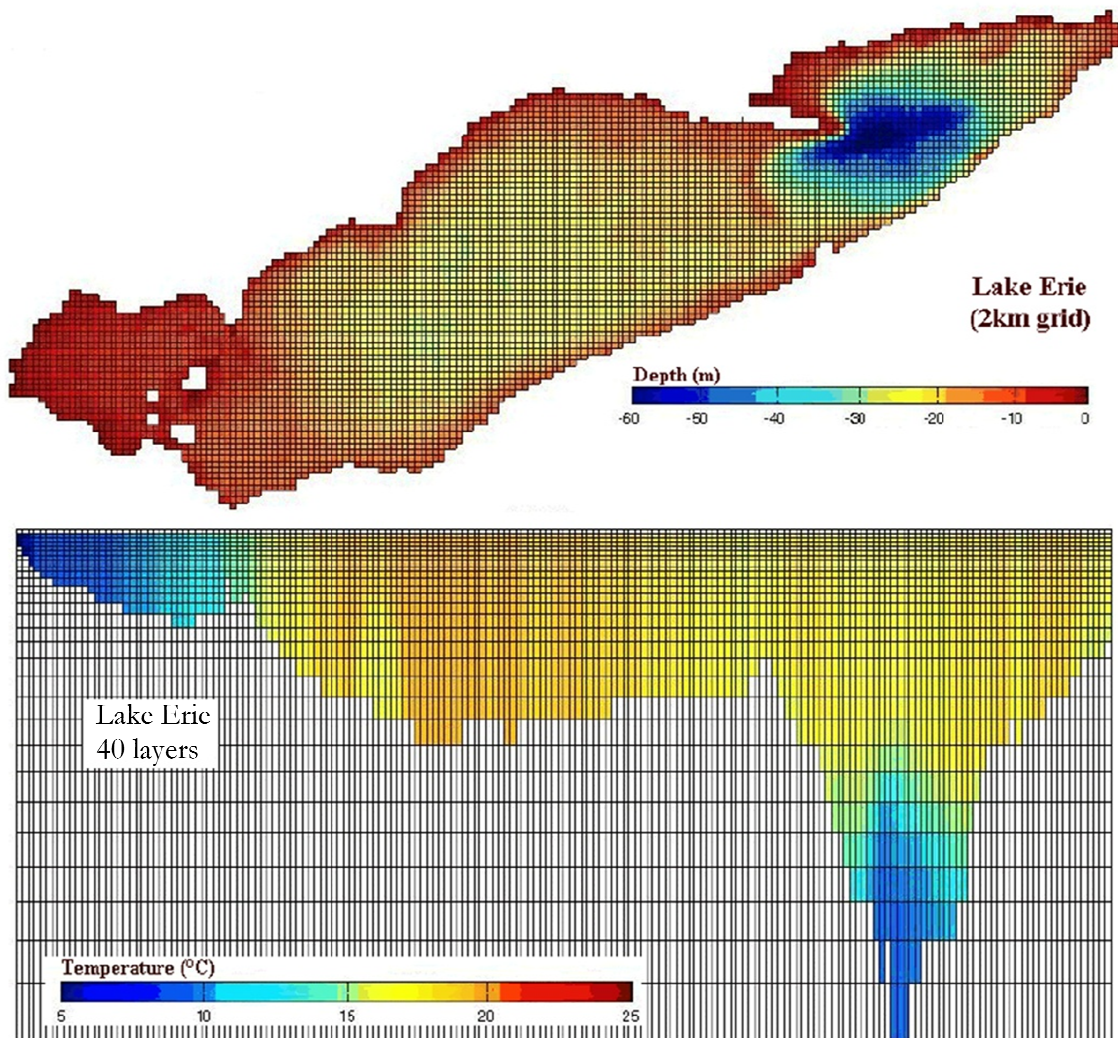


Figure 3-1 Lake Erie ELCOM grid and layer set-up (Leon et al. 2005).

3.2 Ecological model: CAEDYM

The coupled ELCOM-CAEDYM (ELCD) model simulates the three-dimensional transport and interactions of physical processes, biology, and chemistry. CAEDYM is a flexible ecological model that can include comprehensive representations for the nutrient (carbon, nitrogen, phosphorus, and silicon) cycles, dissolved oxygen (DO) profiles, several class sizes of inorganic suspended solids, phytoplankton dynamics and numerous optional state variables. Up to 7 phytoplankton groups, 5 zooplankton groups, bacteria, bivalves, fish, and benthic organisms may all be represented. The model is run at a sub-daily timestep to account for diurnal photosynthesis and nocturnal respiration.

The CWR provides an interactive website to illustrate some of the submodels used by CAEDYM (CWR 2006b) and the process equations and rationale have further been described in the CAEDYM documentation (2006) and previous publications (eg. Robson and Hamilton 2004, Romero et al. 2004). Selected relevant processes in the CAEDYM model are described below.

Nutrients cycle

Phosphorus (P), nitrogen (N), and carbon cycles are modelled in ELCD in both the water column and a layer of sediment at the bottom as dissolved organic and inorganic, and particulate organic components. The nutrients stored within phytoplankton and zooplankton are also part of the nutrient balance. Total nitrogen and total phosphorus are derived by adding together the relevant nitrogen and phosphorus state variables respectively. Dissolved inorganic silica is also modelled and it is only consumed by diatom phytoplankton groups. CAEDYM maintains a balance between settling and resuspension of variables between the sediment and water column. Sediment fluxes of dissolved inorganic and organic nutrients are based on empirical formulations that depend on temperature and oxygen concentration. Particulate forms of C, N and P are degraded from POM (particulate organic matter) to DOM (dissolved organic matter).

Phytoplankton

Up to 7 groups of phytoplankton can be modelled in CAEDYM. Depending on the application, a group can be a specific algal species or a “functional group” that represents the average characteristics and functional responses of types of phytoplankton as opposed to characterizing particular species.

Phytoplankton production and losses are described by a series of submodels in an attempt to capture the mechanisms that exist in nature. These include functions to describe phytoplankton growth (nutrient uptake, photosynthesis) and losses (respiration, sinking, mortality, outflow, and predation). Many of these processes are influenced by temperature. Maximum growth rates for each phytoplankton group are the minimum of nutrient, temperature and light limitation functions. The equations to describe phytoplankton dynamics are described in more detail in the CAEDYM documentation (CWR, 2006b). A table of important CAEDYM equations for phytoplankton dynamics is provided in Appendix A.

Zooplankton

CAEDYM provides the capacity to simulate up to 5 functional groups of zooplankton. The concentration of zooplankton is a balance of growth and losses, just like phytoplankton and any other organism to be modelled. There are a number of sub-functions included in this mass balance. A table of important CAEDYM equations for zooplankton dynamics is also provided in Appendix A.

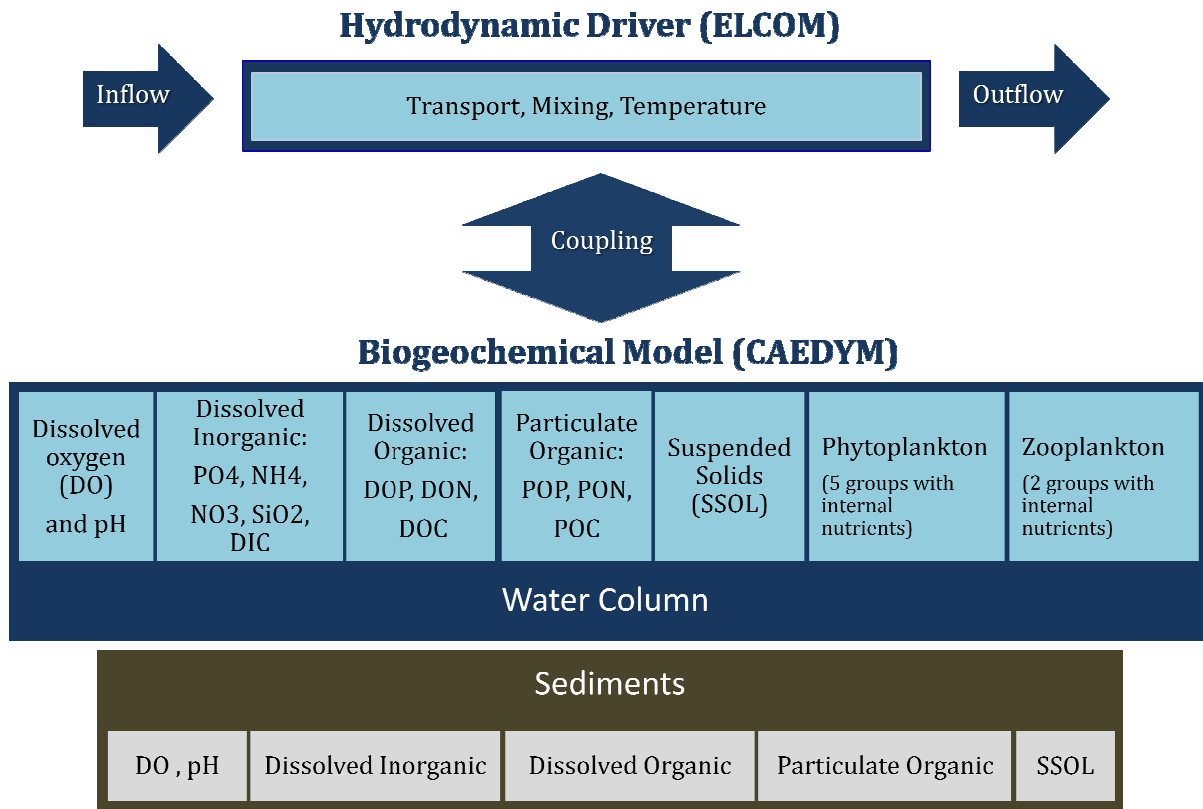
A food preference function is part of the growth model. Higher and lower food preference factors are given to more and less edible phytoplankton groups respectively. For example, zooplankton enjoy eating small diatoms, but not colonies of difficult-to-handle cyanobacteria, therefore, a greater preference for diatoms over cyanobacteria should be assigned. Grazing by zooplankton is a function of prey density and temperature. The zooplankton grazing rate increases with increasing concentrations of prey until the prey reaches a saturation density for the species of zooplankton such that the zooplankton becomes limited by its ability to take up the nutrient rather than the availability of the nutrient (Bowers, 1979). This nutrient uptake behaviour is described with a Michaelis-Menten function. Given optimal food concentration, the grazing rate is maximal at the zooplankton group's "optimal temperature", which is a parameter specified to characterize the temperature function for that group.

The loss terms include respiration as a function of temperature, mortality (which can include predation that is not directly modelled), and flushing of zooplankton through the outflow. Zooplankton grazing on phytoplankton contributes to zooplankton biomass, but is obviously a loss to the phytoplankton mass balance.

3.3 CAEDYM Model of Lake Erie

Leon et al (in press) details the set-up of the Lake Erie ELCD model without the explicit inclusion of zooplankton. In-lake concentrations for water quality variables (including temperature, chlorophyll a concentrations, and other water chemistry variables) at several sites throughout the lake for 2002 are available for calibration efforts and for providing initial conditions for the simulation. The ELCD model in Lake Erie has one outflow (Niagara River) and 11 river inflows including major inputs to the West Basin from the Maumee River and the Detroit River. There are many other inflows, but the 11 included account for over 98% of all inflow to the Lake (Leon et al., in press). Likewise, other outflows are minor compared to the Niagara. Nutrient loading to the lake is accounted for through the 11 inflows. Leon et al provide the specific details and rationale for the daily loading rates assigned to the model (daily loads for most state variables are specified in each inflow). The initialization of state variables is an indirect way to include in the lake the loadings that occurred prior to the beginning of the simulation.

Figure 3-4 presents the state variables modelled by ELCD that are used in the Lake Erie application. CAEDYM relies on the hydrodynamic driver, ELCOM, to model the mixing of variables and the temperature distribution on which so many chemical and biological processes depend.



3-2 Schematic of CAEDYM state variables

The 5 functional groups of phytoplankton represented in the current ELCD Lake Erie application are: Cyanophytes; "Others", Flagellates, Early Diatoms, and Late Diatoms. The cyanophyte group mainly represents N-fixing taxa that are associated with warm stable waters. The "others" group is also associated with warmer waters; it includes some flagellates and nonmotile forms - chlorophytes and some dinoflagellates, chrysophyceans and haptophytes. The flagellates group represents cryptophytes and other flagellates that thrive in cooler waters. The diatoms groups represent taxa that require silica and are also characterized by faster sinking rates. Early diatoms are those that bloom early in the spring and sink rapidly while the late diatoms have lower Si requirements and slower sinking rates and bloom later in the season (this group can include silicified chrysophyceans as well).

Leon et al. (in press) provide details on the functions and chosen parameters that describe the phytoplankton groups. To date, the ELCD model has shown reasonable predictions of phytoplankton biomass and phosphorus concentrations and some other variables as well (Leon et al. in press). The two zooplankton groups listed in Figure 3-2 were added for this thesis and are not included in Leon et al. (in press); their inclusion in the model is described in the next section.

3.4 CAEDYM with Zooplankton in Lake Erie

Towards the goal of modelling the quality of walleye larvae habitat, zooplankton are added to this existing ELCD model of Lake Erie. As in the case of phytoplankton, zooplankton are added as "functional groups": calanoid copepods and cladocerans. These classes were chosen because they are dominant components of zooplankton mass in Lake Erie (Makarawicz, 1993). Rotifers and cyclopoid copepods are also important components of zooplankton, but these groups were not explicitly modelled to reduce the complexity of modelling zooplankton. Rotifers are generally too small to be of greatest interest to walleye larvae; their ecological impact in the simulation would be accounted for indirectly during calibration. For example, the rotifer phytoplankton grazing impact would make up part of the mortality/respiration loss of phytoplankton. Cyclopoids would be particularly complicated to model since they are omnivorous (feeding on phytoplankton and zooplankton). The cyclopoid grazing impacts on modelled zooplankton would also be indirectly accounted for through the calibration of zooplankton loss terms (which would also include losses due to grazing by other higher organisms not explicitly modelled).

Section 4.2.4 discusses the zooplankton parameter values used in the Lake Erie model and gives literature sources for models with similar parameters. The ranges used for zooplankton parameters are based on literature values either measured or used in other models; some parameters are not well constrained initially. With the addition of zooplankton to the ELCD model, the existing nutrient-phytoplankton configuration needs to be altered. For instance, without explicitly simulating zooplankton, it was assumed that the 'flagellates' and 'others' groups would be especially targeted by zooplankton and, therefore, they were assigned higher total loss rates with respiration accounting for a lower fraction of that loss rate. By explicitly simulating zooplankton, the increased loss by predation is directly modelled so the previously assigned loss rate would need adjustment. The sensitivity analysis presented in this thesis is geared towards understanding the effects of various parameters on zooplankton, phytoplankton, and phosphorus and guiding calibration efforts.

3.5 DYRESM-CAEDYM in West Basin of Lake Erie

In order to assess the sensitivity of CAEDYM variables to its parameters, DYRESM is here substituted for ELCOM to vastly decrease the computation time of a single run and thus easily allow thousands of simulations to be executed for analysis. DYRESM is not suitable to model the entire lake due to the major differences in shape and depth between the three distinct basins and the massive size and length of the entire lake. Therefore, only the West Basin was modelled and analysed using DYCD. The West Basin was of special interest for a sensitivity analysis of CAEDYM parameters with respect to zooplankton because it is an important area for walleye larval development. Fortunately, the West Basin was a more suitable basin for DYRESM than the rest of the lake would be. The West Basin is much smaller than the other basins, more uniform in depth, and it is not long and narrow.

The differences between using DYRESM and ELCOM as the hydrodynamic driver for CAEDYM are not trivial. It is important to establish that the CAEDYM variables as modelled by DYCD are comparable to results seen in the ELCD version somewhere in the West Basin so that the results of a

sensitivity analysis of DYCD would validly extend to ELCD (at least in the West Basin). It was expected that the DYCD results would only resemble ELCD results in the centre of the West Basin because that area would be less affected by inflows, nearshore mixing and exchange with the Central basin, and also because the depth in the middle of West Basin (which is important to the simulation of the temperature profile) would be similar to the maximum depth of the DYCD West Basin (WB) model.

The approach in setting up the DYCD model was to use ELCD setup files as much as possible and make suitable approximations when it was not possible. The input files that describe daily inflows and water quality characteristics from the Maumee and Detroit river were identical in DYCD as in ELCD. A hypsographic curve for West Basin was derived from the West end of the 3-D grid used in ELCD. The "full supply" elevation (largest depth in the basin) was 11m and the surface area at that height was 2892km². The daily outflow had to be adjusted however, as the exchange between West and Central basins was not going to be correctly modelled in one dimension. The outflow values were adjusted to achieve similar water levels as the equivalent ELCD simulation. Like the outflow values, the "outlet height" was estimated to achieve similar water levels in DYCD as in ELCD, West Basin. Meteorological forcing data were the same as those used for the WB of the ELCD model. The same CAEDYM parameters file was used and DYCD was initialized with the same initial values profile as that used for ELCD WB stations.

In order to confidently use DYRESM as a tool to assess CAEDYM as applied with ELCOM, one of the most important things to demonstrate was that the DYCD temperature profile would be similar in ranges of magnitude and timing as temperatures modelled in the WB stations of ELCD because the physical mixing of variables and many chemical and biological functions depend on temperature. Figure 3-5 displays the seasonal ELCD temperature results at a site near the centre of the West Basin to the seasonal DYCD temperature results. It was encouraging to see a very similar pattern between the two: the maximum and minimum temperatures were similar and peaks and troughs occurred around the same time. A significant difference, however, was that DYRESM simulated the development of some stable horizontal stratification during the month of July and some of August. Since this could impact vertically averaged concentrations during those times, output results were averaged only for the top 6m to ensure that well mixed epilimnetic waters in both simulations were being compared.

Given that DYCD modelled temperatures in the right range, it further needed to be demonstrated that CAEDYM could perform similarly for ecological variables before using DYRESM as a surrogate hydrodynamic driver for analyzing CAEDYM. Figure 3-6 presents the comparison between DYCD and ELCD for total phosphorus (TP) and total chlorophyll a (i.e. phytoplankton). Since these variables are based on semi-empirical submodels, it is not surprising that the similarity is not as good as that for temperature (in Figure 3-5), but the agreement in timing and magnitudes of these variables' concentrations is still good. It should be noted too that an exact match between the ELCD profile site and the DYCD profile would not be expected since the ELCD profile location is subject to dynamic horizontal fluxes as well as vertical.

Figure 3-7 also demonstrates similarities in magnitude and timing of the zooplankton variables between ELCD and DYCD. The initial attempts at modelling zooplankton in ELCD and DYCD

(Figure 3-7) did not resemble measured data. The purpose of this comparison is to show that given the same CAEDYM parameters, the models would perform similarly – in this case, similarly wrongly. Given the similar results between DYCD and ELCD, it is expected that changing parameter values in DYCD and interrogating the results should give some insight into the effects that those parameter changes would have on the larger ELCD model in the West Basin.

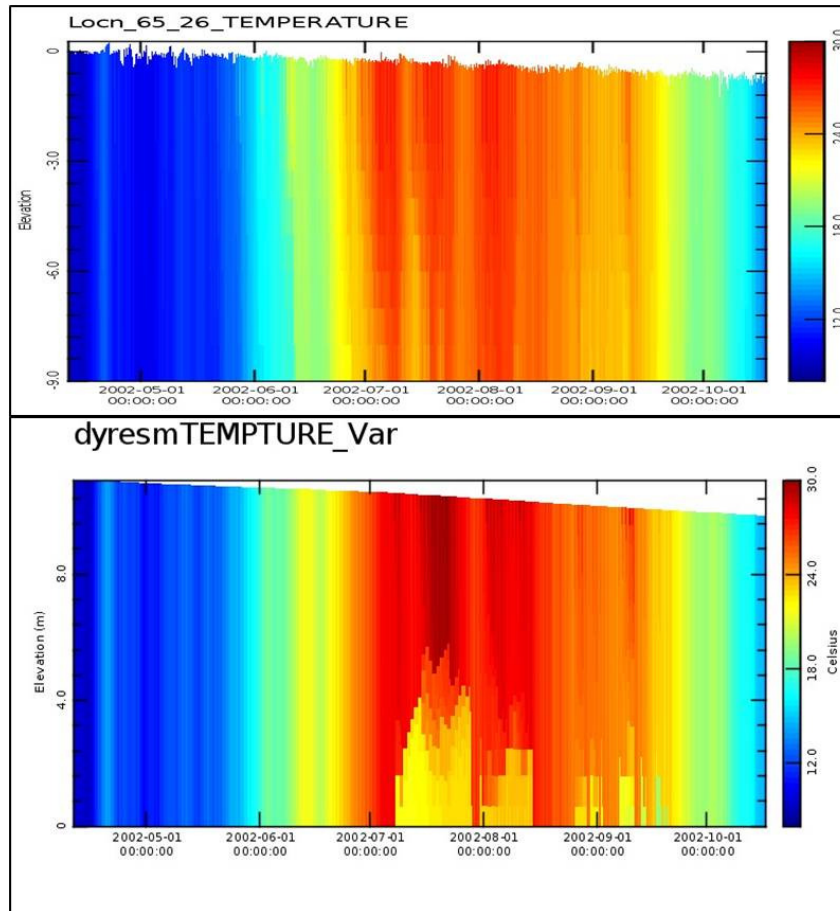


Figure 3-3 Comparison of modelled seasonal temperature profiles. Top: ELCD-modelled temperature at a site in the middle of the West Basin. Bottom: basin-averaged DYCD-modelled temperature.

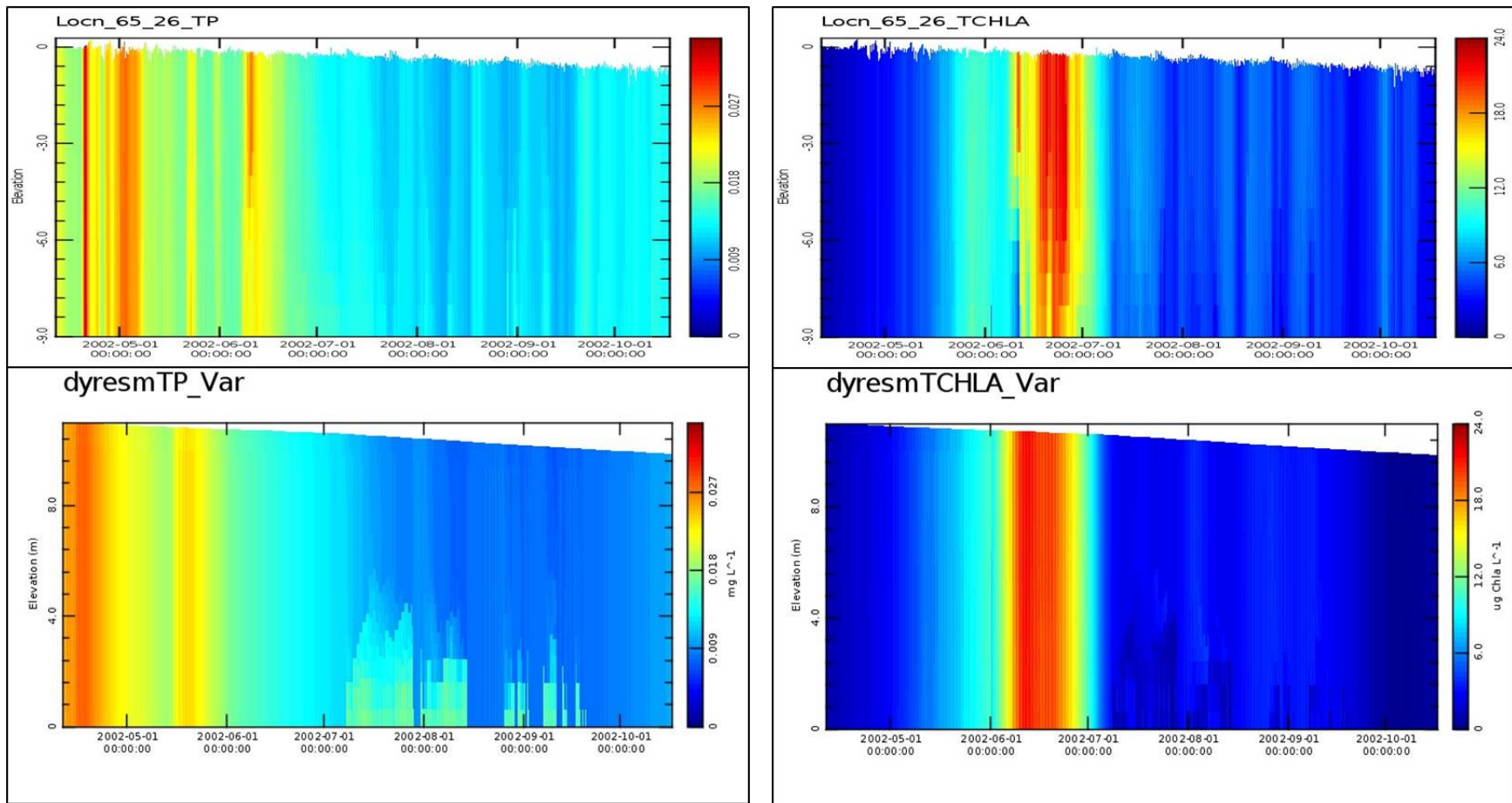


Figure 3-4 Comparison of modelled seasonal total phosphorus (left) and total chlorophyll a (right) profiles. Top: ELCD-modelled variables at a site in the middle of the West Basin. Bottom: basin-averaged DYCD-modelled TChla and TP.

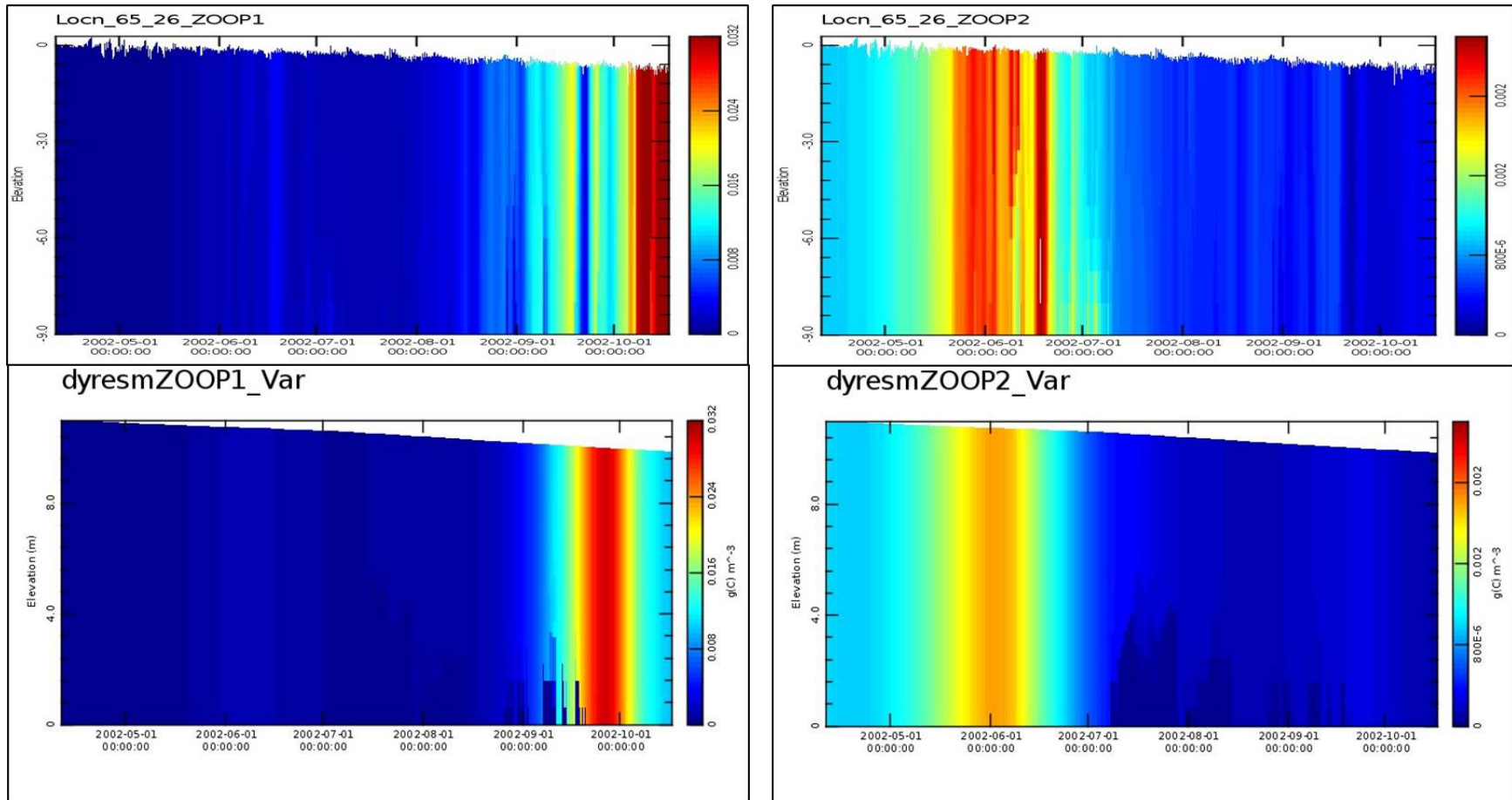


Figure 3-5 Comparison of modelled seasonal cladoceran ("Zoop 1", left) and copepods ("Zoop 2", right) profiles. Top: ELCD-modelled variables at a site in the middle of the West Basin. Bottom: basin-averaged DYCD-modelled zooplankton.

Chapter 4

Sensitivity Analysis

4.1 Morris Sensitivity screening method

The Lake Erie implementation of CAEDYM is a complex non-linear water quality model with hundreds of input parameters. As such, simple methods such as a local sensitivity analysis (in which parameters are varied one at a time while keeping all other parameters constant) or a regression-based sensitivity analysis (in which a simple polynomial function approximates the relationship between an output variable and an input parameter) are inappropriate for obtaining a useful understanding of the impact of parameter choice upon model output and reliability. The parameter space of a model with so many parameters is difficult to thoroughly sample; each parameter has a range of values it could assume and the influence of each parameter depends upon the value of all other parameters. An output variable's response to a change in parameter, x_i , may be (a) zero, (b) constant (i.e. linear and additive), (c) a non-constant function of x_i , or (d) a non-constant function of several parameters (Morris, 1991). To fully understand model sensitivity, a global sensitivity analysis method could be used. However, global methods that quantitatively assess the degree to which output is affected by a parameter and the interaction effects with other parameters is too computationally expensive for application to CAEDYM (i.e. would require many thousands of simulations). Such a method may be more suitable if only a small subset of parameters were investigated.

The method of Morris (1991) is a screening strategy that is global, but computationally inexpensive, and therefore a useful alternative to more rigorous sensitivity analysis approaches. The guiding principle is that a screening method should determine whether a parameter has effects that are (a) negligible, (b) linear and additive, or (c) non-linear or involved in interactions. For parameters where (c) applies, the method cannot distinguish between non-constant functions that are due to important non-linearity or interaction influences of other parameters; a more detailed global analysis would be required to resolve that information. The Morris method is here used to analyse a DYCD model of the West Basin, particularly since this model is a reasonable surrogate for the ELCD model in the West Basin. The information about the most important parameters to outputs of interest (zooplankton, total chlorophyll a, and total phosphorus) is later used to inform calibration of ELCD (Chapter 5).

The Morris method computes the elementary effects of input parameter changes on outputs by randomly sampling parameters one at a time (OAT). It is efficient like a local sensitivity analysis, but additionally ensures that parameters are assessed for a range of possible other parameter configurations. Section 4.1.1 presents a detailed description of the method.

4.1.1 Implementing the Morris screening method

The Morris method uses an intelligent approach to determine the portion of parameter space from which to sample. First, a randomized orientation matrix, B^* , is generated based on the choice of the number of model parameters to evaluate, k , and the number of values or levels at which a parameter may be sampled, p . The orientation matrix supplies a starting configuration of input parameters for a model run (i.e. the first row of the matrix) and subsequent configurations (i.e. the following rows of the matrix); consecutive configurations (rows) differ by only a single parameter (columns). Several

orientation matrices are needed to compute an average effect for each parameter. Table 4-1 lists the variables used to describe this sampling method

Table 4-1 Description of variables used to generate Morris method orientation matrices and elementary effects distributions for all parameters. Variables denoted with an asterisk are randomly generated. Other variables are either selected or computed.

i	index for a column element. Each parameter is assigned to a specific column
j	index for a row element. Each row represents the set of parameter values for one model run in the sensitivity experiment
k	number of parameters to evaluate
p	number of levels at which to sample each parameter, i.e., the sampling resolution
x_i	Value in the interval [0, 1] of parameter i where $1 \leq i \leq k$. In this application, x_i is linearly transformed to a real value for parameter i that is between the parameter's assigned maximum and minimum value (i.e. parameter i is assigned its minimum value if $x_i=0$, its maximum value if $x_i=1$, or the parameter value is linearly interpolated if x_i is a fraction)
X	Full set of x_i parameters for a single model configuration. Contains k elements
$y(X^j)$	Output variable result from the model simulation based on the set of X in row j
x^*	Randomly chosen 'base value' for X
Δ	Increment by which parameter x_i is increased or decreased to give an elementary effect on output. Typically, $\Delta = \frac{p}{2(p-1)}$
B^*	$k+1$ by k "orientation matrix". The first row, X^1 , is derived from an x^* vector. Each subsequent row, X^{j+1} , is different from the previous row, X^j , by only one element, x_i . The x_i from row j is increased or decreased by Δ to give x_i at row $j+1$. Each column is altered only once to generate one elementary effect per input parameter i in an orientation matrix.
B	$k+1$ by k matrix. Strictly a lower triangular matrix of ones.
$J_{k+1,k}$	$k+1$ by k matrix of ones
D^*	k by k diagonal matrix; each element of the diagonal is randomly assigned a value of 1 or -1
P^*	Random k by k permutation matrix. Each column and row contains only one element equal to 1; all other elements are zero. The identity matrix, I , is an example of a possible P^* .
R	Number of orientation matrices (B^*) to include in the analysis. There are r elementary effects computed for each parameter – one elementary effect per parameter per B^* matrix.
d_i	Computed elementary effect on output variable ($y(X)$) for parameter i
μ_i	Average elementary effect of parameter i .
$\bar{\mu}_i$	Average absolute elementary effect of parameter i , as proposed by Saltelli et al. (2004)
σ_i	Standard deviation of elementary effects of parameter i

Equation 4-1 is used to generate a single random orientation matrix for k elementary effects (one elementary effect per input parameter)

$$B^* = J_{k+1,1}x^* + \frac{\Delta}{2}[(2B - J_{k+1,k})D^* + J_{k+1,k}]P^* \quad 4-1$$

In the example given by Saltelli et al. (2004) for a case with 2 parameters ($k=2$) and 4 levels ($p=4$) a Δ value of $2/3$ was computed and B was defined as $\begin{bmatrix} 0 & 0 \\ 1 & 0 \\ 1 & 1 \end{bmatrix}$. The randomly generated components were:

$$x^* = [0 \ 1/3]; \quad D^* = \begin{bmatrix} 1 & 0 \\ 0 & -1 \end{bmatrix}; \quad P^* = \begin{bmatrix} 1 & 0 \\ 0 & 1 \end{bmatrix}.$$

Therefore,

$$B^* = \begin{bmatrix} 1 \\ 1 \\ 1 \end{bmatrix} [0 \ 1/3] + \frac{\Delta}{2} \left[\left(2 \begin{bmatrix} 0 & 0 \\ 1 & 0 \\ 1 & 1 \end{bmatrix} - \begin{bmatrix} 1 & 1 \\ 1 & 1 \end{bmatrix} \right) \begin{bmatrix} 1 & 0 \\ 0 & -1 \end{bmatrix} + \begin{bmatrix} 1 & 1 \\ 1 & 1 \end{bmatrix} \right] \begin{bmatrix} 1 & 0 \\ 0 & 1 \end{bmatrix} \quad 4-2$$

$$B^* = \begin{bmatrix} 0 & 1 \\ 2/3 & 1 \\ 2/3 & 1/3 \end{bmatrix}$$

For this orientation matrix the elementary effect for parameter 1, d_1 , is computed based on the first two simulations as parameter 1 is increased by Δ from row 1 to row 2; the elementary effect for parameter 2, d_2 , is computed based on the 2nd and 3rd simulations as parameter 2 is decreased by Δ from row 2 to row 3. Each elementary effect, d_i , is computed according to

$$d_i^j = \frac{[y(X^{j+1}) - y(X^j)]}{\Delta} \quad 4-3a$$

when x_i has been increased by Δ from row j to row $j+1$, or

$$d_i^j = \frac{[y(X^j) - y(X^{j+1})]}{\Delta} \quad 4-3b$$

when x_i has been decreased by Δ from row j to row $j+1$. $y(X^j)$ is the output variable result from running the model with the parameter configuration from row j of the orientation matrix.

A finite number, r , of B^* matrices is generated to obtain a distribution of r elementary effects per input parameter. Based on previous experiments, Saltelli et al. (2004) suggest that an r -value of 10 with a p -value of 4 is typically sufficient. Using a lower value for r risks not sampling each parameter at all or most of its p levels. The total number of computations, N , in the experiment depends on the choice of r and k : $N = r(k+1)$.

After evaluating the model for r orientation matrices, an average, μ , and a standard deviation, σ , are calculated for each parameter from its distribution of r elementary effect values, d_i . Saltelli et al. (2004) recommend computing an average of absolute elementary effects, $\bar{\mu}$, so that the absolute importance of a parameter is not diminished if its effects on the output can be both positive and negative. Thus, the importance of parameters from most important to least important are ranked by the highest to lowest magnitude of $\bar{\mu}_i$. It is also useful to compare μ_i to $\bar{\mu}_i$. A near zero value of μ_i coupled with a high magnitude of $\bar{\mu}_i$ indicates that parameter i has both positive and negative effects on the output variable whereas an identical magnitude for μ_i and $\bar{\mu}_i$ indicates that changes in parameter i have only had positive (where μ_i is positive) or negative (where μ_i is negative) effects on the output. A high standard deviation, σ , reveals that a parameter has significant non-linear or interactive effects. As with the average values, the magnitude of σ_i is assessed relative to that of the other parameters.

The results from the Morris sensitivity method are best illustrated graphically. An example is discussed in section 4.2.2.

4.1.2 Improved sampling algorithm

Campolongo et al. (2007) proposed an improvement to the Morris sampling design to ensure that the parameter space was optimally sampled given k , p and r without increasing the number of model executions needed. They demonstrated that their improved algorithm produced improved sampling results. A large number, M (~500-1000), of random orientation matrices (B^*) from which to sample r matrices is generated. The combination of r matrices that are the most different from each other is desirable because more of the parameter space will be sampled. Campolongo et al. (2007) optimize the selection of matrices by maximizing the sum of the distances between each element of a matrix and the corresponding elements of the other $r-1$ matrices. The distance, $d_{m,n}$, between 2 matrices, m and n , is defined as:

$$d_{m,n} = \left\{ \sum_{w=1}^{k+1} \sum_{v=1}^{k+1} \sqrt{\sum_{i=1}^k [X_w^m(i) - X_v^n(i)]^2} \right\} \text{ for } m \neq n, \quad 4-4$$

where w and v denote row number for the parameter vector, X , in matrix m and n respectively and i denotes a parameter element of that set of X . The total distance sum, D , for a set of orientation matrices is the square root of the sum of the squares of the $d_{m,n}$ values between all matrices in the set. For example, consider $M=10$ and $r=4$. The sum for the combination M(4-6-7-9) would be computed according to

$$D_{4679} = \sqrt{d_{4,6}^2 + d_{4,7}^2 + d_{4,9}^2 + d_{6,7}^2 + d_{6,9}^2 + d_{7,9}^2} \quad 4-5$$

This sum would be computed for all combinations of r from M . The largest D indicates the optimal combination of r B^* matrices from the M sample. The code that was used to select the combination of r matrices for this thesis did not evaluate every possible combination as described above due to the computational infeasibility when dealing with a large numbers of parameters. A more efficient strategy was employed and is described in section 4.2.1.

4.2 Application of the Morris method to DYRESM-CAEDYM model

4.2.1 Software used for processing

The code for DYRESM and CAEDYM was created in Fortran and compiled as an executable for Windows. These executables were obtained from the Centre for Water Research at the University of Western Australia. A tool called OSTRICH (Mattot, n.d.) was used to run and organise output for thousands of DYRESM-CAEDYM simulations in sequence. The program used to determine the sequence of one-at-time configurations according to the method of Morris was coded in Matlab for this thesis. Modifications to the selection of orientation matrices in the Morris method inspired by Campolongo et al. (2007) were applied to the Morris code to improve the range of parameter space sampled. To reduce the computational cost of selecting the sample of orientation matrices, the program was not coded exactly as presented in Campolongo et al. (2007); the total sum of D distances between all elements of the r elementary effects matrices was not evaluated for every possible combination of r matrices chosen from M random matrices. Instead, the code picked out the two matrices in the selection of M matrices with the greatest value of D_{mi} between them. The next matrix in the set of M was chosen for having the maximum distance between itself and the first two matrices. The following matrix was selected for having the maximum distance between itself and the first three matrices and so on until r matrices were selected. If there were multiple maxima at any step during this process (i.e., multiple matrices shared the same distance from the previously selected matrices) then each trajectory was followed, giving several possible optimal combinations of r matrices. Among those possible combinations, the trajectory with the greatest sum of all distances between its matrices was the optimal combination. This largest sum of distances indicated the selection of matrices that provided the best sample of the parameter space with little duplication of parameter configurations.

For the small number of parameters (low k) used in the trial model discussed in section 4.2.2, the modified code gave identical combinations as those provided by exhaustively evaluating D (the sum of distances between the elements of r matrices) for all possible combinations of r matrices selected from M . It is therefore expected that the modified approach may not produce the absolute best combination when more parameters are included, but it would still provide a significant improvement to the original Morris sampling design, as achieved in Campolongo et al. (2007). The code is included in Appendix B.

Programs for extracting model results from the DYCD Netcdf data files and interpreting the Morris statistics were also written in Matlab.

4.2.2 Initial experiments to test code

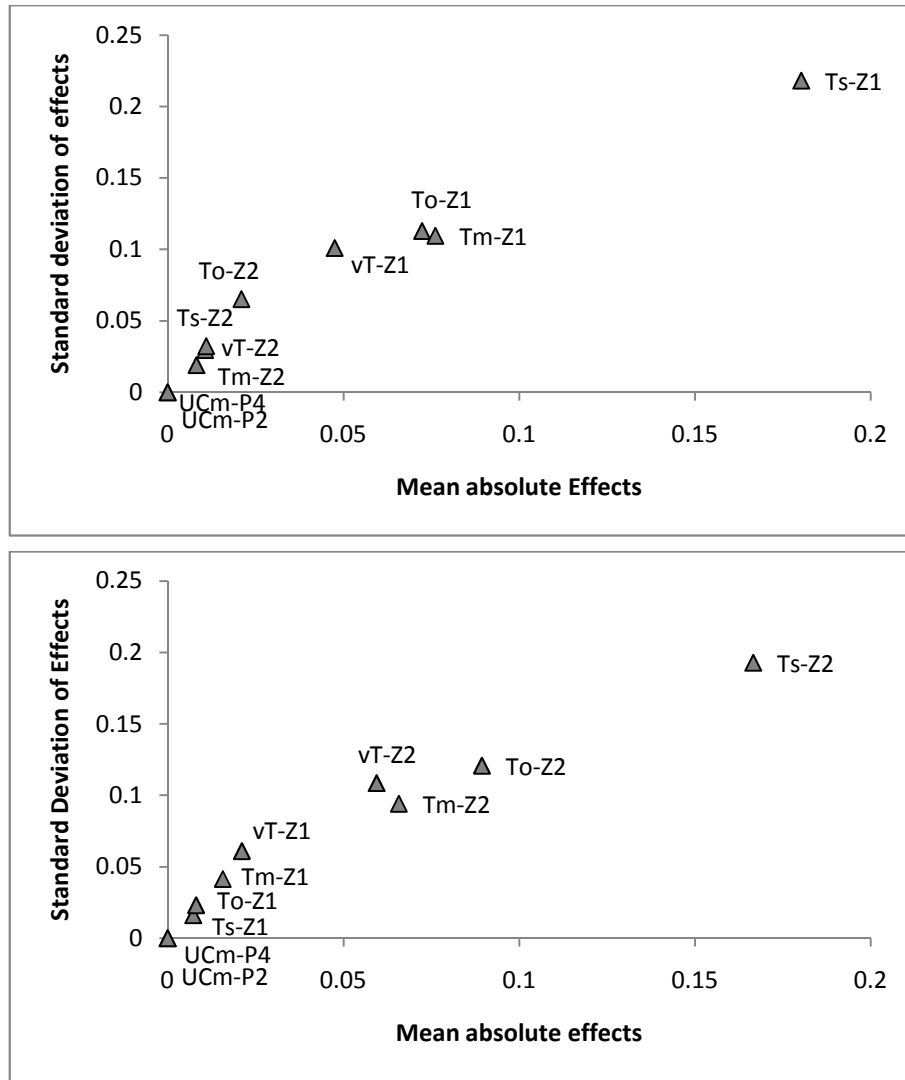
A benchmark model to test the Morris method was implemented in Campolongo et al. (2007) and repeated for this application to test the Matlab code and help determine how to select Morris method variables. The sensitivity analysis performed well, generally ranking the benchmark model parameters in the correct order.

Since Morris (1991) and Campolongo et al. (2007) did not specify why they recommend an r value of 10 (i.e. computing 10 elementary effects per factor via the evaluation of 10 matrices), larger r values were evaluated and compared using the benchmark model. A large sample of M was selected

with r values of 10, 20, and 40. There was negligible improvement between $r=10$ and $r=20$. The most consistent rankings were achieved with $r=40$, and it is assumed that, at this r value, these rankings have converged.

To test the performance of the code on the more complex DYRESM-CAEDYM model, initial runs included only 10 parameters in the screening experiment: 2 parameters that were expected to have no influence on zooplankton output (2 phytoplankton parameters, $UCm-P2$ and $UCm-P4$, with given ranges that should have no impact on the simulation) and 4 parameters that modify the temperature response function in each of the two zooplankton groups (vT -, $Tsta$ -, $Topt$ -, $Tmax$ - Z1 or Z2). These parameters are revisited and defined in the Section 4.2.4. Forty matrices ($r=40$) were chosen from 1000 randomly generated matrices ($M=1000$) of configurations for the 10 parameters. In this test, both zooplankton groups were set up to be identical. If the method performed well the ranking of the effect of Z1 temperature parameters on Z1 output should be the same as the ranking of the corresponding Z2 parameters on the output of Z2 and in both cases the effects of the two phytoplankton parameters should be negligible.

As described in Section 4.1.1, the Morris method generates two statistical criteria for ranking parameters: an average effect, μ , and a standard deviation of effects, σ , on a given output for each parameter. The Saltelli parameter, $\bar{\mu}$, gives an average of absolute effects so that if a parameter has both positive and negative impacts on an output variable, its potency is not underestimated by taking average values. In Figure 4-1, the absolute means for each parameter in the initial $k=10$ experiment are plotted versus their standard deviations. The first plot displays the parameter effects on zooplankton 1 and the second shows the corresponding parameter effects on zooplankton 2. In both plots, $Tsta$ is the most influential parameter on its respective zooplankton group. The next three parameters (vT , $Topt$ and $Tmax$) are important to their respective groups followed by all four parameters for the opposite zooplankton group, and finally the irrelevant phytoplankton parameters, UCm , have no effect on both zooplankton groups as they are plotted in the bottom left corner. These plots demonstrate the importance of a parameter on a given variable relative to the other parameters evaluated. Parameters that are clustered together are of similar importance. Note that the plots are not perfect mirror images, but give the same general sense of the importance of parameters. If the method had stepped through and evaluated every permutation of parameter configurations (10 parameters at 4 levels = 4^{10} configurations) then Figure 4-1(a) and (b) would be identical but with Z1 and Z2 parameters swapped. Since the method uses a streamlined, random sampling procedure, the results are not perfectly mirrored, but they provide a general picture of the relative importance of each factor.



4-1 Morris sensitivity results for seasonal average value of Zooplankton 1, cladocerans, evaluating only 8 zooplankton parameters (4 each for Z1 and Z2) and 2 phytoplankton parameters that were expected to be irrelevant.

The next sections describe the setup and analysis of a larger set of parameters examined in the DYRESM-CAEDYM model.

4.2.3 Selection of sampling experimental design

For the large run in DYRESM-CAEDYM, an r value of 40 was chosen since it should be more reliable than $r=10$, but still computationally manageable. Ninety-one (k) parameters were chosen for sensitivity analysis. A large number of elementary effects matrices were generated ($M=1000$) from which to sample the best combination of r (40) matrices. This sampling design yielded 3680 parameter configurations to run ($N=(k+1) \times r$).

A p -value of 4 was selected thus allowing each parameter to be sampled for one of 4 values between its maximum and minimum value. The rationale for the selection of parameters to be examined and the associated ranges for each parameter are discussed in the next section.

4.2.4 Selection of parameters and ranges

The selection of which parameters to evaluate and what ranges to assign to them is a critical component in any sensitivity analysis. A common approach in local one-at-a-time analyses is to perturb parameters from some starting point by 10% or 50% (Jorgensen & Bendoricchio, 2001), whereas many global methods sample a model parameter from a known or estimated statistical distribution that represents the model parameter's most likely values. Here, a uniform distribution was assumed for all parameters included in the study and an upper and lower limit was chosen. With a p -value of 4, in any given model simulation, each parameter could take on the value of its maximum, minimum, or one of 2 interior points equally spaced between its maximum and minimum. A realistic range for one parameter might span a few orders of magnitude whereas the total realistic range for another might vary by less than 5%. This presents a difficult challenge in setting up and interpreting the results of the sensitivity analysis; parameter ranges must be selected such that the results do not overemphasize the importance of one parameter due to its selected range being too broad or downplay the importance of another parameter because its range was not broad enough.

The ranges for parameters that represent a measurable quantity were assessed based on observed values in Lake Erie and other relevant studies. For some parameters, a measured realistic range is unknown. In these cases, values from relevant published models or judgements based on experience with the ELCD-Erie model were used to choose a range that would be large enough to capture the uncertainty of the parameter, but not so large as to skew the parameter's importance or cause the model to crash due to an extreme parameter choice.

Because there are well over three hundred parameters in the Lake Erie CAEDYM model, not all parameters could be included in the analysis; the parameters removed from consideration were expected to be the least important. Ninety-one parameters were selected for analysis based on the assumption that they would be the most likely to cause significant changes to modelled zooplankton biomass. The effects of parameter changes on total phosphorus and total chlorophyll concentrations were also evaluated because some parameters are expected to be important to zooplankton by exerting their effects indirectly through the nutrient and phytoplankton dynamics. At the same time, the zooplankton are also expected to influence nutrients and phytoplankton so zooplankton parameters can be expected to have some important influences beyond just the zooplankton concentrations.

It was assumed that the phytoplankton concentration (i.e. the zooplankton's food availability) would be important to zooplankton dynamics; therefore, many parameters describing phytoplankton processes were included. Nearly all of the parameters describing zooplankton behaviour were included. Additionally, some parameters describing the fate of particulate organic material (detritus) were included because zooplankton and phytoplankton both feedback into the particulate nutrient pool in significant ways.

Phytoplankton parameters and ranges are summarized in Table 4-2. The literature sources for parameter ranges where available are listed in Table 4-3. Each of the five phytoplankton groups simulated in CAEDYM is modelled by the same set of equations and parameters. The two diatom groups differ slightly from the other groups as they may be limited by silica availability in addition to carbon, nitrogen, and phosphorus concentration. Since each phytoplankton group is modelled by a similar set of equations it was deemed unnecessary to include the parameters for all phytoplankton groups in the sensitivity analysis. Parameters describing phytoplankton groups P4, P5, and P6 ("others", "flagellates", and "late diatoms") were included in the analysis since these three groups dominated the simulated phytoplankton biomass from late spring through early fall in previous simulations of the 2002 season (Leon et al., submitted). It was presumed that small changes to the other two groups (P2 "cyanobacteria" and P7 "early diatoms") brought on by the sensitivity experiment would not greatly impact the modelled total chlorophyll results or the results for total phosphorus and zooplankton. (The P1 and P3 phytoplankton groups are not simulated in the Lake Erie CAEDYM model; only 5 groups of a possible 7 are modelled.) Wherever supported by the literature or otherwise good judgment, identical magnitudes were used for the ranges of a parameter between the three groups, however if there was reason to believe that one group had a more uncertain range (e.g., the carbon:chlorophyll ratio in the flagellates, P5) then it was given a larger range than the other groups for that parameter.

The temperature parameters (12-15) in Table 4-2 define CAEDYM's f^{T1} temperature function (equation 21 in Appendix A), which is part of the growth term. This temperature response function follows a simple exponential function up to the standard temperature ($Tsta$), is maximized at a group's optimal temperature ($Topt$), crashes to zero at the maximum temperature ($Tmax$). These parameters are chosen to reflect the similar seasonal succession patterns of these phytoplankton groups seen in Lake Erie (e.g. Makarewicz et al. 1999, Carrick 2004, Smith et al. 2007). For instance, the "early diatoms" group (P6) with its low temperature parameter values will peak and crash before the "others" (P4) and "flagellates" (P5).

The parameters that describe mortality and losses to respiration were chosen through trial and error and experience with CAEDYM. These processes may be surrogates for processes that are not explicitly modelled in the application. For instance, prior to explicitly modelling zooplankton, phytoplankton loss due to grazing by zooplankton would have been estimated by these bulk loss processes. With the addition of zooplankton, the loss rates of phytoplankton were adjusted according to their suitability as prey for the zooplankton groups modelled. Still, many complex losses, such as filtering by mussels, are modelled indirectly through loss coefficients.

Most of the parameters that describe zooplankton functions for both zooplankton groups were included in the analysis. Zooplankton parameters and ranges are summarized in Table 4-4 and the numbered literature sources are listed, as above, in Table 4-3. As with phytoplankton groups, the ranges for a given parameter value were typically the same for both zooplankton groups.

Table 4-2 Parameters that are included in the sensitivity analysis and describe phytoplankton processes. The ID # represents a given parameter in the plots in section 4.4. P4, P5, P6 represent the "others", "flagellates", and "late diatoms" groups respectively. "Typical" values refer to values typically used to this point for the ELCD-Lake Erie model. Lower and upper are the bounds of the range evaluated for each parameter. The numbered literature sources are given in Table 4-3.

ID #	Name	Units	Description	Typical	Lower	Upper	Sources
1	μ_{max} -P4	/d	Max potential growth rate of phytoplankton.	0.8	0.6	1.6	1, 2, 4, 13, 15
1	μ_{max} -P5			1	0.6	1.6	1, 2, 3, 15
1	μ_{max} -P6			1.7	1.3	2.3	1, 2, 3, 4, 5, 15
2	$Y_{C:Chla}$ -P4	mgC/ mgChla	Average ratio of carbon to chlorophyll a	40	40	100	3, 4
2	$Y_{C:Chla}$ -P5			180	40	180	3, 4, 6
2	$Y_{C:Chla}$ -P6			50	40	100	3, 4
3	I_k -P4	uE/ (m ² s)	Light intensity at which photosynthetic rate is maximal	100	100	200	17
3	I_k -P5			40	35	135	17
3	I_k -P6			60	60	160	17
4	K_p -P4	mg/ L	Half saturation constant for phosphorus	0.003	0.003	0.03	2, 9, 23
4	K_p -P5			0.003	0.003	0.03	2, 9, 23
4	K_p -P6			0.003	0.003	0.03	2, 9, 23
5	K_N -P4	mg/ L	Half saturation constant for nitrogen	0.06	0.03	0.0	2, 4, 9
5	K_N -P5			0.045	0.015	0.075	2, 9
5	K_N -P6			0.045	0.015	0.075	2,9
6	$Sicon$ -P6	mgSi/ mgChla	Constant internal silica concentration	80	40	120	2, 4, 19
7	K_{Si} -P6	mg/L	Half saturation constant for silica	0.062	0.031	0.093	2, 4, 15, 20, 24
8	IN_{MIN} -P4	mgN/ mgChla	Minimum internal nitrogen concentration	3	1.5	3.5	2, 4
8	IN_{MIN} -P5			2	0.5	2.5	2, 4
8	IN_{MIN} -P6			2	0.5	2.5	2, 4
9	IN_{MAX} -P4	mgN/ mgChla	Maximum internal nitrogen concentration	9	7	11	2, 4
9	IN_{MAX} -P5			4	2	6	2, 4
9	IN_{MAX} -P6			4	2	6	2, 4

ID #	Name	Units	Description	Typical	Lower	Upper	Sources
10	IP_{MIN-P4}	mgP/ mgChla	Minimum internal phosphorus concentration	0.3	0.1	0.3	2, 4, 13, 14
10	IP_{MIN-P5}			0.1	0.05	0.25	2, 4
10	IP_{MIN-P6}			0.18	0.05	0.25	2, 4
11	IP_{MAX-P4}	mgP/ mgChla	Maximum internal phosphorus concentration	2	2	5	2, 4, 14
11	IP_{MAX-P5}			1	0.5	3.5	2, 4
11	IP_{MAX-P6}			1.8	0.5	3.5	2, 18
12	$\mathcal{G}-P4$	--	Temperature multiplier	1.06	1.05	1.08	2
12	$\mathcal{G}-P5$			1.06	1.05	1.08	
12	$\mathcal{G}-P6$			1.048	1.045	1.075	
13	T_{sta-P4}	°C	Standard temperature	24	21	27	See text
13	T_{sta-P5}			19	16	22	
13	T_{sta-P6}			7	4	10	
14	T_{opt-P4}	°C	Optimum temperature	28.5	25.5	31.5	See text
14	T_{opt-P5}			21	18	24	
14	T_{opt-P6}			9.8	6.8	12.8	
15	T_{max-P4}	°C	Maximum temperature	35	33.5	40.5	See text
15	T_{max-P5}			27.5	26	33	
15	T_{max-P6}			18.5	14.8	21.8	
16	$kr-P4$	/d	Respiration and mortality rate coefficient	0.102	0.062	0.142	See text
16	$kr-P5$			0.12	0.08	0.16	
16	$kr-P6$			0.118	0.078	0.158	
17	\mathcal{G}_R-P4	--	Temperature multiplier for T2 function (used in respiration)	1.08	1.03	1.13	2
17	\mathcal{G}_R-P5			1.08	1.03	1.13	
17	\mathcal{G}_R-P6			1.09	1.03	1.13	
18	$f_{resp-P4}$	--	Fraction of respiration relative to total metabolic loss rate	0.333	0.25	0.65	See text
18	$f_{resp-P5}$			0.333	0.25	0.65	
18	$f_{resp-P6}$			0.349	0.28	0.68	
19	f_{dom-P4}	--	Fraction of metabolic loss rate that goes to DOM (rest to POM)	0.2	0.1	0.3	See text
19	f_{dom-P5}			0.4	0.3	0.5	
19	f_{dom-P6}			0.4	0.3	0.5	

Table 4-3 List of references for tables 4-2, 4-4 and 4-5.

1. Bierman and Dolan 1981	2. Lehman et al. 1975	3. Griffin et al. 2001
4. Romero et al. 2004	5. Fishman et al. 2009	6. Isvanovics et al. 1994
7. Schladow & Hamilton 1997	8. Spillman et al. 2007	9. Reynolds 1984
10. Bruce et al. 2006	11. Makler-Pick et al. in press	12. Arhonditsis and Brett 2005
13. Grover 1991	14. Isvanovics et al. 2000	15. Scavia et al. 1988
16. Chen et al. 2002	17. Fahnenstiel et al. 1989	18. Smith and Kalff 1983
19. Harrison et al. 1976	20. Ferris and Lehman 2007	21. Wetzel 2001
22. Elser et al. 2000	23. Andersen and Hessen 1991	24. Paasche 1973
25. Scavia 1980	26. Legget et al. 1999	27. Hudson et al. 1999
28. Keeger et al. 1997	29. ODNR, unpub.	30. OMNR, Lake Erie Fisheries Station, unpub.

The modelled zooplankton groups are affected by the same temperature response function (f^T) as the phytoplankton are. Here, temperature parameters were selected to allow for early dominance by copepods and subsequent rise of cladocerans (eg. Barbiero 2001, Arhonditsis et al. 2005, LEPAS and LEB measurements used in Chapter 5). The ranges selected for the other zooplankton parameters were based upon findings from the literature review and applications of CAEDYM to other lake systems that included the zooplankton submodel.

In addition to phytoplankton and zooplankton parameters, some parameters that affect functions of organic matter and suspended solids were included in the study. These are presented in Table 4-5 and the corresponding literature sources are also listed in Table 4-3. It was expected that the transfer rates of particulate to dissolved nutrients may have important effects on zooplankton and phytoplankton since the grazing, excretion and messy feeding of the zooplankton would change the availability of nutrients.

Many input factors were excluded from the sensitivity screening study. As the number of parameters to evaluate increases the ability of the method to span much of the parameter space diminishes. Because a main objective of this study was to add the zooplankton submodel to the working nutrient-phytoplankton model of Lake Erie, only selected equation parameters (as discussed above) and the initial zooplankton concentrations were evaluated. The simulation begins (April 11, 2002) prior to when most zooplankton data are available (typically early May). It is expected that for diagnostics later in the season, initial zooplankton concentrations should have a limited impact since the processes simulated will become more important than the starting conditions as the model progresses. Nevertheless, due to the uncertainty in extrapolating the initial concentration values, these inputs were included in the analysis.

The impact of inflow concentrations and meteorological forcing data were not analysed primarily because the influence of these inputs varies considerably when contrasting DYRESM and ELCOM, and one would not expect the results of the sensitivity analysis to transfer from one to the other. DYRESM models the West Basin as a horizontally uniform basin. Changing inflow concentrations would be expected to have localized effects at the mouths of rivers in the 3-D model, ELCOM. In future studies, it might be worthwhile to consider the effects of initial concentrations of other variables, and the variation in inflow concentrations and meteorological information, but significant computer resources would be needed to do this in ELCD.

Table 4-4 Parameters describing zooplankton processes included in the sensitivity analysis. The ID # corresponds to the plots in section 4.3. Z1 and Z2 represent the cladocerans and copepods respectively. Lower and upper are the bounds of the range evaluated for each parameter. (Since zooplankton have never been modelled before for the ELCD-LE application, there is no column for “typical” values.)

ID #	Name	Units	Description	Lower	Upper	Sources
20	A_z -Z1	--	Messy feeding; portion of food reaching the mouth	0.7	1	10, 11
20	A_z -Z2			0.7	1	10, 11
21	k_{Rz} -Z1	/d	Respiration rate coefficient	0.06	0.18	1, 3, 4, 6
21	k_{Rz} -Z2			0.02	0.14	1, 3, 4, 6
22	k_{Mz} -Z1	/d	Mortality rate coefficient	0.01	0.15	10, 11
22	k_{Mz} -Z2			0.01	0.15	10, 11
23	k_{Fz} -Z1	--	Fecal pellet fraction of Grazing	0.05	0.35	10, 11, 15
23	k_{Fz} -Z2			0.05	0.35	10, 11, 15
24	k_{Ez} -Z1	--	Excretion fraction of grazing	0.05	0.35	10,11,15
24	k_{Ez} -Z2			0.05	0.35	10,11,15
25	k_{ZIN} -Z1	mgN/ mgC	Internal nitrogen to carbon ratio	0.1	0.23	10, 11, 22, 23
25	k_{ZIN} -Z2			0.12	0.25	10, 11, 22, 23
26	k_{ZIP} -Z1	mgP/ mgC	Internal phosphorus to carbon ratio	0.017	0.052	10, 22, 23
26	k_{ZIP} -Z2			0.009	0.03	10, 22, 23
27	ϑ_T -Z1	--	Temperature multiplier in $f(T_1)$	1.05	1.1	*
27	ϑ_T -Z2			1.05	1.1	
28	T_{sta} -Z1	°C	Standard temperature	12	18	*
28	T_{sta} -Z2			7	13	
29	T_{opt} -Z1	°C	Optimum temperature	15	21	*
29	T_{opt} -Z2			9	15	
30	T_{mx} -Z1	°C	Maximum temperature	30	36	*
30	T_{mx} -Z2			27	33	
31	ki -Z1	(gPhyCm ⁻³)/	Maximum grazing rate	0.8	2.8	3, 10, 12, 25
31	ki -Z2	(gZCm ⁻³)/d		0.5	2.5	3, 10, 12, 25
32	ϑ_Z -Z1	--	Temperature dependence $f(T_2)$ for respiration	1.04	1.08	*
32	ϑ_Z -Z2			1.04	1.08	
33	Kj -Z1	gC/m ³	Half saturation constant for grazing	0.1	0.6	3, 10, 12, 25
33	Kj -Z2			0.1	0.6	
34	$iniZ1$	mgC/ L	Initial concentrations zooplankton groups.	4E-05	7E-04	29,30
34	$iniZ2$			0.0006	0.008	29,30

Table 4-5 Parameters describing some other processes relating to particulate matter that were considered in the sensitivity analysis. The ID # represents a given parameter in the plots in section 4.3. Lower and upper are the bounds of the range evaluated for each parameter.

ID #	Name	Units	Description	Typical	Lower	Upper	Literature sources
35	<i>POP1-max</i>	/d	Maximum transfer rate of POC--> DOC	0.01	0.01	0.15	28
36	<i>PON1-max</i>	/d	Maximum transfer rate of PON--> DON	0.01	0.01	0.15	28
37	<i>POM-Dia</i>	m	Diameter of particulate organic matter (POM)	0.00005	5E-06	5E-05	21, 26, 28
38	<i>POM-Dens</i>	kg/m ³	Density of POM	1005	1020	1105	8, 11
39	<i>Tc-POM</i>	N/m ²	Critical shear stress for POM	0.002	0.001	0.003	See text
40	<i>dens-SS1</i>	kg/m ³	Density of suspended solid (SS) particles	2650	1325	3975	See text
41	<i>dia-SS1</i>	M	Diameter of suspended solids	1.8E-06	9E-07	3E-06	See text
42	<i>cShear-SS1</i>	N/m ²	Critical shear stress for SS	0.01	0.005	0.015	See text

4.3 Results

The Morris sensitivity screening analysis method presumes that a single model output value is used to evaluate the effects of changing each parameter. The most appropriate choice of diagnostics to evaluate was not obvious, since DYCD produces profiles for several state variables at every 30-minute timestep for the 142-day simulation. In this case, variation with depth was not important for the DYCD sensitivity analysis since the West basin is shallow and doesn't develop stable stratification, therefore, averages of the top 6m of the basin profile were taken. One of the main objectives for developing the zooplankton submodel was to realistically simulate the timing and magnitude of the peak zooplankton concentrations. State variables of greatest interest and impact to the zooplankton model were presumed to be the zooplankton (cladocerans (Z1) and copepods (Z2)), total algal biomass (approximated as total chlorophyll a), and total phosphorus. Two types of outputs for the four variables were selected for this analysis:

- 1) the maximum mass computed at any given time during the simulation, and
- 2) the day on which the peak mass was reached.

The day of the season is referred to by its Julian date. The first day of the simulation, April 11, is day 101 and the last, September 1, is day 243.

There are 3680 model results for each of the 12 output variables evaluated. Each elementary effect, d_i^j , for a given parameter, i , is computed according to Equation 4-3 by taking the difference between the two consecutive simulation results that correspond to a change in that parameter between two otherwise identical consecutive run configurations and dividing that difference by the interval of parameter change, which in this application is always $2/3 \left(\frac{p}{p-1}\right)$. Each of the 91 (k) parameters was perturbed 40 times ($r=40$), therefore requiring the computation of 40 d_i^j effects. From the distribution of d_i , an average, μ_i , and standard deviation, σ_i , of effects on the given output variable is computed as well as an absolute average, $\bar{\mu}_i$.

The rest of this chapter presents the sensitivity screening results.

4.3.1 Sensitivity of zooplankton

The two zooplankton groups are represented by identical submodel routines in CAEDYM so they are differentiated according to the distinct parameter ranges assigned to them. Of the 15 parameter ranges defined for each zooplankton group in Table 4-3, 7 were identical for both zooplankton groups; the other 8 pairs of parameters (including initial concentration values) are what distinguished the zooplankton groups from each other in the sensitivity experiment. It was expected that a similar set of parameters would prove to be the most significant to both groups' results, but some differences would be expected due to the subtle differences in the tested parameter ranges.

The distributions of zooplankton results for computed seasonal maxima and the days on which maxima are reached are displayed as frequency charts in Figure 4-2. Note that the scale is logarithmic so that the range of higher concentrations and late days of peak concentrations could be seen; this was necessary since in over 2500 simulations each zooplankton group did not grow beyond their initial concentration on April 11 (Day 101). In reality, maximal zooplankton concentrations will occur after April. This unexpected distribution demonstrates the challenge in calibrating the model for zooplankton, even when interrogating the model with reasonable parameter ranges.

When simulations symptomatic of zero growth were removed from the set of simulations for each zooplankton group, the distribution of seasonal maximum concentrations and the days on which those occurred was more realistic. Corrected ranges, medians, and averages are presented in Table 4-6. The sensitivity experiment appears to have a bias for higher copepod concentrations and generally unsuccessful zooplankton simulations. Despite this, the elementary effects produced for the parameters examined should prove useful; certain parameters were significant enough to cause shifts of over several weeks in peak timing and significant swings in concentrations.

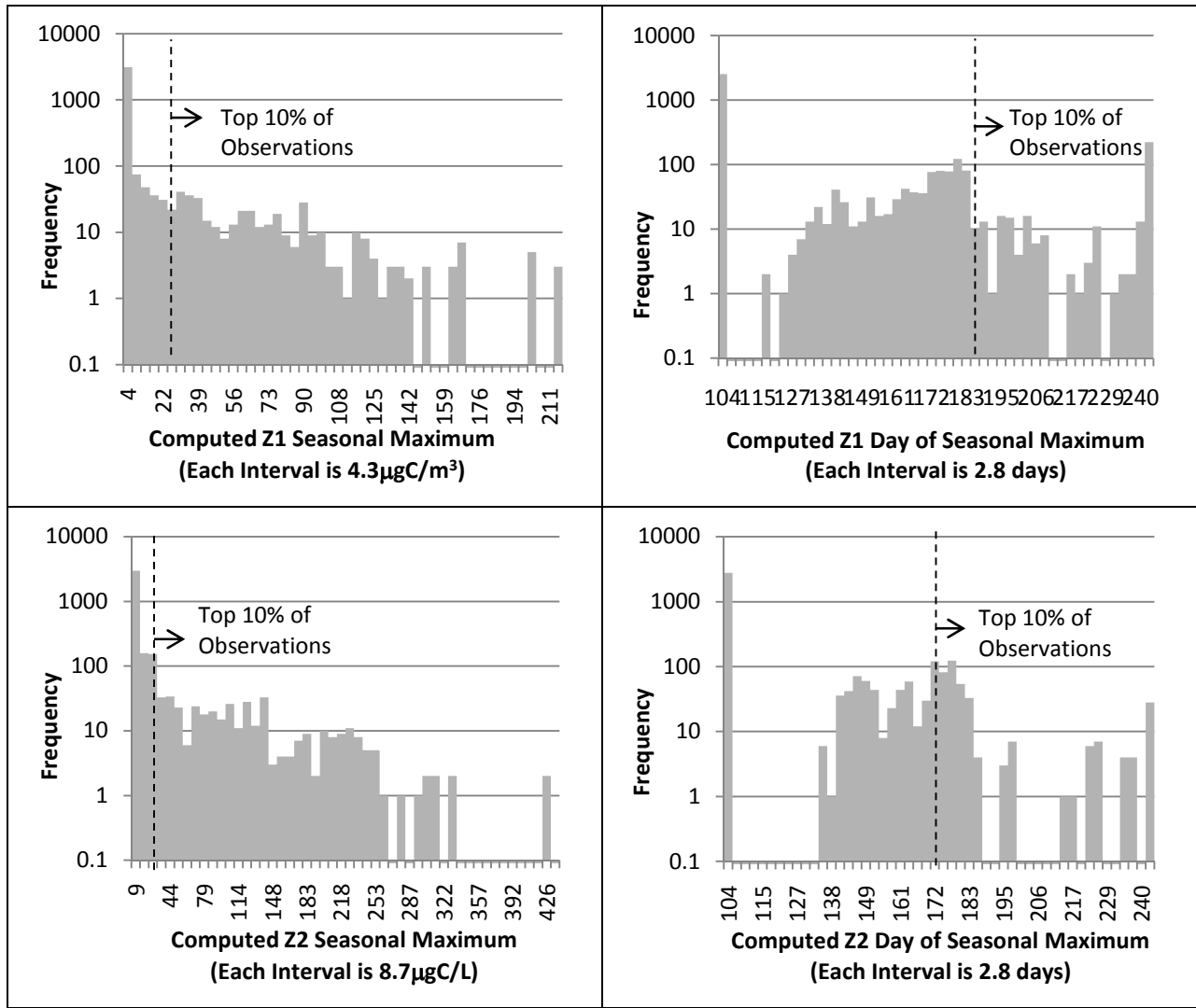


Figure 4-2 Frequency of 3680 computed zooplankton 1 (top) and zooplankton 2 (bottom) outputs for seasonal maximum (left) and the day of seasonal maximum (right). The maximum dates are between 101=April 1 and 243=Sept 1. Due to the large proportion of simulations with early and/or very low peaks the scale is logarithmic. The 90th percentile of computed results is shown in each plot by the dashed line.

Table 4-6 Simulated zooplankton statistics from the Morris experiment for runs that were not symptomatic of a lack of growth.

	Cladocerans (from 1145 simulations)		Copepods (from 915 simulations)	
Corrected statistics	Seasonal Maximum (mgC/L)	Day of Seasonal Maximum	Seasonal Maximum (mgC/L)	Day of Seasonal Maximum
Range	0.00004	18	0.0006	34
	0.215	143	0.435	143
Median:	0.0046	76	0.021	71
Average:	0.0247	84.6	0.055	67.4

Parameter effects on the seasonal maximum biomass of cladocerans (Z1) and copepods (Z2) are presented in Figure 4-3. The axes are unitless since they represent the average and standard deviation of the change in output (ug/m³ for zooplankton) per change in parameter (i.e. divided by $\frac{2}{3} = \frac{p}{p-1}$). This method cannot give a quantitative analysis of a parameter's effects so little notice should be paid to the scale; rather it is the *relative* positions of parameter effects on the plots that are of use. The average plots (right side of Figure 4-3) show the actual average change in zooplankton seasonal maxima per change in the parameter. A negative average indicates a generally negative correlation with variable output; a positive average indicates a positive correlation. The absolute average plots (left side of Figure 4-3) show the average of only the absolute values for the change in seasonal maximum per change in parameter so that the true magnitude and ranking of a parameter's effect is assessed.

If a parameter's average value is less in magnitude than its absolute average value, then that parameter caused both positive and negative changes in variable output. Most parameters had consistent sign effects on output, except the zooplankton's half saturation constants for grazing (Z-33) and the maximum growth rate of the flagellates group (P5-1). Changes caused by these parameters are thus more unpredictable. For example, the half saturation constant for grazing has a generally negative correlation with zooplankton concentration since it limits zooplankton grazing. But this relationship is not always the case. If the grazing term is too favourable (eg. high maximum grazing rate, low half saturation, and optimal conditions) then zooplankton may be so successful early in the simulation that they eat all the food and crash, thus never attaining a high peak concentration. In that way, a lower half saturation value could lead to lower seasonal average and maximum concentrations.

The vertical axis (standard deviation of the distribution of d_i^j effects) is a relative indication of the degree of a parameter's non-linear or interactive effects on the output variable. The Morris screening method cannot distinguish between non-linear or correlated parameter effects on the output variable; it only points out that, under a variety of circumstances, changes in model output are not linearly related to changes in a parameter's value. It is not surprising that most parameters have a high degree of interdependent effects relative to their independent effects since it is already known that CAEDYM models a complex ecological system.

Parameters that are distinctly separate from the cluster of parameters in the bottom left corner are considered to be the most significant to the given output. Nearly all of the zooplankton parameters evaluated appear to be significant parameters for their respective zooplankton group. This confirms that zooplankton parameters are directly affecting zooplankton, as expected, and that all of the modelled zooplankton functions appear to be important to the model output relative to other aspects of the model, as is consistent with expectations. In comparing the two zooplankton groups, the same types of parameters come up as being important with a few differences. (See Appendix A for the specific model equations that use those parameters.) The most important mutually common parameters appear to be the coefficient for mortality (Z-22), the maximum grazing rate (Z-31), the half saturation constant (Z-33), and the internal carbon to phosphorus ratio (Z-26). The next most important mutual zooplankton factors were the fecal pellet fraction of grazing (Z-23), the messy feeding coefficient (Z-20), the respiration coefficient (Z-21), standard and maximum temperature coefficients (Z-28 and Z-30), and the initial value. The temperature multiplier (Z-27) for the fT^1 function and the internal nitrogen to carbon ratio (Z-25) were identified as being significant to Z2, but not Z1.

Only a few phytoplankton parameters had important effects. Phytoplankton parameters that had significant impacts on zooplankton were almost always parameters for "others" (P4) and "flagellates" (P5). This is to be expected since the "early diatoms" (P6) are not as dominant and tend to peak and crash early in the simulation. Specifically, important phytoplankton parameters included the maximum growth rate (P-1), the minimum internal nitrogen concentration (P-8), the respiration and mortality coefficient (P-16), and, for only Z1, the carbon to chlorophyll ratio.

Only one of the "other" parameters – the density of suspended solids (Other-40) – had a notable impact on copepod seasonal maximum. The remaining parameters are clustered near the intersection of the axes in the zooplankton Morris plots; these parameter effects are indistinguishable relative influences on the output and had the least important impact on zooplankton output given the setup of this experiment.

Parameter effects on the day on which seasonal maxima occur for zooplankton are presented in Figure 4-4. As in Figure 4-3, average plots for each output variable are compared beside absolute plots to show the sign and relative magnitude of parameter effects.

A smaller subset of parameters are significant to the simulated days on which the maxima occur. This is not surprising given the frequency of peak concentrations occurring on the first day of the simulation. As with the seasonal maxima, the mortality rate coefficient (Z-22), half saturation constant for grazing (Z-33), maximum grazing rate (Z-31) and internal phosphorus to carbon ratio (Z-26) are at the top of the list of significant parameters for the day of maximum. The diameter of suspended solids (Other-41) appears to be as important as the density of suspended solids. Parameter effects appear to be more unpredictable for the maximum day output value: the average values are much lower than the absolute values for most parameters which indicates that the changes in those parameters can result in either earlier or later maximum peaks.

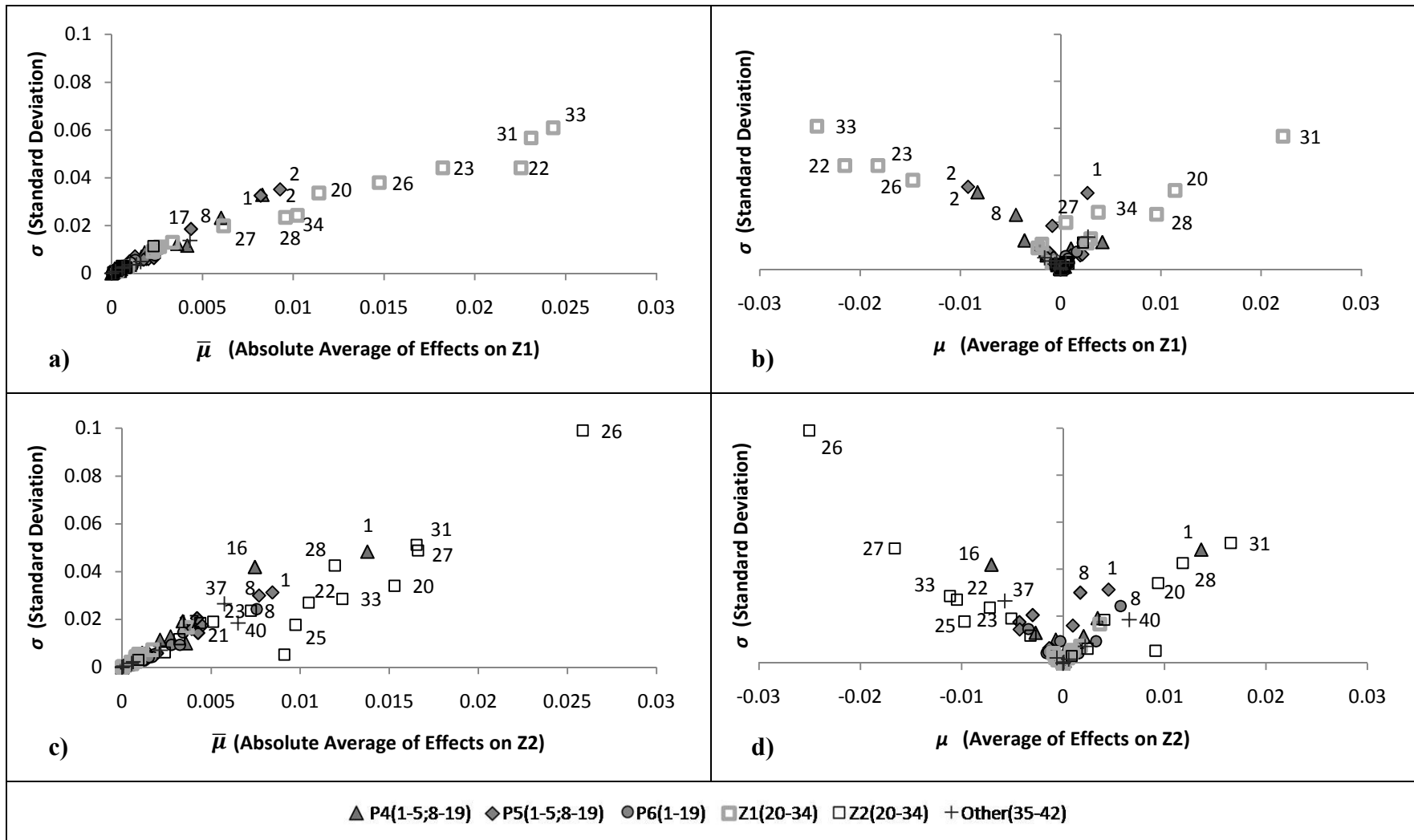


Figure 4-3 Parameter effects on seasonal maxima of [a,b] zooplankton 1 (cladocerans) and [c,d] zooplankton 2 (copepods). [a,c] absolute average and [b,d] average versus standard deviation of parameter effects on output.

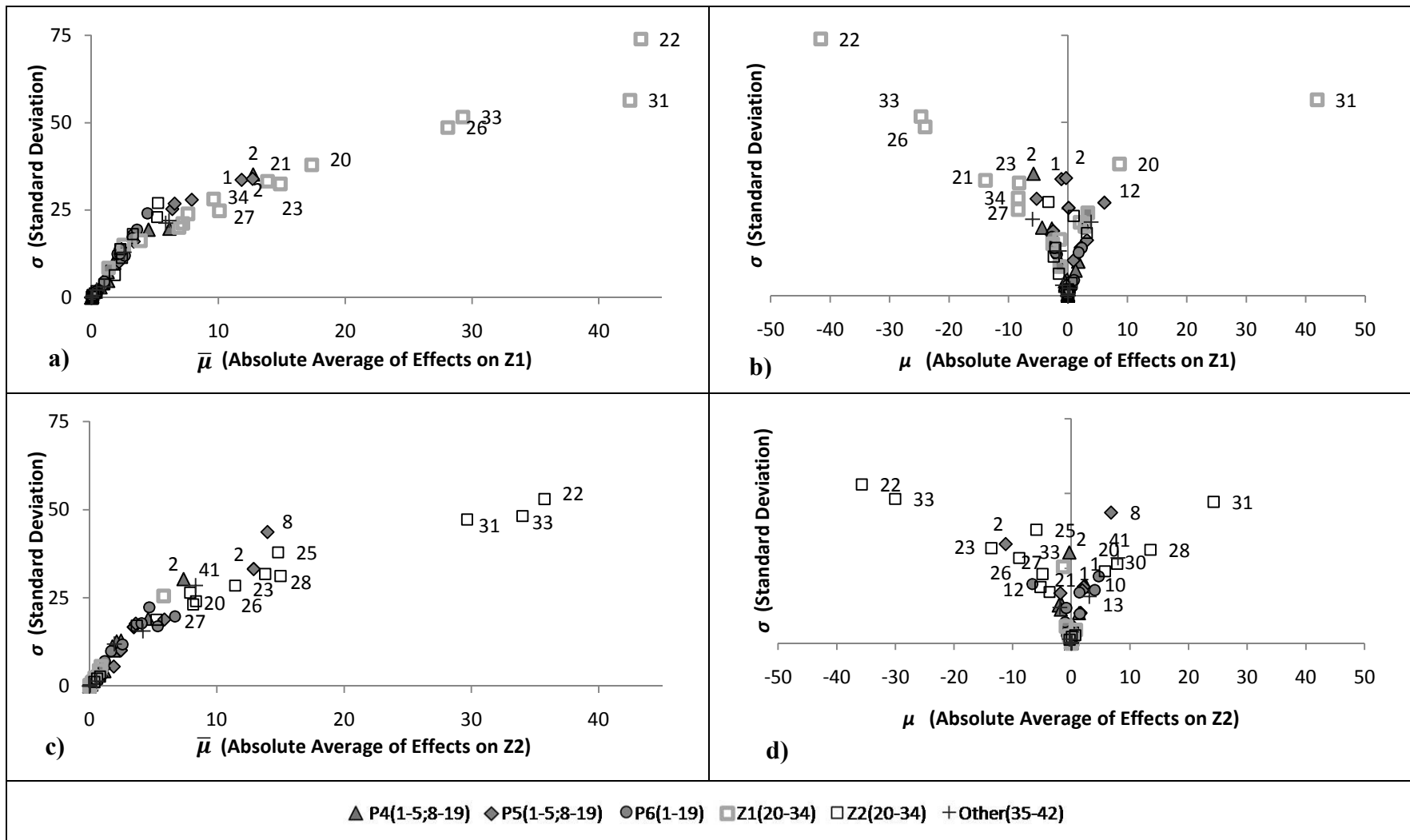


Figure 4-4 Parameter effects on the day at which [a,b] zooplankton 1 (cladocerans) and [c,d] zooplankton 2 (copepods) reach their seasonal maxima. [a,c] absolute average and [b,d] average versus standard deviation of parameter effects on output.

4.3.2 Sensitivity of total phytoplankton and phosphorus

The distributions of total chlorophyll (TChla) and total phosphorus (TP) output results were not as unexpected as they were for zooplankton. A summary of the range, median and average values for TChla and TP from all 3680 simulations is provided in Table 4-7. Total phosphorus was the least affected by the perturbations of this experiment because fewer parameters were altered that directly affect TP and the model describing TP is simpler. Typically, the TP in the lake should be maximal in the spring due to spring runoff. As the season progresses, a net loss of TP to settling occurs (Schwab et al., 1999). It was typical in the existing ELCD nutrient-phytoplankton model of Lake Erie for TP to be at its maximum at the beginning of the simulation; this was most often the case in the Morris experiment too. More variation was seen in total chlorophyll since parameters describing three of the five phytoplankton groups that comprise the total chlorophyll were altered and phytoplankton are further affected by changes in zooplankton and phosphorus.

Table 4-7 Summary of total chlorophyll a and total phosphorus output results from the full set of 3680 runs.

	Seasonal Maximum		Day of Seasonal Maximum (day)	
	(ug/L)	(mg/L)	TChla	TP
Range	2.76	0.0247	118	101
	97.7	0.0334	243	141
Median	16.7	0.0258	161	101
Average	20.69	0.0276	165.5	109.66

Parameter effects on the seasonal maximum concentrations of TChla and TP are presented in Figure 4-5. Again, the average plots (right side of Figure 4-5) show the actual change in seasonal average concentration per change in the parameter. The absolute average plots (left side of Figure 4-5) show only the absolute values for the change in seasonal maximum per parameter.

In general, parameters describing P5 had the greatest impact on TChla output. This is not surprising since P5 was set up to be the most dominant phytoplankton group in the summer. By contrast, parameters directly affecting P6 were the least important phytoplankton parameters since P6 was set up to have the lowest seasonal average biomass of the three groups.

The most significant phytoplankton parameters on TChla are the maximum potential growth rate (P5-1), the minimum internal phosphorus concentration (P5-10), and the coefficient of respiration (P5-16). P-1 is multiplied by the growth term and thus has a positive influence on TChla biomass, whereas P-16 is a loss term due to respiration and “mortality” and therefore has a negative influence on TChla. The importance of P-10 indicates that phosphorus is likely limiting to these phytoplankton groups: an increase in the minimum requirement for phosphorus results in greater phosphorus limitation and thus lower biomass values.

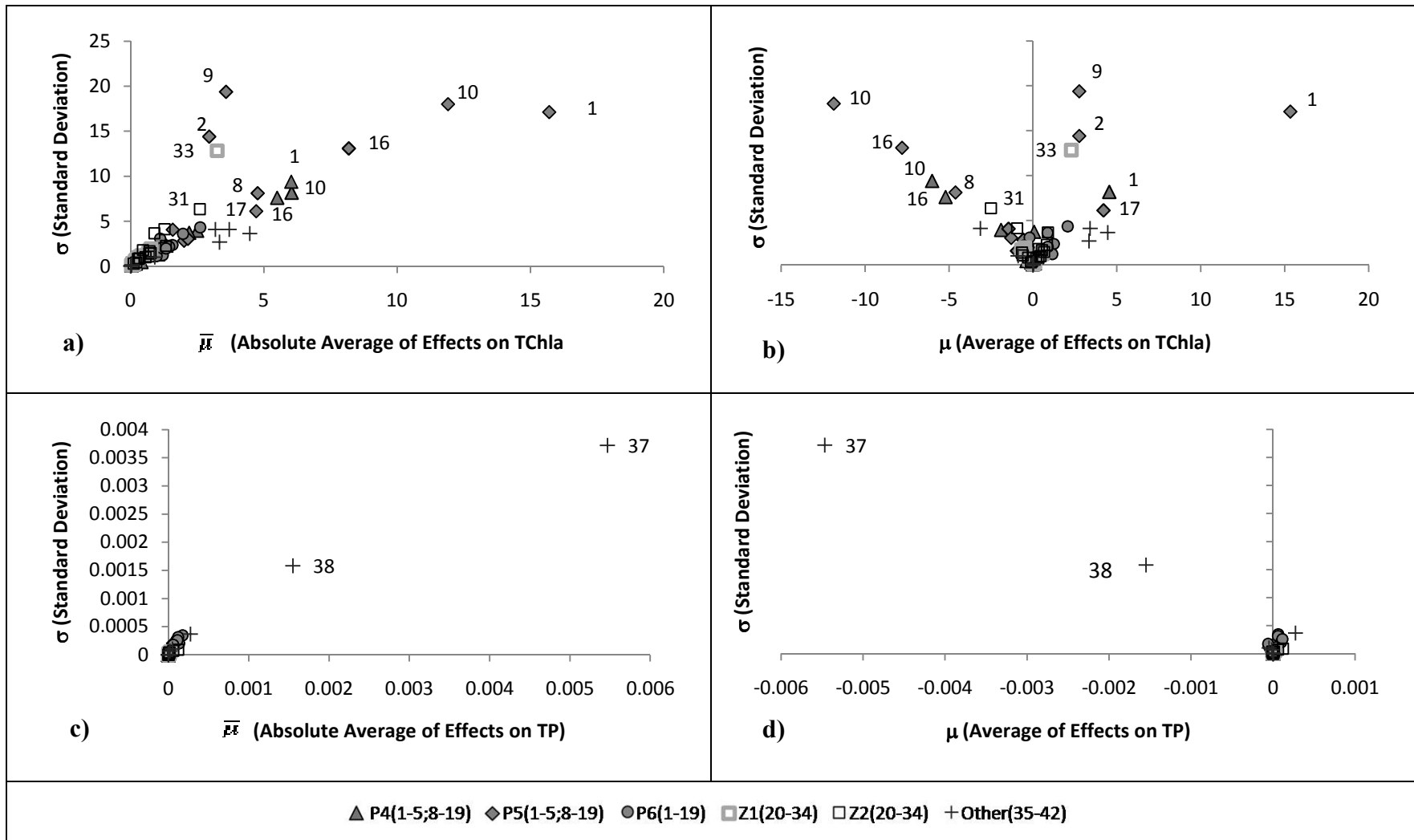


Figure 4-5 Absolute average (a and c) and average effects (b and d) of parameters on predicted seasonal maximum of total chlorophyll (a and b) and total phosphorus (c and d).

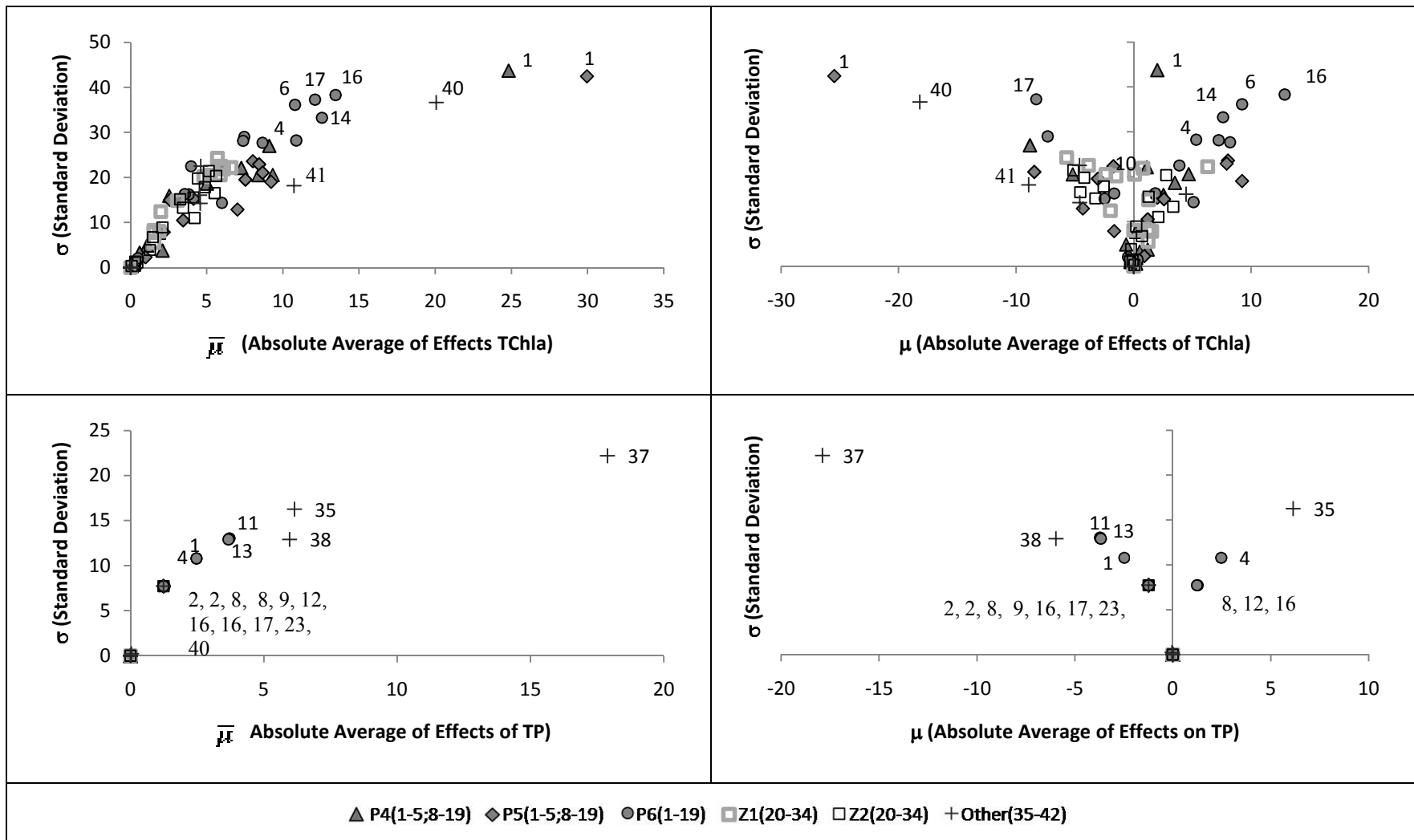


Figure 4-6 Absolute average (a and c) and average effects (b and d) of parameters on the predicted day of the seasonal maximum of total chlorophyll (a and b) and total phosphorus (c and d).

The factors dealing with particulate matter were important to both phytoplankton and TP. In the case of TP, only the maximum transfer rate from particulate to dissolved organic carbon (Other-35), the diameter of particulate organic matter (Other-37), and the density of particulate organic matter (Other-35) were important. This indicates that settling is the main pathway for decreasing total phosphorus concentration which has implications for the biota - if settling is increased then less TP is available for phytoplankton and if it is decreased then more TP is available. In this way, these parameters are also important to phytoplankton.

The most influential zooplankton factors on total phytoplankton were the maximum grazing and half-saturation constants (Z-31 and Z-33 respectively). Thus, in the model, zooplankton primarily impact phytoplankton through their direct grazing. It is possible that some other important zooplankton parameter effects were underestimated given that numerous runs resulted in no zooplankton growth. In those runs, all zooplankton parameters would likely have negligible impacts on total chlorophyll.

4.4 Discussion

A summary of the most significant parameters identified by this Morris sensitivity screening exercise is provided in Table 4-8. In each of the four diagnostic output columns, it is indicated whether a listed parameter had significant impacts on either, both, or neither of the two diagnostic outputs (seasonal maximum and maximum timing). The outputs were not sensitive to 47 parameters, which were not listed in Table 4-8.

Zooplankton parameter sensitivity revealed a mixture of expected and more surprising results, including some high sensitivities to parameters that do not appear to be well-constrained by existing information. Mortality rates, respiration rates, maximum grazing rates and half saturation constants for control of grazing rates by phytoplankton concentration were important and likely should be, as they directly affect feeding and survival rates. Tissue elemental composition (C and P) would also affect the nutritional demands of the animals so their importance is understandable.

Temperature functions for feeding activity were also important but primarily in terms of the steepness of the functions (multiplier) and onset of near-maximal values (Tsta); cardinal values for optimal and maximum temperatures were less important. This would suggest that below-optimal temperatures, rather than above-optimal temperatures were of greater influence. Temperature response of respiration was comparatively unimportant.

The importance of the messy feeding parameter might also be expected, because it also determines the effective ration, but the literature to support choices for this parameter is surprisingly sparse suggesting that further research on this process could be valuable. The fecal pellet fraction and the messy feeding coefficient (Z-20) represent losses to zooplankton that contribute mass to the particulate matter cycle.

That so many simulations were symptomatic of very low and early peak concentration is an indication of the difficulty associated with calibrating the zooplankton model. Zooplankton functions and parameters are not as well understood and characterized as many of the phytoplankton submodels.

Table 4-8 Parameters showing significance (relative to clustered parameters) in any of the sensitivity diagnostics. "Both" in a variable's column indicates that the parameter was significant for both the seasonal maximum and day of seasonal maximum. For brevity, zooplankton parameters are labelled as Zx- to include either zooplankton 1 or 2 (zooplankton parameters significantly impacted only their respective zooplankton groups; where they were significant to TChla 'x' indicates which zooplankton group parameter was significant).

ID #		Description	Cladoceran (x=1)	Copepod (x=2)	TChla	TP
Zx-20	A_z	Messy feeding; portion of food reaching the mouth	both	both		
Zx-21	k_{Rz}	Respiration rate coefficient	day	max		
Zx-22	k_{Mz}	Mortality rate coefficient	both	both		
Zx-23	k_{Fz}	Fecal pellet fraction of Grazing	both	both		
Zx-25	k_{ZIN}	Internal nitrogen to carbon ratio		both		
Zx-26	k_{ZIP}	Internal Phosphorus to carbon ratio	both	both		
Zx-27	ϑ_T	Temperature multiplier in $f(T_1)$	both	both		
Zx-28	T_{sta}	Standard temperature in $f(T_1)$	max	both		
Zx-30	T_{mx}	Maximum temperature in $f(T_1)$		day		
Zx-31	K_i	Maximum grazing rate	both	both	max (x=2)	
Zx-33	K_j	Half saturation constant for grazing	both	both	max (x=1)	
Zx-34	Ini	Initial concentration of zooplankton	both	max		
P4-1	μ_{max}	Max potential growth rate of phytoplankton.		max	both	
P5-1	μ_{max}	Max potential growth rate of phytoplankton.	both	max	both	
P4-2	$Y_{C:Chl_a}$	Average ratio of carbon to chlorophyll a	both	day		
P5-2	$Y_{C:Chl_a}$	Average ratio of carbon to chlorophyll a	both	day	both	
P6-4	K_P	Half saturation constant for phosphorus			day	
P6-6	$Sicon$	Constant internal silica concentration			day	

P4-8	IN_{MIN}	Minimum internal nitrogen concentration		max		
P5-8	IN_{MIN}	Minimum internal nitrogen concentration	max	both	max	
P6-8	IN_{MIN}	Minimum internal nitrogen concentration		max	max	
P5-9	IN_{MAX} x	Maximum internal nitrogen concentration			max	
P4-10	IP_{MIN}	Minimum internal phosphorus concentration			max	
P5-10	IP_{MIN}	Minimum internal phosphorus concentration			max	
P6-14	T_{opt}	Optimum temperature			day	
P4-16	Kr	Respiration and mortality rate coefficient		max	max	
P5-16	Kr	Respiration and mortality rate coefficient			max	
P6-16	Kr	Respiration and mortality rate coefficient			day	
P5-17	g_R	Temperature multiplier for T2 function (used in respiration)			max	
P6-17	g_R	Temperature multiplier for T2 function (used in respiration)			day	
O-35	POP_{max}	Maximum transfer rate of POC to DOC			max	max
O-37	POM_{-Da}	Diameter of particulate organic matter (POM)		max	max	both
O-38	POM_{-De}	Density of POM				both
O-40	$dens_{SS1}$	Density of suspended solid (SS) particles		max	max	
O-41	dia_{SS1}	Diameter of suspended solids		day	both	

The parameters directly defining the given zooplankton group were by far more important than other types of parameters, as would be expected. In terms of intergroup influences, phytoplankton parameters commonly important to zooplankton were almost exclusively for groups P4 and P5 ("others" and "flagellates", which dominate phytoplankton biomass) and included the maximum potential growth rates (P-1), minimum internal nitrogen (P-8), respiration and mortality (P-16) and, curiously, the carbon to chlorophyll a ratio (P-2).

The factors relating to particulate matter were expected to have a significant impact on total phosphorus, but they also appeared to be important to phytoplankton biomass and even the copepods. The size and density of particles proved particularly important. Particles settle to the sediments according to Stokes' law (CWR, 2006b); in the settling function the diameter is squared and multiplied by density. An increase in size would therefore significantly accelerate settling, making nutrients less available to phytoplankton uptake. In some initial sensitivity experiments prior to completing the sensitivity screening analysis, DYCD was run using POM diameters or POM densities exceeding the ranges assigned in Table 4-5. These parameters, given overly large ranges, had dramatic effects on the results; often the model crashed. The parameters were therefore constrained in the main sensitivity experiment to avoid this problem. It is a weakness that these parameters are so important since they are not easily measured and not well characterized. Makler-Pick et al. (in press) also found POM diameter and density to be of great significance in their sensitivity analysis.

The phytoplankton seasonal maximum was sensitive to relatively fewer parameters compared to the zooplankton especially given that there were more phytoplankton parameters evaluated and that phytoplankton are also influenced by changes in zooplankton and TP. This may reflect that the phytoplankton functions and parameters are better constrained in the analysis. Alternatively, since total chlorophyll includes 5 functional groups the TChla diagnostic would not convey changes in groups that effectively cancel out. The timing of phytoplankton maximum appeared to be sensitive to very many parameters; it is difficult to distinguish the significant parameters from the cluster.

Phytoplankton were particularly sensitive to parameters pertaining to particulate matter. Zooplankton parameters were largely absent from the list, except for two parameters relating to the grazing of phytoplankton. Had the experiment favoured higher concentrations of zooplankton there may have been more zooplankton parameters significant to total chlorophyll a output.

The results of this experiment - both the identifications of important and unimportant parameters - provide a useful guideline for calibration of the model with respect to zooplankton. Initial calibration efforts using this information are described in Chapter 5.

Chapter 5 Calibration of ELCOM-CAEDYM

5.1 Zooplankton data available for comparison

In any given year where surveys of zooplankton densities were conducted, the spatial distribution and timing of zooplankton abundance is not thoroughly characterized for a lake as large as Lake Erie. Ideally, for the purposes of model calibration and verification for given years, there would be zooplankton concentration data available for hundreds of sites sampled at many times throughout the season. This type of data set is not available and not feasible. An impressive sampling effort in 2002 (the year the model was set up for in this study) provided hundreds of measurements over the course of the season, but many parts of the lake and some periods during the simulation were not well described. In this chapter, the strategy for assessing the model's performance is to use measured data across many sites over several years as guidance for achieving an appropriate pattern of zooplankton distribution and peak timing for a simulated growing season.

Measured zooplankton values in Lake Erie at various sites between 1997 and 2006 were obtained from two sampling programs: Lake Erie Biomonitoring (LEB) (OMNR, Lake Erie Fisheries Station, unpub.) and the Lake Erie Plankton Abundance Study (LEPAS) (ODNR, unpub.). Only the concentrations for cladocerans and calanoid copepods were used in this study. The locations of all LEPAS and LEB sites with available zooplankton measurements are presented in Figure 5.1.

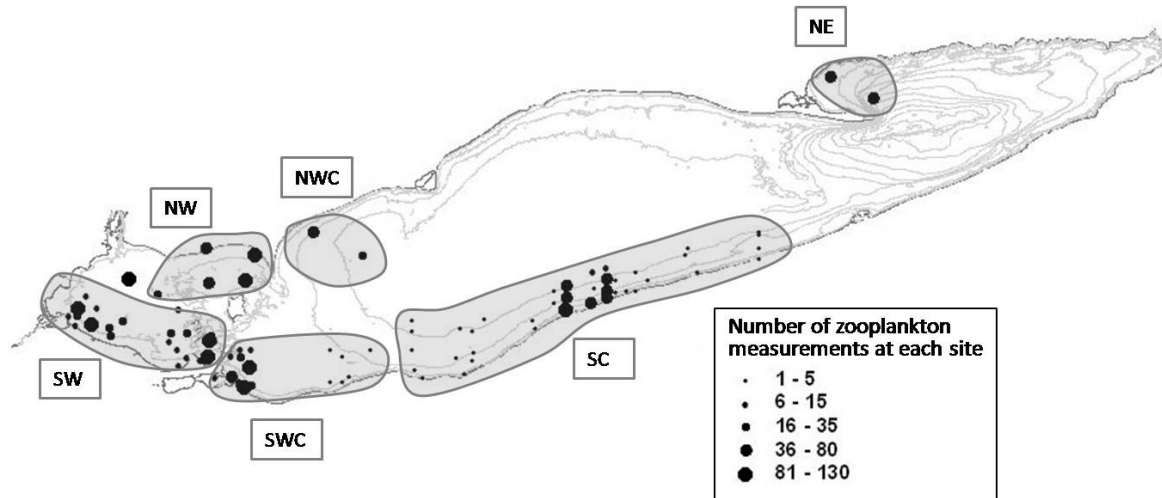


Figure 5-1 Location of sites at which zooplankton surveys were conducted between 1997 and 2006 via the LEPAS or LEB sampling programs. Zones are delineated for the purpose of comparison between data sets and modelled results. The size of the dots is an indication of how many times a particular site was sampled for cladocerans and copepods.

LEB sampling sites are located in the North half of the Lake Erie basins. Very few sites with zooplankton measurements were located in the Central and East basins. Johansson et al. (2000) provide some details on the rationale and sampling protocols for the LEB program. The LEPAS program sampled zooplankton densities at sites along the south half of the West and Central basins, but no sites were sampled for zooplankton in the East Basin. Details on LEPAS sampling protocols are available from Conroy et al. (2005).

The complete data set (from 1997 to 2006) at these sites was used to estimate the general patterns in the lake for comparison to the modelled results for the year 2002. To facilitate this comparison, the sites were divided into six zones and the data from sites within each zone were pooled to give an estimate of median and variation expected within a zone. These zones are indicated in Figure 5.1 by the following acronyms: NW=North West-Basin; SW=South West-Basin; NWC=Northwest Central-Basin; SWC=Southwest Central-Basin; SC=South Central-Basin; and NE=North East-Basin. Figure 5.1 also expresses the availability of measurements for zooplankton at each site. For example, both sites in the East basin have between 36 and 80 measurements available for each of the two zooplankton groups. A site with only 1 to 5 measurements was likely only sampled once or a few times in one year whereas a site with many measurements may have been sampled for several, but not necessarily all, of the years between 1997 and 2006. Within one season, a site may have been sampled once or several times.

The LEB and LEPAS zooplankton biomass is reported as a concentration of dry weight: $\mu\text{gDW L}^{-1}$. Zooplankton results computed by CAEDYM are reported in units of carbon: $\mu\text{gC m}^{-3}$. To compare measured zooplankton to modelled zooplankton, measured values were converted to $\mu\text{g m}^{-3}$ and multiplied by a factor of 0.48, which is a typical carbon content in crustacean zooplankton (Andersen and Hessen, 1991).

5.2 Modelled zooplankton in the ELCD Lake Erie model

5.2.1 The zooplankton set-up in the existing ELCD Lake Erie model

Two zooplankton groups, cladocerans and copepods, were added to the existing ELCD_LE model. The CAEDYM submodel for zooplankton requires that several zooplankton parameters are defined for each group modelled and that initial concentration profiles and inflow concentrations are included as with other CAEDYM state variables. The parameter choices for these groups were selected based on a literature review (presented in Table 4-4). The incoming concentration of zooplankton from rivers was considered negligible (Mion et al. 1998), so inflow concentrations were set to zero. Initial values were estimated based on Barbiero et al.'s 1998 survey (2001), which has measurements from earlier in the season than LEB or LEPAS data, and extrapolating the trends for early April from the LEB and LEPAS data.

Initial uncalibrated zooplankton modelling attempts produced impossibly low zooplankton estimates, especially in the West end of the lake, which did not agree well with the data; very low peak concentrations occurred in April or May and the modelled cladocerans all but disappeared after that. The initial modelling of copepods was less of a failure as it did predict more reasonable peak

timing, but the magnitudes of concentration were also much too low. It was clear that the parameters affecting zooplankton required calibration. Since so many factors were likely to affect the concentrations of both zooplankton groups, the sensitivity analysis presented in Chapter 4 was used to guide the calibration of parameters to produce more reasonable simulations of cladocerans (Z1) and copepods (Z2).

5.2.2 Sensitivity screening results applied to initial calibration efforts

As a starting point, the modelled zooplankton results from the 3680 simulations in the DYCD West Basin sensitivity screening experiment were mined to find a parameter setup that gave reasonable maximal seasonal zooplankton concentrations that occurred around late June. There were only a few sets of runs that satisfied these criteria for both zooplankton groups since many of the zooplankton results from the screening were invalid (due to zooplankton not growing beyond their initial value). The most promising parameter set from the DYCD experiment was applied to the ELCD model. This presented a significant improvement over initial attempts to incorporate zooplankton prior to the sensitivity analysis, but still required more calibration. The sensitivity analysis was used to guide the subsequent manual adjustments to the parameter configurations. Significant parameters such as internal phosphorus concentration (k_{ZIP} or Z-26), standard temperature for the temperature function (T_{sta} or Z1-28), the maximum grazing rate (ki or Z-31), the half saturation constant for grazing (kj or Z-33), the coefficient for loss to respiration (k_{RZ} or Z2-21), and the initial value ($iniZ2$ or Z2-34) were altered to shift the applicable zooplankton group in a more desirable direction. For instance, to address the issue that cladocerans (Z1) were not reaching high enough peak concentrations, $ki-Z1$ might be increased or $kj-Z1$ decreased. Calibration is not complete yet, but plausible ranges of concentrations and seasonal patterns for zooplankton have emerged; the best results to date, in terms of zooplankton, are presented in this chapter.

The 91 parameters that were evaluated in Chapter 4 are presented in Table 5-1 (phytoplankton parameters), Table 5-2 (zooplankton parameters), and Table 5-3 (other parameters) with the set of values used in the model run discussed in this chapter. The ID numbers and parameter names are consistent with the introduction of these parameters in Tables 4-2, 4-4, and 4-5. The values for these parameters that were taken directly from the best run from the sensitivity analysis are shown in the tables under "SA value". Parameters that were manually calibrated are indicated by the final altered numbers in the "final value" column of the tables. The complete CAEDYM parameters file, which includes these 91 parameters as well as other parameters that were not included in the sensitivity screening, is provided in Appendix C.

The rest of Chapter 5 displays results from this recent simulation compared with data pooled by the zones delineated in Figure 5-1.

5-1 Phytoplankton parameter values used in the semi-calibrated model simulation presented in this chapter. ID numbers are those used in the sensitivity analysis presented in Chapter 4. "SA" value indicates the initial parameter configuration used from the best sensitivity analysis run and "Final Value" indicates which parameters were manually altered in calibration.

ID	Name	Units	Description	SA Value	Final Value
1	μ_{max} -P4	/d	Max potential growth rate of phytoplankton.	0.6	Same
1	μ_{max} -P5			0.6	Same
1	μ_{max} -P6			1.6	Same
2	$Y_{C:Chla}$ -P4	mgC/ mgChla	Average ratio of carbon to chlorophyll a	40.0	Same
2	$Y_{C:Chla}$ -P5			40.0	Same
2	$Y_{C:Chla}$ -P6			80.0	Same
3	I_k -P4	uE/ (m ² s)	Parameter for initial slope of P-I curve	108.	Same
3	I_k -P5			65.0	Same
3	I_k -P6			68.3	Same
4	K_p -P4	mg/ L	Half saturation constant for phosphorus	0.01	Same
4	K_p -P5			0.00	Same
4	K_p -P6			0.03	Same
5	K_N -P4	mg/ L	Half saturation constant for nitrogen	0.03	Same
5	K_N -P5			0.04	Same
5	K_N -P6			0.06	Same
6	$Sicon$ -P6	mgSi/ mgChla	Constant internal silica concentration	93.3	Same
7	K_{Si} -P6	mg/L	Half saturation constant for silica	0.09	Same
8	IN_{MIN} -P4	mgN/ mgChla	Minimum internal nitrogen concentration	2.2	Same
8	IN_{MIN} -P5			0.5	Same
8	IN_{MIN} -P6			1.8	Same
9	IN_{MAX} -P4	mgN/ mgChla	Maximum internal nitrogen concentration	7.0	Same
9	IN_{MAX} -P5			2.0	Same
9	IN_{MAX} -P6			4.7	Same
10	IP_{MIN} -P4	mgP/ mgChla	Minimum internal phosphorus concentration	0.17	Same
10	IP_{MIN} -P5			0.12	Same

ID	Name	Units	Description	SA Value	Final Value
10	IP_{MIN-P6}			0.25	Same
11	IP_{MAX-P4}			5.0	Same
11	IP_{MAX-P5}	mgP/ mgChla	Maximum internal phosphorus concentration	1.5	Same
11	IP_{MAX-P6}			2.5	Same
12	$\mathcal{G}-P4$				1.06
12	$\mathcal{G}-P5$	--	Temperature multiplier	1.06	Same
12	$\mathcal{G}-P6$			1.05	Same
13	T_{sta-P4}				23.0
13	T_{sta-P5}	°C	Standard temperature	16.0	Same
13	T_{sta-P6}			4.0	Same
14	T_{opt-P4}				31.5
14	T_{opt-P5}	°C	Optimum temperature	18.0	Same
14	T_{opt-P6}			12.8	Same
15	T_{max-P4}				40.5
15	T_{max-P5}	°C	Maximum temperature	26.0	Same
15	T_{max-P6}			21.8	Same
16	$kr-P4$				0.14
16	$kr-P5$	/d	Respiration and mortality rate coefficient	0.08	0.10
16	$kr-P6$			0.08	0.10
17	\mathcal{G}_R-P4				1.03
17	\mathcal{G}_R-P5	--	Temperature multiplier for T2 function (used in respiration)	1.06	Same
17	\mathcal{G}_R-P6			1.13	Same
18	$f_{resp-P4}$				0.52
18	$f_{resp-P5}$	--	Fraction of respiration relative to total metabolic loss rate	0.65	Same
18	$f_{resp-P6}$			0.28	Same
19	f_{dom-P4}				0.30
19	f_{dom-P5}	--	Fraction of metabolic loss rate that goes to DOM (rest to POM)	0.50	Same
19	f_{dom-P6}			0.37	Same

5-2 Zooplankton parameter values used in the semi-calibrated model simulation. Initial parameter configuration used from the best sensitivity analysis run are shown in "SA value" and "Final Value" indicates which parameters were manually altered in calibration.

ID	Name	Units	Description	SA Value	Final Value
20	A_z -Z1	--	Messy feeding; portion of food reaching the mouth	0.90	Same
20	A_z -Z2			0.90	Same
21	k_{Rz} -Z1	/d	Respiration rate coefficient	0.14	Same
21	k_{Rz} -Z2			0.06	0.09
22	k_{Mz} -Z1	/d	Mortality rate coefficient	0.01	Same
22	k_{Mz} -Z2			0.01	Same
23	k_{Fz} -Z1	--	Fecal pellet fraction of Grazing	0.05	Same
23	k_{Fz} -Z2			0.15	Same
24	k_{Ez} -Z1	--	Excretion fraction of grazing	0.05	Same
24	k_{Ez} -Z2			0.15	Same
25	k_{ZIN} -Z1	mgN/ mgC	Internal nitrogen to carbon ratio	0.19	Same
25	k_{ZIN} -Z2			0.12	Same
26	k_{ZIP} -Z1	mgP/ mgC	Internal phosphorus to carbon ratio	0.029	0.027
26	k_{ZIP} -Z2			0.023	Same
27	ϑ_T -Z1	--	Temperature multiplier in $f(T_1)$	1.10	Same
27	ϑ_T -Z2			1.05	Same
28	T_{sta} -Z1	°C	Standard temperature	18.0	Same
28	T_{sta} -Z2			13.0	Same
29	T_{opt} -Z1	°C	Optimum temperature	21.0	Same
29	T_{opt} -Z2			13.0	Same
30	T_{mx} -Z1	°C	Maximum temperature	32.0	34.0
30	T_{mx} -Z2			33.0	Same
31	k_i -Z1	(gPhyCm ⁻³)/ (gZCm ⁻³)/d	Maximum grazing rate	2.80	2.40
31	k_i -Z2			1.17	Same
32	ϑ_Z -Z1	--	Temperature dependence $f(T_2)$ for respiration	1.07	Same
32	ϑ_Z -Z2			1.04	Same
33	K_j -Z1	gC/m ³	Half saturation constant for grazing	0.43	0.35
33	K_j -Z2			0.27	0.30
34	$iniZ1$	mgC/ L	Initial concentrations zooplankton groups.	0.000	Same
34	$iniZ2$			0.000	0.0008

5-3 Other parameter values used in the semi-calibrated model simulation. Initial parameter configuration used from the best sensitivity analysis run are shown in "SA value" and "Final Value" indicates which parameters were manually altered in calibration.

ID	Name	Units	Description	SA Value	Final Value
35	<i>POP1-max</i>	/d	Maximum transfer rate of POC--> DOC	0.06	Same
36	<i>PON1-max</i>	/d	Maximum transfer rate of PON--> DON	0.01	Same
37	<i>POM-Dia</i>	m	Diameter of POM	0.000005	Same
38	<i>POM-Dens</i>	kg/m ³	Density of POM	1020.0	Same
39	<i>Tc-POM</i>	N/m ²	Critical shear stress for POM	0.003	Same
40	<i>dens-SS1</i>	kg/m ³	Density of suspended solid (SS) particles	3091.7	Same
41	<i>dia-SS1</i>	M	Diameter of suspended solids	0.000003	Same
42	<i>cShear-SS1</i>	N/m ²	Critical shear stress for SS	0.0083	Same

5.3 Current calibration results: spatial distribution of zooplankton

The spatial variation in measured and modelled zooplankton concentrations is compared in this section. Variation in depth was not considered since measured data was given as a vertically averaged concentration; therefore, modelled zooplankton is also presented as vertically averaged concentrations. The variation in modelled zooplankton output throughout the lake near in the last week of each month simulated is presented along with zooplankton measurements that were made within the last week of that month between 1997 and 2006 (the years for which data were available). The zones discussed in section 5.1 are again delineated on the ELCD output sheets to facilitate the comparison with the data from those zones.

5.3.1 Last week in May

Modelled zooplankton results from the last week in May are presented with the concentrations of zooplankton measured within the last week of May in Figure 5-2. The box plots indicate the 25th to 50th percentile (light grey) and 50th to 75th percentile (dark grey) of the measurements, which were taken in a given zone during that week in any of the years between 1997 and 2006. Error bars show the total variation of the measurements. Fewer measurements were available in May than in later months. Since only a few measurements were available in each of the zones, the box plots are rough estimates of the expected variation in concentration of zooplankton at this time of year. Measured values were typically well under 0.04µg m⁻³, except in the South Central Basin where more variation was observed for both zooplankton groups. The NW basin had the most available measurements and a modest amount of variation between zero and 0.04µg m⁻³.

Modelled cladoceran concentrations throughout the lake were uniformly less than $0.01 \mu\text{gC m}^{-3}$, which is appropriate given the data available except in the SC zone where higher concentrations and variability would have been more consistent with measured cladocerans. Modelled copepod concentrations were generally between zero and $0.02 \mu\text{gC m}^{-3}$; the modelled copepods were slightly more successful than cladocerans in the South and Southwest parts of the central basin. These results are generally consistent with what data is available at this point in the simulation, but again, higher and more variable concentrations in the SC zone would have been more consistent with copepod observations.

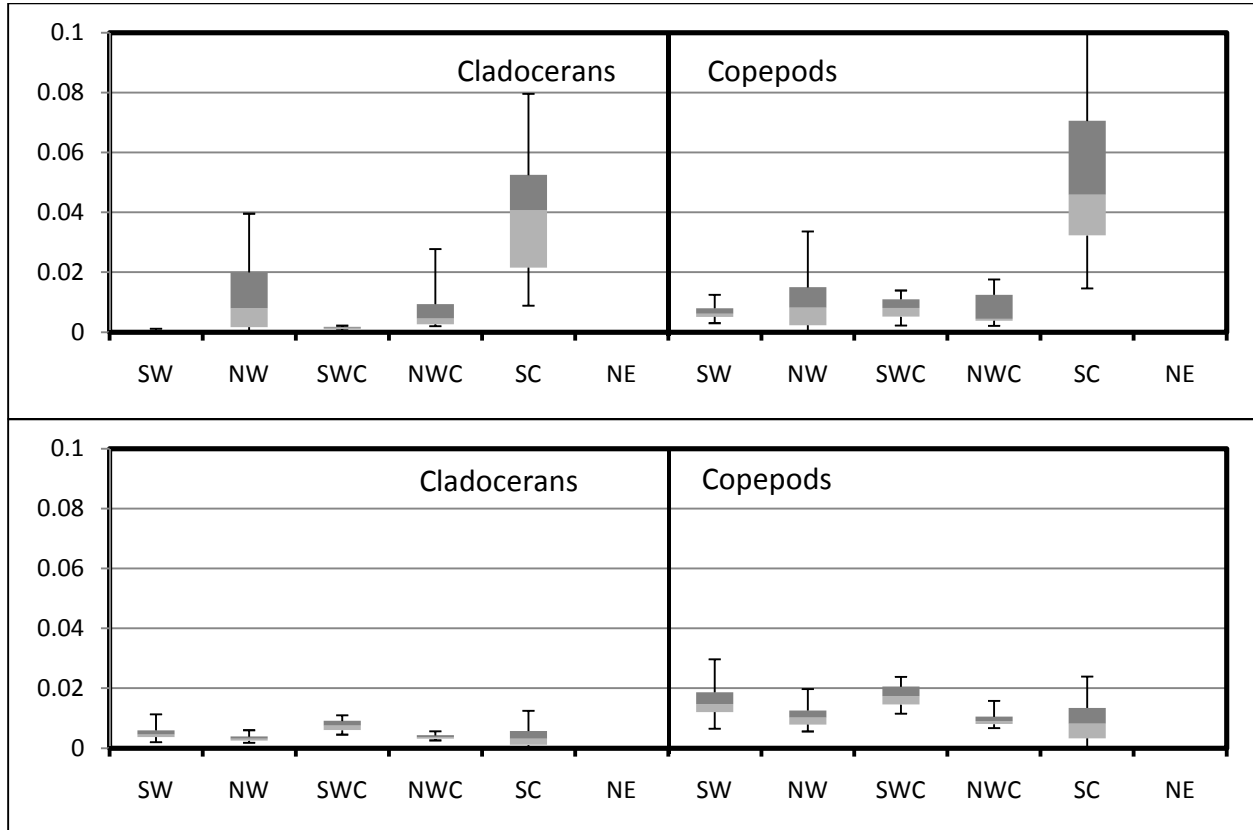


Figure 5-2 Spatial distributions of measured cladocerans and copepods (top left and right) and computed cladocerans and copepods (bottom left and right) grouped by zone during the last week of May. Concentrations are in $\mu\text{gC/m}^3$.

5.3.2 Last week in June

Figure 5-3 presents the modelled zooplankton results from the last week of June and the concentrations of zooplankton measured within the last week of June. Data are presented in a similar fashion as in Figure 5-2.

Again, given the measured data, the results for both zooplankton groups should generally be low (under $0.04 \mu\text{gC m}^{-3}$) with somewhat higher and more varied concentrations for cladocerans in June than in May. Measured values indicate that by the end of June the cladocerans should be as successful

as copepods and may even have a slight advantage over copepods, particularly in the West half of the lake. These data do not support the modelled result in which copepods were distinctly more successful than cladocerans in the West end of the lake. The low values of cladocerans and the slight variation in concentrations seen in modelled results are similar to available measured values, but copepods are predicted to be more successful than the data suggest, with concentrations often exceeding $0.05 \mu\text{gC m}^{-3}$ in the West end.

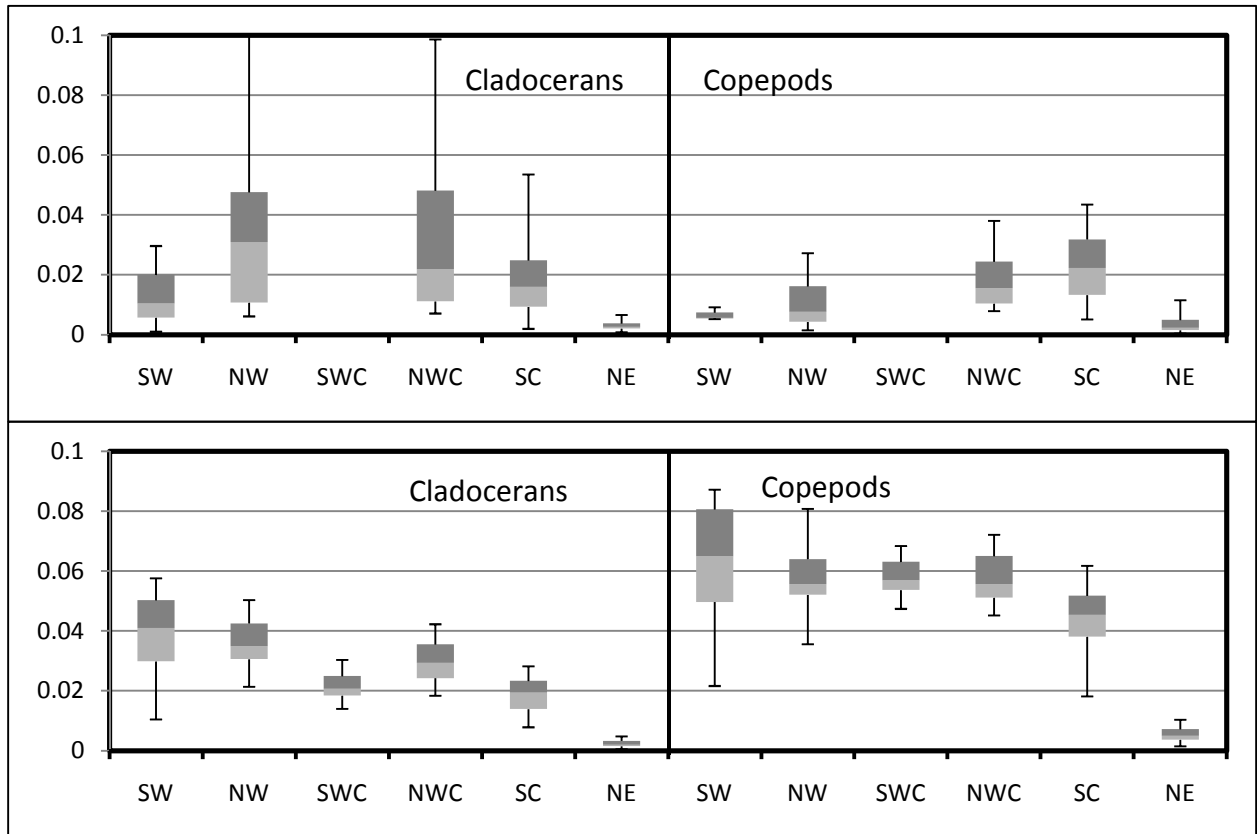


Figure 5-3 Spatial distributions of measured cladocerans and copepods (top left and right) and computed cladocerans and copepods (bottom left and right) grouped by zone during the last week of June. Concentrations are in $\mu\text{gC/m}^3$.

5.3.3 Last week in July

Measured zooplankton concentrations from the last week in July are shown above computed concentrations in Figure 5-4 with the same format as in Figure 5-2. More measured values were available at this time of the season. Measurements indicated a much higher degree of variability in both groups and generally higher concentrations of cladocerans throughout the lake. Note that a different scale ($0-0.2 \mu\text{gCm}^{-3}$) was used to show the variability of measured data.

The most notable error in the simulation at this time is that higher and more variable densities for both cladocerans and copepods are not seen in the modelled SWC basin. Furthermore, the cladocerans throughout the lake are generally unsuccessful (near zero concentration) when there

should be much higher concentrations (above $0.04 \mu\text{gCm}^{-3}$) in the west half of the lake and along the south shore. Modelled copepod concentrations generally appear to be in the right ranges, but the model is not exhibiting much of the variability in the SW basin that is indicated by measured values.

Unexpected results are seen at the mouth of the Detroit River in the North West corner of the West Basin (not included in the zones shown), but not enough data were available for comparison. It appears that the inflow characteristics from the Detroit River are providing modelled zooplankton with a more favourable environment than the surrounding basin.

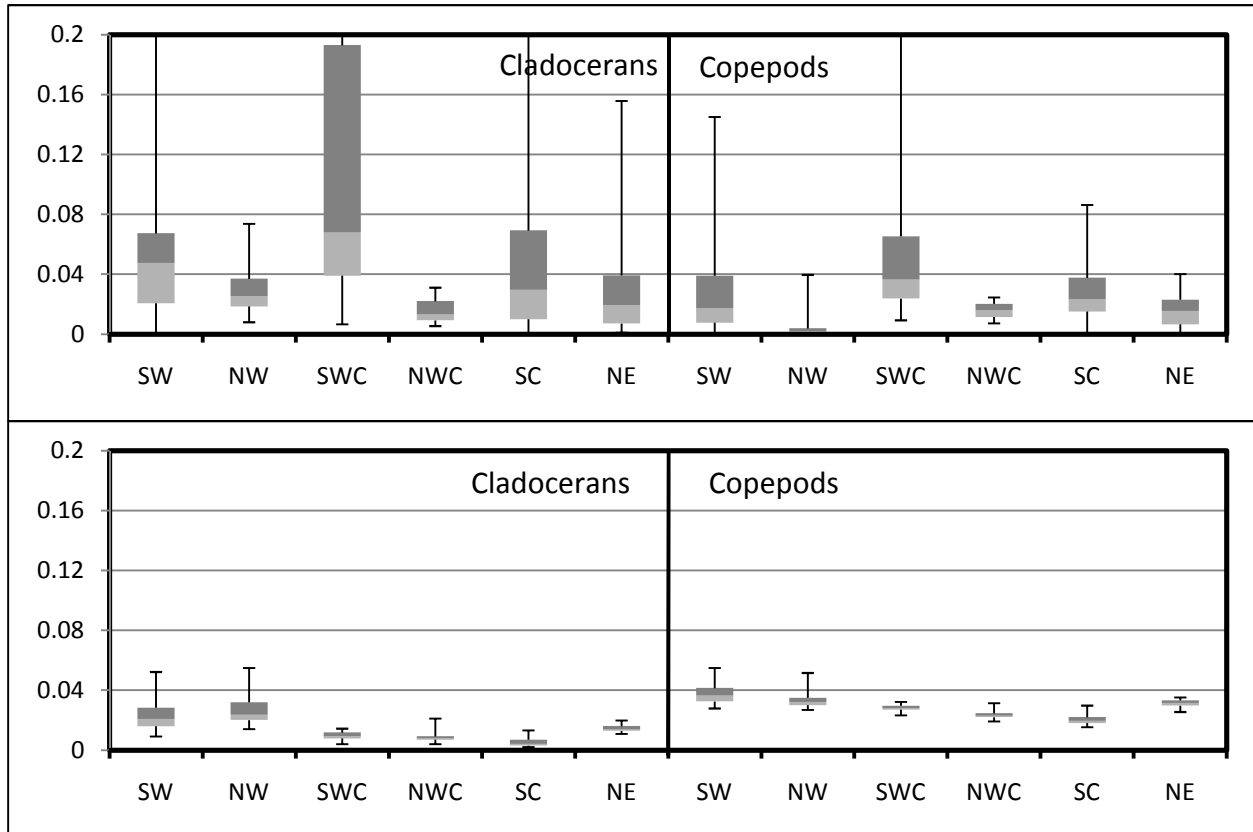


Figure 5-4 Spatial distributions of measured cladocerans and copepods (top left and right) and computed cladocerans and copepods (bottom left and right) grouped by zone during the last week of July. Concentrations are in $\mu\text{gC}/\text{m}^3$.

5.3.4 Last week in August

Modelled results and zooplankton measurements for the final week of the simulation – the last week in August – are presented in Figure 5-5 with the same format as the foregoing sections. By the end of the simulation, copepods are still generally more successful than cladocerans, which is not supported by the data. Modelled cladocerans appear a little low in the SW and SWC basins, but otherwise seem to be in range of measured concentrations.

Both groups appear to enjoy much higher concentrations at the mouth of the Detroit River (not shown) than at any other time or location in the simulation. Measured data are not available to confirm this; but it is not likely accurate. Further calibration will require reviewing the conditions modelled in the West Basin compared to the inflow characteristics of the Detroit River towards the end of the simulation to determine why there is a hot spot there.

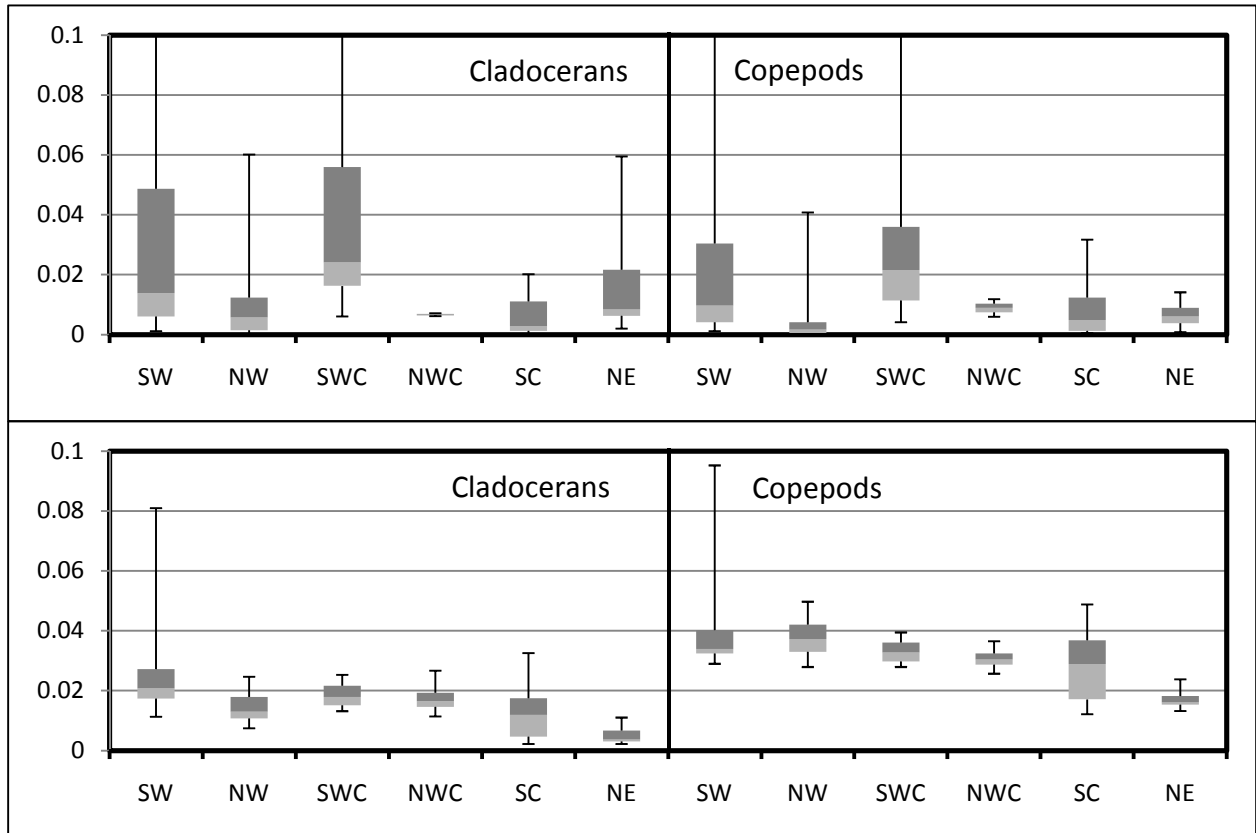


Figure 5-5 Spatial distributions of measured cladocerans and copepods (top left and right) and computed cladocerans and copepods (bottom left and right) grouped by zone during the last week of August. Concentrations are in $\mu\text{gC}/\text{m}^3$.

5.4 Current calibration results: temporal distribution of zooplankton

This section presents the temporal distribution of zooplankton at each zone. Measured data are presented in a consistent fashion as section 5.3. To show modelled results over time, vertically averaged profiles at a few locations within a zone are presented with the measured data.

5.4.1 West Basin (NW and SW)

Measured data in the West Basin, grouped by week and zone, for cladocerans and copepods are presented with modelled profiles in Figure 5-5. Each bar (25th to 75th percentile of observations) and its range (shown by error bars) represents all observations available between 1997 and 2006 in a

given zone for a particular week in the season. Again, numbers above the error bars indicate how many measurements were available for that week. Measurements that were specifically taken in 2002 are indicated by the dots. The lines show vertically averaged computed results at various sites within the given zone to give an impression of the variability of predicted concentrations over time.

Predicted values for cladocerans are within the range of measurements, but copepods are generally overestimated, especially in the NW basin. In the NW basin, the timing of predicted cladoceran growth is encouraging, but in the SW basin, their early success in the model appears to be premature.

The modelled results presented here, with reasonable seasonal patterns and concentration ranges that are within realistic ranges represent, a major improvement over modelling attempts prior to the sensitivity analysis.

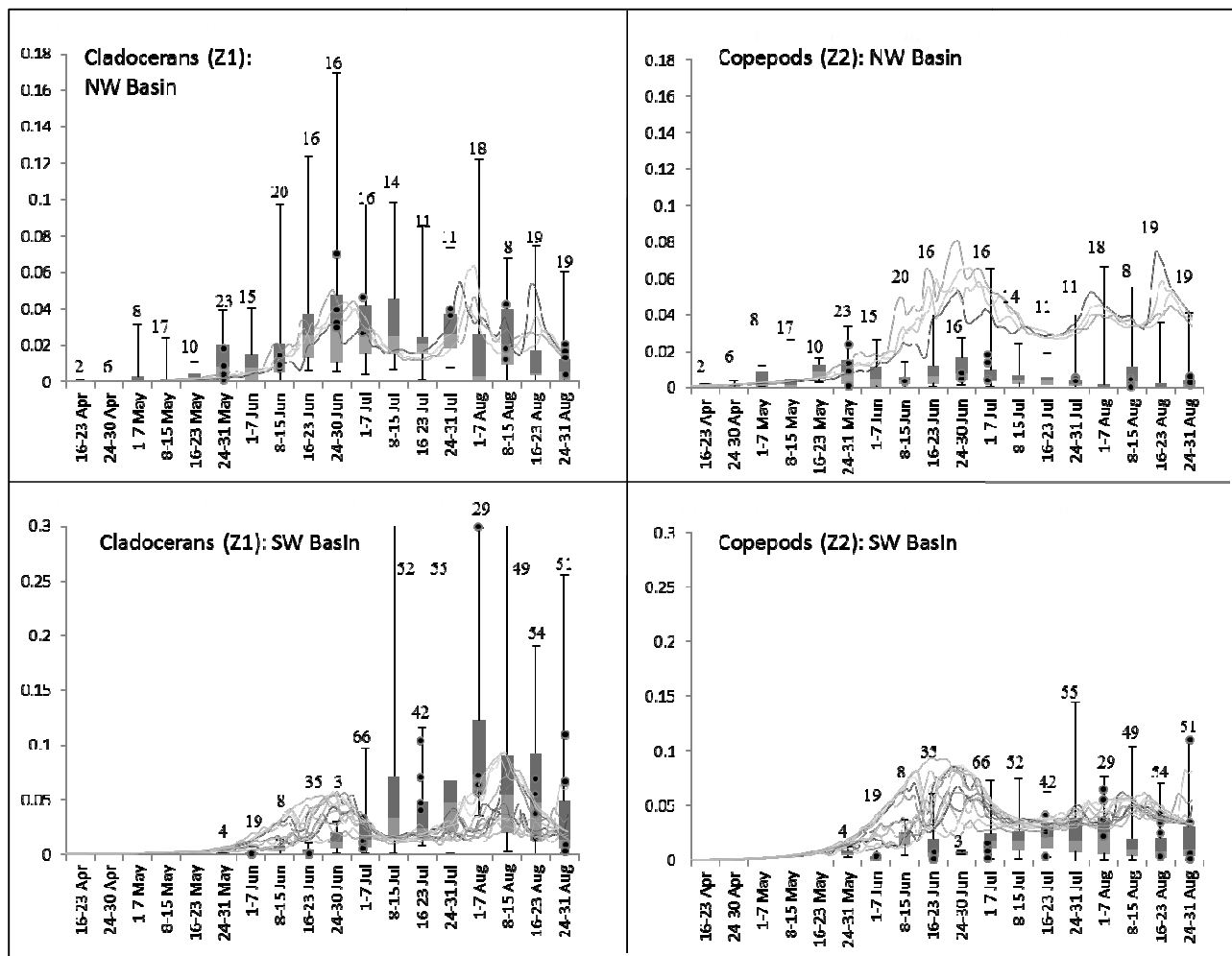


Figure 5-6 Computed cladoceran (left) and copepod (right) concentrations (grey lines, $\mu\text{gC}/\text{m}^3$) throughout the simulated season at sites within a specified zone in the West Basin. Top: North end of the West basin; Bottom: South end of the West Basin. Grey boxes: 25th to 50th and 50th to 75th percentile of measured data available in the given zone. Dots: measurements from 2002.

5.4.2 Central Basin (NWC, SWC and SC)

Measured data in the Central Basin, grouped by week and zone, for cladocerans and copepods are presented with modelled profiles in Figure 5-6 using the same format as in Figure 5-5.

Unfortunately, only two sites with zooplankton measurements were available in the NWC zone, but there were a few measurements available in every week from the end of May to the end of August. Many of these data were from 2002 (the dots in Figure 5-6). The cladocerans reach peak concentrations in this zone in late June/early July and their concentration declines subsequently from late July to early August. Cladocerans rise again in concentration towards the middle of August. Predicted cladocerans profiles in the NWC zone also exhibit a peak-decline-peak pattern consistent with the observations. Observed copepods also appear to peak in late June, but if there is a subsequent decline and resurgence it is subtler. Copepod concentrations in this zone appear to be generally lower than cladocerans. The predicted copepod profiles resemble the observations of cladocerans more so than the observations of copepods as the peak-decline-peak pattern is too distinct and concentrations are somewhat too high.

The highest variation and magnitudes in measured zooplankton concentrations are seen in the SWC zone (note the scales in Figure 5-6). In this section, modelled copepods are actually not overestimated; they are within the commonly observed ranges of observation, although, the distinct peak-decline-peak pattern modelled in this zone is not well supported by the observations. Modelled cladoceran profiles are the least accurate in the SWC basin; concentration profiles are far too low and the predicted two-peak pattern is not supported by the data. Cladoceran measurements in this zone are surprising because an appreciable increase in measured concentrations does not occur until July, after which point cladocerans remain abundant. Modelled profiles do not capture the timing of that growth or the magnitude and variability of cladocerans in the late summer. As the lakewide model is improved with further calibration, this zone will likely remain the most difficult to simulate.

The simulated cladoceran profiles in the SC basin are also too low given the data, but the timing of the peak is better. Copepod predictions along the SC zone are well within the commonly observed ranges and the timing was realistic, although they should probably peak a little sooner in late May.

Apart from the underproductive predicted cladocerans along the south and southwest zones, magnitudes and patterns in the Central basin are also realistic. This is encouraging given that the sensitivity analysis and calibration efforts were geared towards the results in the West Basin.

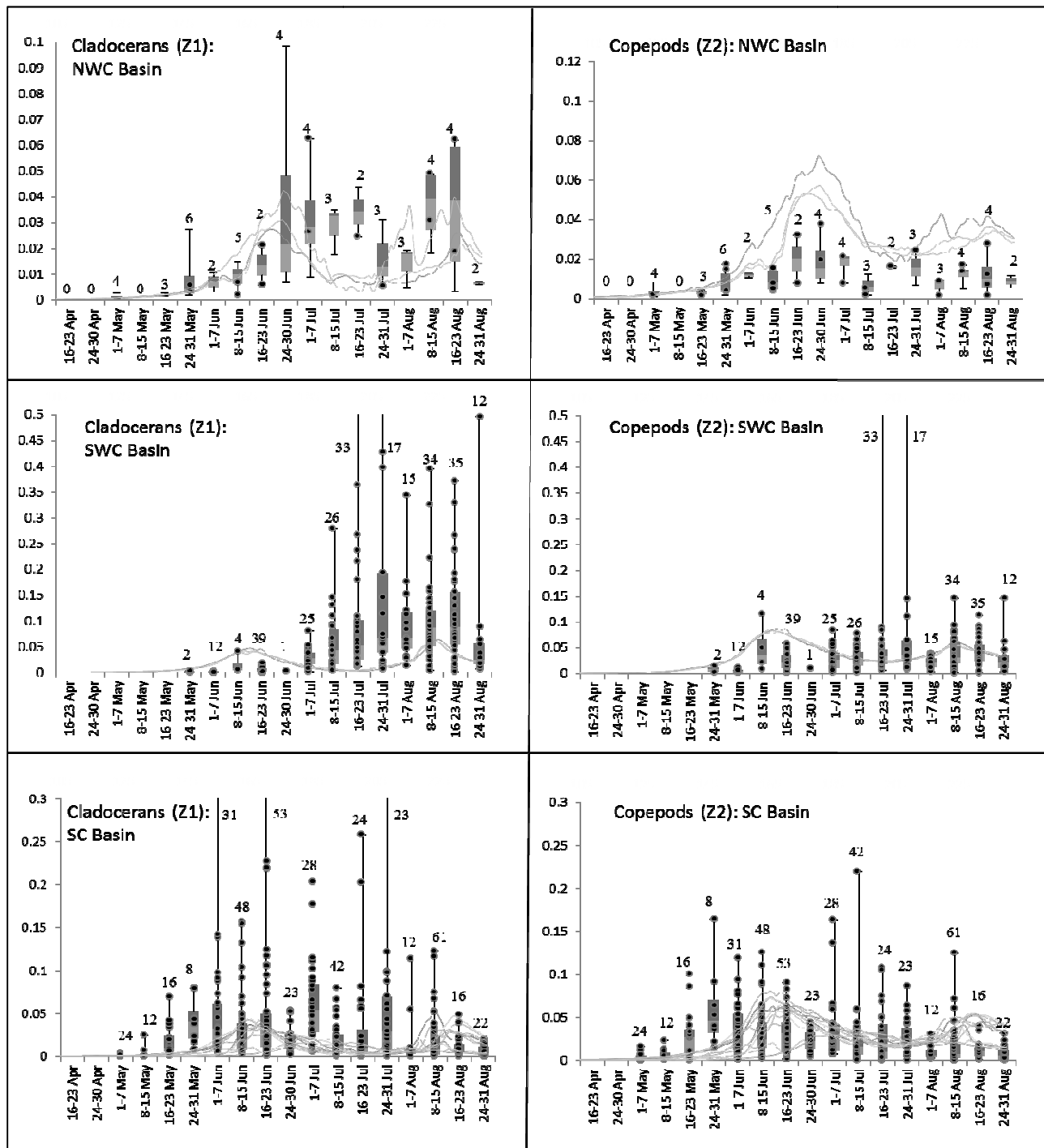


Figure 5-7 Computed cladoceran (left) and copepod (right) concentrations (grey lines, $\mu\text{gC}/\text{m}^3$) throughout the simulated season at sites within a specified zone in the Central Basin. Top: North West end of the central basin; Middle: South West zone; Bottom: South shore zone. Grey boxes: 25th to 50th and 50th to 75th percentile of measured data available in the given zone. Dots: measurements from 2002.

5.4.3 East Basin (NE)

Measured data in the NE zone of the East Basin, grouped by week, for cladocerans and copepods are presented with modelled profiles in Figure 5-7 using the same format as in Figure 5-5. Only two sites were available in this zone, as in the NWC zone, but again at least a few measurements were available for all weeks. Like measured values, modelled zooplankton concentrations in the NE zone are near zero until early July where they gradually increase to peak in the latter half of July. Except for the anomalous two cladoceran measurements during the week of August 8, predicted cladoceran profiles were all within measured ranges. Peak copepod concentrations were again too high in this zone. In general, predicted concentrations and seasonal patterns resemble the available data in this zone, which is the furthest zone from the West Basin for which calibration efforts were targeted.

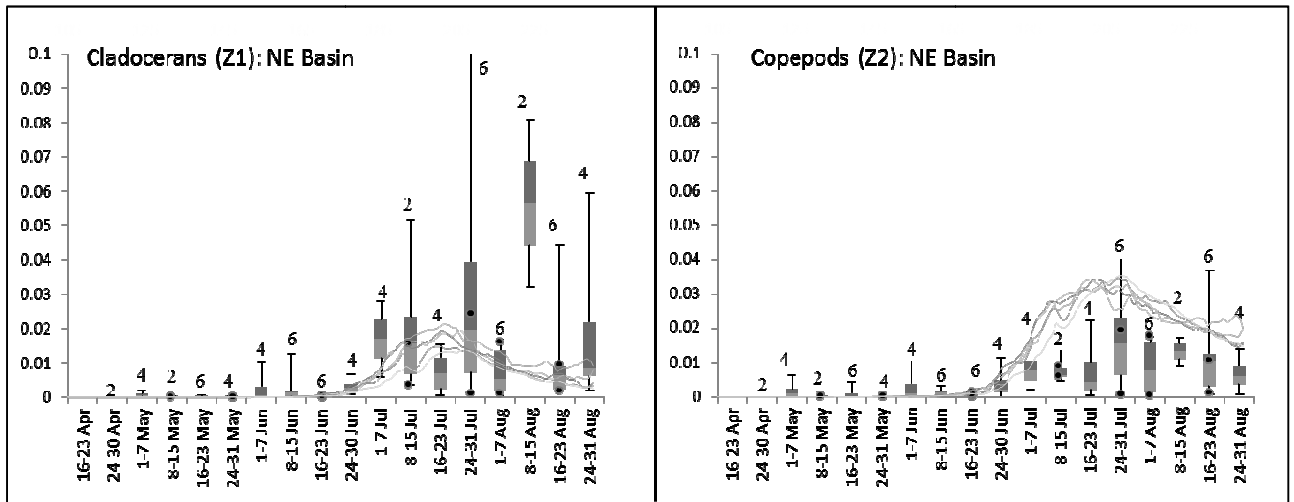


Figure 5- Computed cladoceran (left) and copepod (right) concentrations (grey lines, $\mu\text{gC}/\text{m}^3$) throughout the simulated season at sites within a specified zone in the East Basin zone. Grey boxes: 25th to 50th and 50th to 75th percentile of measured data available within the East zone. Dots: measurements from 2002.

5.5 Discussion

Since performing the sensitivity analysis, calibration efforts have resulted in predicted zooplankton concentrations and seasonal patterns that are close to observations throughout the lake, except for cladocerans in the SW and SWC zones. Overall, modelled copepods were too abundant compared to modelled cladocerans. Further calibration is needed to address this problem.

The sensitivity analysis and much of the rough calibration efforts for CAEDYM parameters were conducted using the DYCD model of the West Basin. When DYCD results returned plausible West Basin concentrations and seasonal patterns, the parameter configurations were ported to ELCD. ELCD zooplankton results, even in the middle of the West Basin which most closely resembled the DYCD conditions, were not identical to DYCD results and they were not expected to be due to the complexity of physical and bio-chemical processes modelled in three dimensions. Nevertheless, DYCD was a useful tool to estimate the seasonal patterns that a change in the CAEDYM configuration would produce in the West Basin of the ELCD model. Although calibration was geared

towards the West Basin, predicted ELCD zooplankton results were often as good or better in other zones of the lake.

In the NW and NWC basins, the measured data and predicted profiles suggest that zooplankton concentrations peak in June, decline in July and partially recover in August. Modelled results are consistent with the presence of a clear-water phase. The clear-water phase refers to the increased transparency of water that accompanies a severe decline in phytoplankton in eutrophic or mesoeutrophic lakes (Wetzel 2001, p 441), such as the West end of Lake Erie. Herbivorous zooplankton – especially daphnids (the major contributor to cladoceran biomass) – play a significant role in this decline (Kalf 2002, p388). In late spring or early summer as temperatures warm and algae is abundant, zooplankton biomass reaches its maximum. The grazing pressure imposed on algae contributes to a decline in algal biomass (hence the clear-water phase) and, in turn, the decline in available food results in a marked decline in zooplankton biomass. Zooplankton concentrations increase again as the edible algal populations recover. As the lake turns over in the fall and the water cools, diatoms would become more abundant again and it is expected that the zooplankton presence would remain strong well into the fall months.

The predicted concentration profiles of zooplankton throughout the season displayed plausible seasonal patterns in most of the zones. It is difficult to assess the success of the model in July and August in all southern zones because the data are so varied; to that end the model did not capture that variability well. The model performed quite poorly in the SW and SWC zones especially for cladocerans: measured cladoceran concentrations remain low until July with high values occurring in late July through August, whereas modelled cladocerans peak in June, decline in July, and resume high concentrations in August. The mismatch between the model and data in the first few months may indicate a much higher prevalence of walleye larvae in this part of the lake. Walleye larvae (and other zooplanktivores) are not directly simulated in the Lake Erie ELCD model. Their grazing effect on zooplankton is simplistically modelled through a temperature function multiplied by a loss term that is applied uniformly throughout the lake. It is believed that most of the walleye harvested in the West and Central basins originated in three major spawning areas: the Maumee River, the Sandusky River, and the mid-lake reef complex in the South half of the West Basin (Jones et al., 2003) so it is reasonable to expect higher concentrations of walleye larvae in this part of the lake (in the SW and SWC zones) during the spring and early summer. Qin and Culver (1995) demonstrated that the concentration of stocked walleye larvae in ponds had significant impacts on cladocerans and copepods: in ponds that initially had similar plankton densities, higher concentrations of stocked walleye larvae resulted in lower concentrations of cladocerans and copepods compared to ponds stocked with lower densities of walleye larvae. This also impacted the algal types and densities. It is therefore not surprising that the zooplankton loss term to grazing does not adequately account for the probable higher concentrations of walleye larvae in the southwest end of the lake.

In the Northern zones, predictions of seasonal patterns are much better. The pattern of measured zooplankton in the NE zone is similar to those of the SW and SWC zones (although with much lower concentrations): zooplankton concentrations remain low until July and peak values occur in late July and August. However, unlike the SW and SWC zones, the model correctly predicts low initial concentrations and one late peak. The double peak pattern of zooplankton does not occur in the East end of the lake because it is oligotrophic; plankton are not as productive. The increased plankton

concentrations at the end of the simulation in Lake Erie can be attributed to warmer temperatures and some transfer of nutrients and plankton from the Central basin.

In this semi-calibrated model, copepods were often too successful with peak concentrations exceeding observed ranges in all of the northern zones. Cladocerans were not successful enough in the southern zones. Lakewide patterns (i.e. overly successful copepods and underachieving cladocerans) could benefit from further fine tuning of the parameters discussed in this thesis, but future calibration work may require adjustments to factors not discussed, such as inflow characteristics. The Sandusky River outlets near the SWC zone. Mion et al. (1998) reported such low concentrations of zooplankton in the Sandusky River in April and May that the model assumed no zooplankton in the inflow. It is possible that zooplankton are being seeded into the SWC basin by the Sandusky during the summer and this may contribute to the high peak cladoceran values. Likewise, the Maumee River might be seeding cladocerans into the SW zone in the summer. Other state variable concentrations in the Sandusky inflow could also contribute to higher cladocerans densities in the SWC basin. Further calibration should consider several variables specified in the inflow. This analysis should also include the Detroit River since an unexpected hotspot for zooplankton growth in the model developed at the mouth of the Detroit River. Next steps should involve a comparison between the Detroit River inflow variables applied to the model and the modelled variables adjacent to the Detroit River plume of high zooplankton. The relevant variables are likely temperature and phytoplankton concentrations, but may also include some particulate matter variables and parameters.

The effects of the latest modelling efforts on phytoplankton were not presented here as the first objective was to bring zooplankton concentrations to within measured ranges. Future calibration efforts must consider the effects on total chlorophyll in more detail concurrently with the effects on zooplankton concentrations. Calibrating the model for phytoplankton may improve the simulation of zooplankton as well.

The model presented here was developed based on 2002 conditions because many water quality variables were thoroughly sampled in that year. Vertical hauls of zooplankton – giving depth-averaged concentrations – were taken at discrete coordinates at a few discrete times during the season. Zooplankton were also sampled heavily in 2002 – especially in the south half of the central basin – but the 2002 data alone set could not provide enough of a detailed pattern of spatial and temporal variation in zooplankton concentration to guide calibration. To increase the number of measurements available and better illustrate the seasonal patterns of zooplankton, measured data from 1997 to 2006 were used. Thus the model is theoretical in terms of its applications to 2002 specifically. The magnitude and temporal patterns of zooplankton concentrations vary from year to year. If the model were applied to conditions from another year, the model will provide an estimate of the expected patterns given that year's conditions.

Chapter 6

Conclusions and Recommendations

Simple mass balance models for phosphorus have been useful in guiding policy decisions that led to reduced eutrophication in Lake Erie, but new, confounding threats to the ecological health of Lake Erie continue to appear. Managers continue to need useful tools to better understand the lake. The walleye fishery in Lake Erie is economically very important. Walleye recruitment has been highly variable from year to year since the 1990s. An ecological model that could shed some light on the conditions in which walleye find themselves during their vulnerable larval stage from year to year would be useful.

The ELCOM-CAEDYM model in Lake Erie simulates thermal dynamics, mixing, and several chemical and biological variables (including phosphorus and 5 functional groups of phytoplankton) in three-dimensions. The ecological functions and variables are deeply interconnected; the model is very complex and it is also time-consuming to run (6 days per full simulation). The objectives of this study were to better understand the ELCOM-CAEDYM model of Lake Erie through a sensitivity analysis (SA), which has not been done before for the Lake Erie application, and to explicitly simulate zooplankton in this model for future inferences of walleye habitat.

A local SA was deemed inappropriate because local SA's ignore the possibility of a parameter's effects being correlated to the status of other parameters; local analyses do not interrogate parameter space well so results are biased by the configuration of the baseline chosen. A global analysis, which samples all of the parameter space, would be prohibitively computationally expensive. DYRESM, the one-dimensional counterpart to ELCOM, was coupled with CAEDYM to simulate the West Basin of Lake Erie allowing for vastly faster run times (about 1 minute). The DYCD West Basin model proved to be an extremely useful tool to study ELCD. Of course, DYRESM is very different than ELCOM: DYRESM simulates variables as a function of depth and area: there is no horizontal mixing and results are somewhere between being a profile of a basin average and a profile at the deepest point in the middle of the basin. ELCD output variables profiles (for temperature, Z1, Z2, TP, TChla) from deep stations near the middle of West basin were similar enough to the West-basin-averaged DYCD results in concentration magnitudes and seasonal patterns to justify using DYCD as an efficient surrogate to evaluate the sensitivity of CAEDYM variables to its parameters in Lake Erie.

Parameter ranges were supplied to the sensitivity experiment. These ranges were selected based on literature values, where available, which included both measured observations and calibrated values that were used in similar models. Some parameters, especially those concerning zooplankton and particulate matter, were poorly known. The Morris sensitivity screening method revealed the importance of some parameters that are not well-constrained. Zooplankton were sensitive to almost all of the zooplankton parameters perturbed in the analysis. This may indicate that modelling zooplankton is extremely complex, relying on many dynamic processes, or that evaluated ranges were not constrained well enough. For instance, temperature is certainly a significant factor in the seasonal development of zooplankton and phytoplankton, yet parameters relating temperature to grazing and respiration did not consistently stand out as being highly important in the context of other parameter perturbations. This may be because those parameters were well constrained; the effects of

temperature have been well-studied. The sensitivity results implicating other parameters are valid though because the sensitivity should be subject to the uncertainty of parameter values. Bruce et al (2006) presented a DYRESM-CAEDYM model for Lake Kinneret. They found that many of their diagnostic variables were sensitive to less than 10% of the parameters they evaluated, although, predatory zooplankton was sensitive to most zooplankton parameters. In their analysis, parameters were uniformly varied one-at-a-time from a baseline configuration by +/- 10% regardless of the uncertainty or natural variation in a given parameter. Individual parameter results are therefore easy to compare to one another, but have limited usefulness in the context of different parameter sets. Makler-Pick et al. (in press) performed a rigorous sensitivity analysis on the same model using global methods. Two parameters they noted as being particularly significant were particulate organic matter (POM) diameter and POM density. Makler Pick et al.'s assigned range for POM density was greater than that evaluated in this study (1020 to 2000, compared to 1020-1105 in this study). During some initial attempts using DYCD in Lake Erie with higher POM diameter or density values it was noted that these factors led to precipitously low phosphorus levels and could result in the model crashing before completing. Further review of the limited literature supported using lower ranges (Spillman 2007, Keeger et al. 1997, Wetzel 2001). Modelled particles settle to the sediments according to Stokes' law (CWR, 2006b) wherein the diameter is squared and multiplied by density. An increase in size would therefore significantly accelerate settling, making nutrients less available to phytoplankton uptake. It is a weakness that these parameters are so important since they are not easily measured and not well characterized for Lake Erie specifically. Thus it is difficult to know how important these factors should be.

Another example of sensitivity to a poorly known parameter is the messy feeding parameter. It is not surprising that this parameter had notable impacts on both zooplankton groups since it directly affects their ability to assimilate food. Reducing the uncertainty of this parameter would improve the confidence in the zooplankton assimilation submodel. Other parameters that stood out for being especially significant to zooplankton were: the respiration rate, mortality rate, internal phosphorus to carbon ratio, the temperature multiplier and standard temperature for feeding dynamics, the half saturation constant, and initial values. Most of these are easily explained as they directly aid or impede growth or they directly affect zooplankton losses. Only cladocerans were notably sensitive to initial concentration; this higher sensitivity compared to copepods is due to the lower range assigned to them and the fact that so many simulations predicted no growth of zooplankton beyond initial concentrations. Given these conditions, it is unlikely that seasonal maxima should be terribly sensitive to initial zooplankton values, which is fortunate since measured values of zooplankton in April are scarce. Also not surprising was zooplankton and phytoplankton sensitivity to the maximum grazing rate of the most dominant summer phytoplankton groups ('others' and 'flagellates'), but the sensitivity of zooplankton to the ratio of carbon to chlorophyll a was surprising. There is a good deal of uncertainty associated with that parameter (Conroy, 2005).

The Morris screening method was an appropriate tool to provide information about model sensitivity. The method samples more of parameter space than a local method could, but is still computationally manageable. It must be emphasized that results are only qualitative; they provide a general idea of the sensitivity to given parameters in the context of the parameter value ranges selected. As the matrices are randomly generated (with an optimization algorithm to improve the

diversity of the sampling) different results would be obtained each time a Morris experiment is performed: the ordering of parameters may change given a different matrix selection. It is difficult to know whether evaluating each parameter at 4 levels and the use of 40 matrices (providing 40 elementary effects per parameter from which to sample average and standard deviation of effects) was sufficient. It may be useful to repeat the experiment a few times to produce more confidence in the resulting ordering of parameter importance. A quantitative uncertainty and sensitivity analysis (Monte Carlo filtering or Bayesian analysis) on a smaller, more manageable subset of parameters will provide more than just the parameter effects rankings; it would identify model elements that are most responsible for realistic model simulations (Saltelli et al. 2004).

Another useful aspect of the sensitivity exercise was the volume of results produced by sampling parameter space; the best model realisations of zooplankton taken from this set of 3680 runs provided a starting point for calibration. Prior to the analysis, manual calibration efforts on the time-consuming ELCD model were largely fruitless in generating reasonable zooplankton concentrations and seasonal patterns. The challenge in calibrating for zooplankton was further emphasized by poor zooplankton representations in the vast majority of the 3680 configurations simulated in the analysis.

In addition to enabling the use of a global sensitivity screening method, the DYCD approach is very useful during manual calibration of ELCD. It provides a quick initial estimate of the effects a parameter change will have on ELCD output in the West Basin. Using the best SA realisations and then calibrating zooplankton by manually adjusting the most important zooplankton parameters, as identified by the SA, resulted in zooplankton concentrations and seasonal patterns that were much more consistent with observations than initial modelling attempts.

Modelled zooplankton results were least consistent with observations in the south west area of the lake: zooplankton were overestimated in late June-early July and they subsequently crashed and were underestimated in late July-August. It is supposed that this is due to higher grazing pressure from fish larvae in that area of the lake. Given the current model setup, where zooplankton loss to predations is uniformly characterized throughout the lake by one loss coefficient (albeit mediated by temperature) it is unlikely that the entire lake will be satisfactorily calibrated as far as zooplankton are concerned because predators are not explicitly modelled. As discussed by Qin and Culver (1993) grazing pressure exerted by walleye larvae in the first few months of summer on zooplankton abundance can be significant. Walleye larvae are expected to be most abundant in the south west end of the lake in May-June (Jones et al. 2003) and would therefore likely exert a greater grazing pressure than zooplankton experience elsewhere in the lake. Previous diet studies of larval walleye in western Lake Erie showed that pelagic larval walleye consumed cyclopoid and calanoid copepods and large cladocerans during April, May, and early June (Roseman et al. 2005). Yellow perch and other zooplanktivores may also contribute to increased razing presser at this time of year. If a different mortality coefficient could be assigned in the south west end of the lake then we could test the hypothesis without adding extra complication by explicitly modelling fish.

Mion et al (1998) reported insignificant concentrations of zooplankton in the Sandusky and Maumee rivers in April and May, but no data were presented after that. If zooplankton are being seeded from the Sandusky and Maumee rivers in the latter summer months, accounting for this influx could further improve the simulation of zooplankton concentration along the south shore in the West and Central basins. The Maumee and Sandusky rivers (as well as other rivers) should be re-evaluated for the possibility that they are contributing significant zooplankton concentrations after May. The accuracy of the simulations in July and August is not of great importance since the critical walleye

larval period where feeding on zooplankton is significant lasts only up to June, but to get a good model fit with data through the end of August would be gratifying and would increase the confidence in the model's credibility.

Although it is anticipated that the south west seasonal zooplankton patterns will not be substantially improved through parameter calibration, further calibration is needed since copepods are overestimated and cladocerans underestimated in much of the rest of the lake; this problem can likely be addressed through continued calibration. Phytoplankton groups must also be calibrated simultaneously to ensure that they are still operating within reasonable concentrations given more successful zooplankton simulations.

Bibliography

- Andersen, T., Hessen, D.O. 1991. Carbon, Nitrogen, and Phosphorus Content of Freshwater Zooplankton. *Limnology and Oceanography*. 36:807-814.
- Antenucci, J.P., R. Alexander, J.R. Romero, & J. Imberger. 2003. Management strategies for a eutrophic water supply reservoir – San Roque, Argentina. *Water Sci. Technol.* 47:149-155.
- Arhonditsis, G.B., and M.T. Brett. 2005. Eutrophication model for Lake Washington (USA) Part I. Model description and sensitivity analysis. *Ecol. Mod.* 187:140-178.
- Atanasova, N, L. Todorovski, S. Džeroski & B. Kompare. 2006. Constructing a library of domain knowledge for automated modelling of aquatic ecosystems. *Ecol. Mod.* 194(1-3): 14-36.
- Barbiero, R.P., Little, R.E., Tuchman, M.L. 2001. Results from the U.S. EPA's Biological Open Water Surveillance Program of the Laurentian Great Lakes: III. Crustacean Zooplankton. *J Great Lakes Res.* 27:167-184.
- Bierman, V.J. Jr., & D.M. Dolan. 1981. Modeling of phytoplankton-nutrient dynamics in Saginaw Bay, Lake Huron. *J. Great Lakes Res.* 7:409-439.
- Bierman, V.J. Jr., J. Kaur, J.V. DePinto, & T.J. Feist. 2005. Modeling the role of zebra mussels in the proliferation of blue-green algae in Saginaw Bay. *J. Great Lakes Res.* 31:32-55.
- Bowers, J.A. 1979. Chapter 3: Zooplankton grazing in simulation models: the role of vertical migration. In D. Scavia and A. Robertson (Eds.) *Perspectives on Lake Ecosystem Modeling* (pp. 53-73). Ann Arbor: Ann Arbor Science Publishers Inc.
- Bruce, L.C., D. Hamilton, J. Imberger, & G. Gal. 2006. A numerical simulation of the role of zooplankton in C, N and P cycling in Lake Kinneret. *Ecol. Mod.* 193:412-436.
- Campolongo, F., J. Cariboni, A. Saltelli. 2007. An effective screening design for sensitivity analysis of large models. *Env. Mod. & Software.* 22:1509-1518.
- Canfield, D.E. Jr. & R.W. Bachmann. 1981. Prediction of total phosphorus concentrations, chlorophyll a, and Secchi depths in natural and artificial lakes. *Can. J. Fish. Aquat. Sci.* 38: 414-423.
- Chapra, S.C. & W.C. Sonzogni. 1979. Great Lakes total phosphorus budget for the mid 1970s. *J. Water Pollution Control Fed.* 51:2524-2533.
- Chen, C, R. Ji, D.J. Schwab, D. Beletsky, G.L. Fahnenstiel, M. Jiang, T.H. Johengen, H. Vanderploeg, B. Eadie, J.W. Budd, M.H. Bundy, W. Gardner, J. Cotner, P.J. Lavrentyev. 2002. A model study of the coupled biological and physical dynamics in Lake Michigan. *Ecol. Mod.* 152:145-168.
- Conroy, J.D., Kanel, D.D., Dolan, D.M., Edwards, W.J., Charlton, M.N., Culver, D.A. 2005. Temporal Trends in Lake Erie Plankton Biomass: Roles of External Phosphorus Loading and Dreissenid Mussels. *J. Great Lakes Res.* 31(Suppl2):89:110.

- Cushing, D.H. 1990. Plankton production and year-class strength in fish populations: an update of the match/mismatch hypothesis. *Advances in Marine Biology* 26: 249-293.
- [CWR] Centre for Water Resources. 2006a. "CAEDYM Documentation." University of Western Australia. Accessed 10 April 2008.
<http://www.cwr.uwa.edu.au/services/models/caedym/caedym_docs.php>.
- [CWR]. 2006b. ELCOM Documentation. University of Western Australia. Accessed 10 April 2008.
<http://www.cwr.uwa.edu.au/services/models/elcom/elcom_docs.php>.
- [CWR]. 2008. DYRESM Documentation. University of Western Australia. Accessed 10 April 2008.
<<http://www.cwr.uwa.edu.au/services/models/dyresm/documentation>>.
- Dillon, P.J. & F.H. Rigler. 1974. The phosphorus-chlorophyll relationship in lakes. *Limnol. Oceanogr.* 19:767-773.
- Dolan, D.M., McGunagle, K.P. 2005. Lake Erie Total Phosphorus Loading Analysis and Update: 1996-2002. *J. Great Lakes Res.* 31(suppl. 2):11-22.
- Elliott, J.A., A. E. Irish, C. S. Reynolds & P. Tett. 1999. Sensitivity analysis of PROTECH, a new approach in phytoplankton modelling. *Hydrobiologia* 414: 45-51.
- Elser, J.J., Fagan, W.F., Denno, R.F., Dobberfuhl, D.R., Folarin, A., Huberty, A., Interland, S., Kilham, S.S., McCauley, E., Schultz, K.L., Siemann, E.H., Sterner, R.W. Nutritional constraints in terrestrial and freshwater foodwebs. *Nature.* 408:578-580.
- Fahnenstiel, G.L., Chandler, J.F., Carrick, H.J., Scavia, D. 1989. Photosynthetic characteristics of phytoplankton communities in lakes Huron and Michigan: P-I parameters and end-products. *J. Great Lakes Res.* 15:394-407.
- Ferris, J.A., Lehman, J.T. 2007. Interannual variation in diatom bloom dynamics: roles of hydrology, nutrient limitation, sinking, and whole lake manipulation. *Water Research.* 41:2551-2562.
- Fishman, D.B., Adlerstein, S.A., Vanderploeg, H.A., Fahnenstiel, G.L., Scavia, D. Causes of phytoplankton changes in Saginaw Bay, Lake Huron, during the zebra mussel invasion. *J. Great Lakes Res.* 35:482-495.
- GLERL and NOAA. Great Lakes Environmental Research Laboratory, United States National Oceanic and Atmospheric Administration. 2004 Nov 15. About our Great Lakes: Lake by Lake Profiles. Accessed Jun 27 2010. <<http://www.glerl.noaa.gov/pr/ourlakes/lakes.html>>
- Griffin, S.L., Herzfeld, M., Hamilton, D.P. 2001. Modelling the impact of zooplankton grazing on phytoplankton biomass during a dinoflagellate bloom in the Swan River Estuary, Western Australia. *Ecological Engineering* 16:373-394.
- Grover, J.P. 1991. Resource Competition in a Variable Environment: Phytoplankton Growing According to the Variable-Internal-Stores Model. *The American Naturalist.* 138:811-835.
- Hamilton, D.P. and S.G. Schladow. 1997. Prediction of water quality in lakes and reservoirs. Part I – Model description. *Ecol. Mod.* 96: 91-110.

- Harrison, P.J., Conway, H.L., Dugdale, R.C. 1976. Marine Diatoms Grown in Chemostats under Silicate or Ammonium Limitation. I. Cellular Chemical Composition and Stead-State Growth Kinetics of *Skeletonema costatum*. *Marine Biology*. 35:177-186.
- Hartig, J.H., Zarull, M.A., Ciborowski, J.J.H., Wilke, G.E., Norwood, G., Vincent, A.N. 2009. Long-term ecosystem monitoring and assessment of the Detroit River and Western Lake Erie. *Environ Monit Assess* 158:87-104.
- Hecky, R.E., Smith, R.E.H., Barton, D.R., Guildford, S.J., Taylor, W.D., Howell, T.D., and Charlton, M.N. 2004. The nearshore shunt: a consequence of ecosystem engineering by dreissenids in the Laurentian Great Lakes. *Can J. Fish Aquatic Sci.* 61:1285-1293.
- Hipsey, M.R., Romero, J.R., Antenucci, J.P., Hamilton, D.P. 2004. CAEDYM v2: V2.2 User Manual, Centre for Water Research, University of Western Australia, Perth.
- [IJC] International Joint Commission. Jun 27 2010. The Great Lakes Water Quality Agreement between the United States of America and Canada. Accessed Jun 27 2010. <http://www.ijc.org/en/activities/consultations/glwqa/guide_3.php>
- Isvanovics, V., Pdisak, J., Pettersson, K., Pierson, D.C. 1994. Growth and phosphorus uptake of summer phytoplankton in Lake Erken (Sweden). *Journal of Plankton Res.* 16(9):1167-1196.
- Isvanovics, V. Shafik, H.M. Presing, M., Juhos, S. 2000. Growth and phosphate uptake kinetics of the cyanobacterium, *Cylindrospermopsis raciborskii* (Cyanophyceae) in throughflow cultures. *Freshwater Biology*. 43:257-275.
- Jones, J.R., and R.W. Bachmann. 1976. Prediction of phosphorus and chlorophyll levels in lakes. *J. Water Pollut. Control Fed.* 48: 2176-2182.
- Jorgensen, S.E., Bendricchio, G. *Fundamentals of Ecological Modelling*. 3rd Ed. Oxford, UK. Elsevier Science Ltd. 2001.
- Kalff, J. 2002. *Limnology*. Upper Saddle River, NJ: Prentice-Hall, Inc.
- Kasprzak, P., J. Pdisak, R. Koschel, L. Krienitz, and F. Gervais. 2008. Chlorophyll a concentration across a trophic gradient of lakes: An estimator of phytoplankton biomass? *Limnologica*. 38:327-338.
- Lam, D. C. L., W. M. J. Schertzer, & Fraser, A.S. J. 1987. A Post-Audit Analysis of the NWRI Nine-Box Water Quality Model for Lake Erie. *Great Lakes Res.* 13(4):782-800.
- Lehman, J.T., D.B. Botkin, and G.E. Likens. 1975. The assumptions and rationales of a computer model of phytoplankton population dynamics. *Limnol. Oceanogr.* 20:343-364.
- Leon, L.F., Imberger, J., Smith, R.E.H., Lam, D. and Schertzer, W. 2005. Modeling as a tool for nutrient management in Lake Erie. *J. Great Lakes Res.* 31: 309-318.
- Leon, L.F., Smith, R.E.H., Hipsey, M.R., Bocaniov, S.A., Higgins, S.N., Hecky, R.E., Antenucci, J.P., Guildford, S.J., and Imberger, J. In press. Spatial and temporal variability of nutrients and phytoplankton in Lake Erie as portrayed by a three dimensional model.

- Lesht, B.M., T.D. Fontaine, D.M. Dolan. 1991. Great Lakes Total Phosphorus Model: Post Audit and Regionalized Sensitivity Analysis. *J. of Great Lakes Res.* 17(1):3-17.
- Lewis, D.M., Brookes, J.D. and Lambert, M.F. 2004. Numerical models for management of *Anabaena circinalis*. *J. Appl. Phycol.* 16: 457-468.
- Makarewicz, J.C. 1993a. Phytoplankton biomass and species composition in Lake Erie, 1970 to 1987. *J. Great Lakes Res.* 19:258-274.
- Makarewicz, J.C. 1993b. A Lakewide Comparison of Zooplankton Biomass and Its Species Composition in Lake Erie, 1983-87. *J. Great Lakes Res.* 19:275-290.
- Makler-Pick, V., G. Gal, M. Gorfine, M.R. Hipsey, Y. Carmel. In press. Sensitivity analysis for complex ecological models – a new approach.
- Matott, L.S. n.d. Ostrich: An Optimization Software Tool; Documentation and User's Guide v1.6. <<http://www.civil.uwaterloo.ca/lsmatott/Ostrich/OstrichMain.html>>
- Morris, M.D. 1991. Factorial Sampling Plans for Preliminary Computational Experiments. *Technometrics.* 33:161-174.
- Omlin, M, P. Reichert, & R. Forster. 2001a. Biogeochemical model of Lake Zurich: model equations and results. *Ecol. Mod.* 141:77-103.
- Omlin, M., Brun, R., Reichert, P. 2001b. Biogeochemical model of Lake Zurich: sensitivity, identifiability and uncertainty analysis.
- [OMNR] Ontario Ministry of Natural Resources. 2010 Mar 23. Lake Erie and Lake St. Clair. Accessed 2010 Jun 27. Available from: http://www.mnr.gov.on.ca/en/Business/GreatLakes/2ColumnSubPage/STEL02_173905.html.
- Pace, M.L. 1984. Zooplankton Community Structure, but not Biomass, Influences the Phosphorus-Chlorophyll a Relationship. *Can. J. Fish. Aquat. Sci.* 41: 1089-1096.
- Paasche, E. 1973. Silicon and the Ecology of the Marine Plankton Diatoms. I. *Thalassiosira pseudonana* (*Cyclotella nana*) Grown in a Chemostat with Silicate as Limiting Nutrient. *Marine Biology.* 19:117-126.
- Qin, J. and Culver D.A. 1995 Effect of young-of-the-year walleye (*Percidae: Stizostedion vitreum*) on plankton dynamics and water quality in ponds. *Hydrobiologia* 297:217-227.
- Reynolds, C.S. 1984. Phytoplankton periodicity: the interactions of form, function and environmental variability. *Freshwater Biology.* 14(2):111-142
- Riley, G.A. 1965. A Mathematical Model of Regional Variations in Plankton. *Limnology and Oceanography.* 10(Supplement: Alfred C. Redfield 75th Anniversary): 202-215.
- Robson, B.J. & D.P. Hamilton. 2004. Three-dimensional modelling of a Microcystis bloom event in the Swan River estuary. *Ecol. Mod.* 174:203-222.
- Romero, J.R. & J. Imberger. 2003. Effect of a flood underflow on reservoir water quality: Data and three dimensional modeling. *Arch. Hydrobiol.* 157:1-25.

- Romero, J.R., J.P. Antenucci, & J. Imberger. 2004. One- and three-dimensional biogeochemical simulations of two differing reservoirs. *Ecol. Mod.* 174:143-160.
- Roseman, E.F., Taylor, W.W., Hayes, D.B., Haas, R.C., Knight, R.L., Paxton, K.O. 1996. Walleye egg deposition and survival on reefs in Western Lake Erie (USA). *Ann Zool. Fennici* 33:341-351.
- Saltelli, A., Tarantola, S., Campolongo, F., Ratto, M. *Sensitivity Analysis in Practice: A Guide to Assessing Scientific Models*. West Sussex, England. John Wiley & Sons Ltd. 2004.
- Scavia, D., G.A. Lang, & J.F. Kitchell. 1988. Dynamics of Lake Michigan plankton: a model evaluation of nutrient loading, competition, and predation. *Can J. Fish. Aquat. Sci.* 45:165-177.
- Scavia, D. 1980. An ecological model of Lake Ontario. *Ecological Modelling*. 8:49-78.
- Schladow, S.G. and D.P. Hamilton. 1997. Prediction of water quality in lakes and reservoirs: Part II - Model calibration, sensitivity analysis and application. *Ecol. Mod.* 96:111-123.
- Smith, R.E.H., Kalff, J. 1983. Competition for Phosphorus Among Co-Occurring Freshwater Phytoplankton. *Limnology and Oceanography*. 28:448-464.
- Spillman, C.M., Imberger, J., Hamilton, D.P., Hipsey, M.R., Romero, J.R. 2007. Modelling the effects of Po River discharge, internal nutrient cycling and hydrodynamics on biogeochemistry of the Northern Adiratic Sea. *Journal of Marine Systems*. 68:167-200.
- Stockwell, J.D., Sprules, W.G. 1995. Spatial and temporal patterns of zooplankton biomass in Lake Erie. *ICES J. Mar. Sci.* 52:557-564.
- [USEPA] United States Environmental Protection Agency. 2006 Mar 9. Lake Erie Lakewide Management Plan (LaMP): A Primer on Phosphorus in Lake Erie. Accessed 2010 Jun 27. Available from: <http://www.epa.gov/glnpo/lakeerie/primer.html>.
- Wetzel, R.W. 2001. *Limnology: Lake and River Ecosystems*. Elsevier: New York.
- Zhao, Y., Jones, M., & Shuter, B. 2009. A biophysical model of Lake Erie walleye (*Sander vitreus*) explains interannual variations in recruitment. *Canadian Journal of Fisheries and Aquatic Sciences*, 66(1):114-25.

Appendix A

CAEDYM Equations for Phytoplankton and Zooplankton Dynamics

Table A-1: Selected functions, fractions, and mass balance equations for variables not including phytoplankton and zooplankton.

<p>Light (I, $\mu\text{mol photons m}^{-2} \text{ s}^{-1}$)</p> $I(\eta, z) = f_{PAR} I_0 \exp(-\eta z);$ $\eta(A, SS, DOC, POC) = \eta_w + \sum_a \eta_{A_a} A_a + \sum_s \eta_{SS_s} SS_s + \eta_{DOC} DOC + \eta_{POC} POC$	1
<p>Inorganic Particles (SS1 1.8 μm diameter respectively)</p> $\frac{\partial SS_s}{\partial t} = \underbrace{f_{SS_s}^{RES}(\tau, SS_s)}_{\text{resuspension}} - \underbrace{f_{SS_s}^{SET}(SS_s)}_{\text{sedimentation}}$	2
<p>Dissolved Oxygen (DO, g O m^{-3})</p> $\frac{\partial DO}{\partial t} = \underbrace{f_{O_2}^{ATM}(DO)}_{\text{atmospheric flux}} + \underbrace{[f_{CO_2}^{BUP}(A, DIC) - f_{CO_2}^{BRE}(A)] Y_{O_2:C}}_{\text{algal photosynthesis \& respiration}} - \underbrace{[k_{rZ} Z] Y_{O_2:C}}_{\text{denitrification}} - \underbrace{\mu_{NIT} f_{NIT}^{T2}(T) f_{NIT}^{DO1}(DO) NH_4 Y_{O_2:N}}_{\text{nitrification}}$ $- \underbrace{k_{SOD} f_{SOD}^{T2}(T) f_{SOD}^{DO1}(DO) \frac{1}{\Delta z_{bot}}}_{\text{sediment oxygen demand}}$	3
<p>Carbon (inorganic, DIC; dissolved organic, DOC; detritus, POC; algal internal, IC_i; g C m^{-3})</p> $\frac{\partial DIC}{\partial t} = \underbrace{f_{pCO_2}^{ATM}(pCO_2)}_{\text{atmospheric flux}} + \underbrace{f_{CO_2}^{BRE}(A, Z)}_{\text{respiration}} - \underbrace{f_{CO_2}^{BUP}(A, CO_2)}_{\text{photosynthesis}} + \underbrace{f_{DIC}^{DSF}(T, DO)}_{\text{sediment flux}}$	6
<p>Phosphorus (phosphate, FRP; dissolved organic, DOP; detritus, POP; algal internal, IP_i; g P m^{-3})</p> $\frac{\partial FRP}{\partial t} = \underbrace{f_{DOP}^{DEC}(T, DO, DOP)}_{\text{mineralization}} - \underbrace{f_{FRP}^{BUP}(A, FRP)}_{\text{algal uptake}} + \underbrace{f_{FRP}^{DSF}(T, DO)}_{\text{sediment flux}}$	7
<p>Nitrogen (Ammonium, NH_4; nitrate, NO_3; dissolved organic, DON; detritus, PON; algal, A_N; g N m^{-3})</p> $\frac{\partial NH_4}{\partial t} = \underbrace{f_{DON}^{DEC}(T, DO, DON)}_{\text{mineralization}} - \underbrace{f_{NH_4}^{BUP}(A, NH_4)}_{\text{algal uptake}} + \underbrace{f_{NH_4}^{DSF}(T, DO)}_{\text{sediment flux}} - \underbrace{\mu_{NIT} f_{NIT}^{T2}(T) f_{NIT}^{DO1}(DO) NH_4}_{\text{nitrification}}$ $\frac{\partial NO_3}{\partial t} = - \underbrace{f_{NO_3}^{BUP}(A, NO_3)}_{\text{algal uptake}} + \underbrace{f_{NO_3}^{DSF}(T, DO)}_{\text{sediment flux}} + \underbrace{\mu_{NIT} f_{NIT}^{T2}(T) f_{NIT}^{DO1}(DO) NH_4}_{\text{nitrification}} - \underbrace{\mu_{DEN} f_{DEN}^{T2}(T) f_{DEN}^{DO2}(DO) NO_3}_{\text{denitrification}}$	8
<p>Silicon (Algal, A_{Si}; soluble reactive, RSi; g Si m^{-3}):</p> $\frac{\partial RSi}{\partial t} = \underbrace{f_{RSi}^{BUP}(A, RSi)}_{\text{algal uptake}} + \underbrace{f_{RSi}^{DSF}(T, DO)}_{\text{dissolved sediment flux}}$	9

Table A-2: Phytoplankton (A) functions (see Table A-3 for notation).

Phytoplankton (A_i , g Chla m^{-3} ; $i = 1$ to 5 and denotes group)	10
$\frac{\partial A_i}{\partial t} = \underbrace{\mu_i(A_i)}_{\text{photosynthesis}} - \underbrace{R_i(A_i)}_{\text{respiration}} - \underbrace{E_i(A_i) - M_i(A_i)}_{\text{excretion \& mortality}} - \underbrace{f_{A_i}^{SET}(A_i)}_{\text{settling}} + \underbrace{f_{A_i}^{RES}(\tau, A_i)}_{\text{resuspension}}$	
Algal growth rate: $\mu_i(A_i) = \mu \max_i(T) f_i^{T1} \min[f_i(N), f_i(P), f_i(I), f_i(Si)]$	11
N and P limitation functions, $f_i(N)$, $f_i(P)$: $f_i(X) = \frac{IX_i}{IX_{\max i} - IX_{\min i}} \left(1 - \frac{IX_{\min i}}{IX_i} \right)$	12
Silica limitation functions, $f_i(Si)$: $f_i(Si) = \frac{RSi}{RSi + KSi_i}$	13
Light limitation function: $f_i(I) = 1 - \exp\left(-\frac{I}{I_k}\right)$	14
Phosphorus uptake: $U_{FRP}(A_i) = UP_{MAX_i} f_{A_i}^{T1}(T) \left[\frac{IP_{MAX_i} - IP_i}{IP_{MAX_i} - IP_{MIN_i}} \frac{FRP}{FRP + K_{P_i}} \right] A_i$	15
NH ₄ uptake: $U_{NH_4}(A_i) = P_{N_i} UN_{MAX_i} f_{A_i}^{T1}(T) \left[\frac{IN_{MAX_i} - IN_i}{IN_{MAX_i} - IN_{MIN_i}} \frac{NH_4 + NO_3}{NH_4 + NO_3 + K_{N_i}} \right] A_i$	16
NO ₃ uptake: $U_{NO_3}(A_i) = (1 - P_{N_i}) UN_{MAX_i} f_{A_i}^{T1}(T) \left[\frac{IN_{MAX_i} - IN_i}{IN_{MAX_i} - IN_{MIN_i}} \frac{NH_4 + NO_3}{NH_4 + NO_3 + K_{N_i}} \right] A_i$	17
Ammonium Preference: $P_{N_i} = \left[\frac{NH_4 \cdot NO_3}{(NH_4 + K_{N_i})(NO_3 + K_{N_i})} \right] \left[\frac{NH_4 \cdot K_{N_i}}{(NH_4 + NO_3)(NO_3 + K_{N_i})} \right]$	18
Algal losses (respiration, excretion, mortality): $R_i = k_{Ri} \mathcal{G}_{Ri}(T^{-20})$	19
Intracellular N and P: $\frac{dIX_i}{dt} = \frac{U_{X_i} - R_i(1 - f_{resp})IX_i A_i}{A_i} - f_{A_i}^{SET}(A_i)IX_i + f_{A_i}^{RES}(\tau, A_i)IX_i$	20
Temperature dependence: $f^{T1}(T) = \mathcal{G}^{T-20} + \mathcal{G}^{C1(T-C2)} + C3$	21
C1, C2, C3 such that: at Tsta, $f(T)=1$; at Topt, $\frac{\partial f(T)}{\partial t} = 0$; and at Tmax, $f(T)=0$.	
Settling: $f_i^{SET} = \frac{V_{s_i}}{\Delta z}$ and Resuspension: $f_i^{RES}(\tau, i) = \alpha_i \left(\frac{\tau - \tau_{c_i}}{\tau_{ref}} \right) \left(\frac{j^{SED}}{K_{T_i} + j^{SED}} \right) \frac{1}{\Delta z_{bot}}$	22

Table A-3: Parameter definitions for phytoplankton characteristics and processes.

Parameter	Description	Parameter	Description
$Y_{C:Chla}$	Ratio of C to chla (mg C (mg chla) ⁻¹)	I_k	Onset of light saturation of photosynthesis ($\mu E m^{-2} s^{-1}$)
μ_{max}	Maximum growth rates of algae (d ⁻¹)	η_A	Algal effect on the extinction coefficient ((g chla m ⁻³) ⁻¹ m ⁻¹)
ϑ	Temperature multiplier for growth (-)	K_{Si}	Si ¹ / ₂ saturation constant for algal uptake (mg SiO ₂ L ⁻¹)
T_{STD}	Standard temperature for algal growth (°C) where f^{T1} = 1.0	UP_{MAX}	Maximum phosphorus uptake rate (mg P (mg Chla) ⁻¹ d ⁻¹)
T_{OPT}	Optimum temperature for algal growth (°C) where f^{T1} = maximum	K_P	Half saturation constant for phosphorus uptake (mg P L ⁻¹)
T_{MAX}	Maximum temperature for algal growth (°C) where f^{T1} = 0	IP_{MAX}	Maximum internal phosphorus concentration (mg P (mg Chla) ⁻¹)
R	Algal respiration, mortality, and excretion (d ⁻¹)	IP_{MIN}	Minimum internal phosphorus concentration (mg P (mg Chla) ⁻¹)
ϑ_{Ri}	Temperature multiplier for respiration (-)	UN_{MAX}	Maximum nitrogen uptake rate (mg N (mg Chla) ⁻¹ d ⁻¹)
f_{dom}	Fraction of mortality & excretion that is DOM (remainder is POM)	K_N	Half saturation constant for nitrogen uptake (mg N L ⁻¹)
f_{resp}	Fraction of algal losses that is respiration (remainder is mortality and excretion)	IN_{MAX}	Maximum internal nitrogen concentration (mg N (mg Chla) ⁻¹)
v_s	Settling velocity at 20 °C (m ds ⁻¹)	IN_{MIN}	Minimum internal nitrogen concentration (mg N (mg Chla) ⁻¹)

Table A-4: Zooplankton processes (see Table A5 for parameter notation).

Zooplankton (Z_i , g C m ⁻³ ; $i = 1$ to 2 and denotes group)	23
$\frac{\partial Z_i}{\partial t} = \underbrace{a_z G(A_i)}_{\text{grazing}} - \underbrace{E_{\text{particulate}}(Z_i) - E_{\text{dissolved}}(Z_i)}_{\text{excretion \& mortality}}$	
(Note: if fish or omnivorous zooplankton were modelled, there would be a predation loss.)	
Potential rate of carbon consumption: $f_{Z_z}^{ZFD}(A) = \frac{\sum_a^{N_A} A_a Y_{C:Chla_a}}{K_{j_z} + \sum_a^{N_A} A_a Y_{C:Chla_a}}$	24
Carbon consumed: $G_C(Z_Z) = g_{MAX_Z} f_{Z_z}^{T1}(T) f_{Z_z}^{ZFD}(A) Z_Z$ (f^{T1} was defined in Table 2 equation 21)	25
Nitrogen consumed: $G_N(Z_Z) = \sum_a^{N_A} G_C(Z_Z) \frac{P_{Za} A_a Y_{C:Chla_a}}{\sum_a^{N_A} P_{Za} A_a Y_{C:Chla_a}} \frac{AIN_a}{A_a}$	26
Phosphorus consumed: $G_P(Z_Z) = \sum_a^{N_A} G_C(Z_Z) \frac{P_{Za} A_a Y_{C:Chla_a}}{\sum_a^{N_A} P_{Za} A_a Y_{C:Chla_a}} \frac{AIP_a}{A_a}$	27
Respiration loss: $R_{DIC}(Z_Z) = k_{R_z} g_z(T-20) Z_Z$	28
Carbon lost via mortality, excretion, and egestion Excretion: $E_{DOCL}(Z_Z) = k_{Ez} G_C(Z_Z)$ Faecal pellets and mortality: $E_{POCL}(Z_Z) = k_{Fz} G_C(Z_Z) + k_{Mz} g^{T-20} Z_Z$	29
Nitrogen lost to particulate detrital pool via zooplankton fecal pellets and mortality: $E_{PONL}(Z_Z) = k_{Fz} G_N(Z_Z) + k_{Mz} g^{T-20} k_{ZIN} Z_Z$	30
Phosphorus lost to particulate detrital pool via zooplankton fecal pellets and mortality: $E_{POPL}(Z_Z) = k_{Fz} G_P(Z_Z) + k_{Mz} g^{T-20} k_{ZIP} Z_Z$	31
If P is limiting then: $E_{DONL}(Z_Z) = \frac{ZIN_z^* Z_z^{t+1} k_{ZINz}}{\Delta t}$	32
If N is limiting then: $E_{DOPL}(Z_Z) = \frac{ZIN_z^* Z_z^{t+1} k_{ZIPz}}{\Delta t}$	33

Table A-5: Parameter definitions for zooplankton characteristics and processes.

Parameter	Description	Parameter	Description
A_z	Messy feeding; portion of food that reaches the mouth	\mathcal{G}_T	Temperature multiplier for grazing in f^{T1}
k_{Rz}	Respiration rate coefficient (d^{-1})	T_{sta}	Standard temperature for grazing ($^{\circ}C$) where $f^{T1} = 1.0$
k_{Mz}	Mortality rate coefficient	T_{opt}	Optimum temperature for grazing ($^{\circ}C$) where f^{T1} is maximized
k_{Fz}	Fecal pellet fraction of Grazing	T_{max}	Maximum temperature for grazing ($^{\circ}C$) where $f^{T1} = 0$
k_{Ez}	Excretion fraction of grazing	k_i	Maximum grazing rate (d^{-1})
k_{ZIN}	Internal nitrogen to carbon ratio	K_j	Half saturation constant for grazing
k_{ZIP}	Internal phosphorus to carbon ratio	P_{za}	Zooplankton group z's preference for phytoplankton group, a.
\mathcal{G}_Z	Temperature multiplier for respiration (-)		

Appendix B

Matlab Code for Modified Morris Selection Matrix

```

% Output combo matrices to a file

%--- get run specs, BStar*M, d, filenames, etc. ----
% k=number of parameters to test (columns)
% p=number of levels per parameter
% M=total number of B matrices to create (i.e. like 500 or 1000)
% runs=number of B matrices to run selected from M

M=500; runs=10; k=91; p=4;

OUTFolder=strcat('MorrisOut-M',num2str(M),'-r',num2str(runs),...
    '-k',num2str(k));
if exist(OUTFolder,'dir')==0; mkdir(OUTFolder); end
OutFileM=strcat(OUTFolder,'\BSTAR-M',num2str(M),...
    '-k',num2str(k),'.txt');
OutFileC=strcat(OUTFolder,'\Combo-M',num2str(M),'-k',num2str(k),....
    '-r',num2str(runs),'.txt');

BS=zeros(k+1,k,M);
for i=1:M
    BS(:, :, i)=BStar(k,p); %%% See sub-function BStar %%%
end
d=dLength(M,BS,k); %%% See sub-function dLength %%%

% find the best combo of 'runs' from 'M'
combo=zeros(1,runs);
max1=max(max(d)); root=2;
for i=1:M-1;
    for j=i+1:M
        if(d(i,j)==max1)
            col(1)=i; col(root)=j;
            for z=1:M
                if d(z,i)==0 || d(z,j)==0
                    Sum(root,z)=0;
                else
                    Sum(root,z)= d(z,i)+d(z,j);
                end
            end
        end
        % Pass runs=5 M=10, root, Sum, global d
        combo=FindCombo(root,M,runs,Sum,d,col,combo,d(i,j));
        %%% See sub-function FindCombo %%%
    end % End the first if (the max of first 2 columns)
end
if mod(i,5)==0
    i

```

```

    end
end

% Eliminate duplicate combos and sort combo in ascending order
COMBO=sort(combo,2);
COMBO=unique(COMBO,'rows');
[DMax, row]=max(COMBO(:,numel(COMBO(1,:)))));
COMBO=COMBO(row,1:numel(COMBO(1,:))-1);
clear i j z row max1 root col Sum;

%Output the entire thing to a file:
fid=fopen(OutFileM,'w');
fprintf(fid, '%s', 'Combination:');
for i=1:runs
    fprintf(fid, '%d ', COMBO(i));
end
fprintf(fid, '\n DMax: %5.2f\n', DMax);
fprintf(fid, '%s %d \n','DivideBy:',p-1);
for m=1:M
    for i=1:k+1;
        for j=1:k;
            fprintf(fid,'%3d',BS(i,j,m)*(p-1));
            % *(p-1) use whole numbers instead of truncated numbers
        end
        fprintf(fid,'\n');
    end
    fprintf(fid,'\n');
end
fclose(fid);

% Output just the combination matrices to file (no blank lines)
fid=fopen(OutFileC,'w');
for m=1:runs
    for i=1:k+1
        for j=1:k
            fprintf(fid,'%d ', BS(i,j,COMBO(m))*(p-1));
        end
        fprintf(fid,'\n');
    end
end
fclose(fid);

```

```

% Generate one B* matrix

function [Bs] = BStar(k,p)

delta=p/(2*(p-1));

```

```

% Array of k params - 4 levels between 0 and 1
X=randint(1,k,[0, p-1])*1/(p-1);
B=zeros(k+1,k);
tempD=randint(k,1,[0, 1])*2-1; % Array of k values radomly 1 or -1
D=zeros(k,k);
J=zeros(k+1,k);
for i=1:k+1
    for j=1:k
        if(i>j); B(i,j)=1; end % B is a lower triangular matrix
of ones
        if(i==j); D(i,j)=tempD(j); end
        %D has a diagonal of 1 or -1; otherwise zeroes
        J(i,j)=1; % J is a k+1 by k+1 matrix of
ones
    end
end

perm=randperm(k);
I=eye(k,k);
P=I(perm,:);

%B=[0,0,0;1,0,0;1,1,0;1,1,1]; X=[2/3,1,1]; delta=2/3;
%D=[-1,0,0;0,-1,0;0,0,-1]; P=[1,0,0;0,0,1;0,1,0]; J=ones(4,3);
Bs=(J(:,1)*X+delta/2*((2*B-J)*D+J))*P;

```

```

Bs=mod(Bs,2*delta);

```

```

% Calculate all the d-lengths for the selection of matrices
function [d]=dLength(M, BS,k)
sum=0; sumRoot=0; sumSumRoot=0;
d=zeros(M,M);
for n=1:M-1
    for l=n+1:M
        for i=1:k+1
            for j=1:k+1
                for z=1:k
                    sum=sum+(BS(i,z,n)-BS(j,z,l))^2;
                end
                sumRoot=sumRoot+sqrt(sum);
                sum=0;
            end
            sumSumRoot=sumSumRoot+sumRoot;
            sumRoot=0;
        end
        d(n,l)=sumSumRoot;
        sumSumRoot=0;
    end
end

```

```

end
for l=1:M-1
    for n=l+1:M
        d(n,l)=d(l,n);
    end
end
end

```

```

% Recursive loop to find the max combos in the FullMorris code

```

```

function combo=FindCombo(root, M, runs, Sum, d, col,combo,FirstMax)
global count; global DMax;
if combo(1,1)==0; count=0; end

```

```

MAX=max(Sum(root,:));
root=root+1;
if root==3;
    DMax(root)=MAX+FirstMax;
else
    DMax(root)=MAX+DMax(root-1);
end

```

```

for k=1:M
    if Sum(root-1,k)==MAX
        col(root)=k;
        if root==runs
            count=count+1;
            combo(count,1:numel(col))=col;
            combo(count,numel(col)+1)= DMax(root);
        else
            for m=1:M
                if d(m,k)==0 || Sum((root-1),m)==0
                    Sum(root,m)=0;
                else
                    Sum(root,m)=Sum(root-1,m)+d(m,k);
                end
            end
            end
            %Call recursive loop again if root<runs
            combo=FindCombo(root, M, runs, Sum, d, ...
                col,combo,FirstMax);
        end
    end
end
end
end

```

Appendix C

CAEDYM Parameters File for Chapter 5 Simulation

```

! CAEDYM PARAMETER FILE: Valid for v2.3 only
!-----!
! LIGHT constants *****!
!-----!
!-- Base extinction coefficient          !
  1.00000    0.410    : NIR, Near InfraRed
  0.20000    0.450    : PAR, Photosynthetically Active
  1.80000    0.035    : UVA, UV-A Region
  2.50000    0.005    : UVB, UV-B Region
!-----!
! PHYTOPLANKTON constants *****!
!-----!
! Pmax (/day) : Maximum potential growth rate of phytoplankton      !
  0.60000    !1-DINOF -
  0.80000    !2-CYANO - Cyanonephron/Aphanocapsa (was 1.1 - 01-10-2003)
  1.20000    !3-NODUL - Using this as another CHLOR group - Closterium/Staurastrum/Cosmarium
(was 1.0)
  6.000000E-001    !4-CHLOR - Sphaerocystis
  6.000000E-001    !5-CRYPT - Cryptomonas/Chroomonas
  1.600000E+000    !6-FDIAT - Aucleseira Icelandica, spring (2006_ScottMatt)
  1.99000    !7-FDIAT - Generic FWater diatom, summer (2006_ScottMatt)
! Ycc (mg C/mg chla) : Average ratio of C to chlorophyll a          !
  300.00000    !DINOF -
  50.00000    !cyanobacteria JRR 08/05 50 O'Conner et al. (1973)
  50.00000    !nodularia JRR 08/05 50 O'Conner et al. (1973)
  4.000000E+001    !chlorophytes
  4.000000E+001    !cryptophytes - Istvanovics et al 1994
  8.000000E+001    !freshwater diatoms (2006_ScottMatt)
  50.00000    !freshwater diatoms JRR 08/05 50 O'Conner et al. (1973)
!-----!
! Light limitation (2=no photoinhibition, 3=photoinhibition)      !
! algt (no units) : Type of light limitation algorithm            !
  3    ! DINOF
  2    ! CYANO
  2    ! NODUL
  2    ! CHLOR
  2    ! CRYPT
  2    ! MDIAT
  2    ! FDIAT
! IK (microE/m^2/s) : Parameter for initial slope of P_I curve      !
  140.00000    !DINOF
  130.00000    ! 530.0 Wallace and Hamilton 1999 [Stage 1 = 65]
  100.00000    ! values based on relative relationships given in Reynolds 1984
  1.083000E+002    !CHLOR
  6.500000E+001    !CRYPT
  6.830000E+001    !MDIAT
  60.00000    !FDIAT
! ISt (uEm^-2s^-1) : Light saturation for maximum production      !

```

390.00 ! Whittington et al 2000 [Stage 1 = 140]
 1300.00 ! Wallace and Hamilton 1999 [Stage 1 = 130]
 200.00
 100
 200
 70
 70.00
 ! Kep (ug chlaL^-1m^-1) : Specific attenuation coefficient !
 0.014 ! Whittington et al 2000 [Stage 1 = 0.0067]
 0.020 ! JRR 08/05: Megard et al (1980) 0.022/Smith and Baker (1978) 0.016
 0.020 ! JRR 08/05: Megard et al (1980) 0.022/Smith and Baker (1978) 0.016
 0.014
 0.014
 0.020 ! JRR 08/05: Megard et al (1980) 0.022/Smith and Baker (1978) 0.016
 0.020 ! JRR 08/05: Megard et al (1980) 0.022/Smith and Baker (1978) 0.016
 !-----!
 ! Nutrient Parameters !
 ! KP (mg/L) : Half saturation constant for phosphorus !
 0.00383 ! 0.00083 Istvanovics et al 1994 Table III [Stage 1 - 0.0038]
 0.00900 ! 0.006 Holm and Armstrong 1981, Robson 2001 (was 0.003/6 JRR 1/03)
 0.00800 ! was 0.006 08/10/03 from Reynolds 1984 (was 0.0025/5 JRR 1/03)
 1.000000E-002 ! based on oligotrophic dominance (Reynolds 1984) (was 0.001/3 JRR 1/03)
 3.000000E-003 ! Istvanovics 1994, quoting Smith and Kalff 1983 (was 0.002/2 JRR 1/03)
 3.000000E-002 ! Reynolds - 0.008 {0.0042 Grover et al 1999} (was 0.002/4 JRR 1/03)
 0.00600 ! Reynolds - 0.008 {0.0042 Grover et al 1999} (was 0.002/4 JRR 1/03)
 ! Po (mg/L) : Low concentrations of PO4 at which uptake ceases !
 0.00000
 0.00000
 0.00000
 0.00000
 0.00000
 0.00400
 0.00150
 ! KN (mg/L) : Half saturation constant for nitrogen !
 0.01980 ! DINOF
 0.04500 ! Robson et al 2001 (was 0.03 10/09/03)
 0.04500 ! NODUL
 3.000000E-002 ! based on relative relationship from Reynolds 1984
 4.000000E-002 ! based on relative relationship from Reynolds 1984
 6.000000E-002 ! Grover et al. 1999 [Stage 1 - 0.03]
 0.04500 ! Grover et al. 1999 [Stage 1 - 0.03]
 ! No (mg/L) : Low concentrations of N at which uptake ceases !
 0.00000
 0.00000
 0.00000
 0.00000
 0.00000
 0.00000
 0.00000
 ! Sicon (mg Si/mg Chla) : Constant internal Silica concentration !
 0.00000 ! dinoflagellates
 0.00000 ! fwater cyanobacteria

0.00000 ! nodularia
 0.00000 ! chlorophytes
 0.00000 ! cryptophytes
 9.330000E+001 ! fwater diatoms - JRR 08/05 Harrison et al (1971)
 40.0000 ! fwater diatoms - JRR 08/05 Harrison et al (1971)
 ! KSi (mg/L) : Half saturation constant for silica !
 0.00000
 0.00000
 0.00000
 0.00000
 0.00000
 9.000000E-002 ! (0.06200<--not sure why this number was there) JRR 08/05 Paasche (1973)
 0.05500 ! JRR 08/05 Paasche (1973)
 ! Sio (mg/L) : Low concentrations of Si at which uptake ceases !
 0.00000
 0.00000
 0.00000
 0.00000
 0.00000
 0.1000
 0.0200
 ! KCa (mg/L) : Half saturation constant for carbon !
 2.00000
 2.00000
 2.00000
 2.00000
 2.00000
 2.00000
 2.00000
 ! INmin (mg N/mg Chla) : Minimum internal N concentration !
 36.0000 ! Istvanovics et al 1994, for C/Chla = 300 [Stage 1 = 3.5]
 2.00000 ! JRR 08/05 average 4.4, min 2.2 FWPCA (1968)
 2.00000 ! JRR 08/05 average 4.4, min 2.2 FWPCA (1968)
 2.200000E+000
 5.000000E-001
 1.800000E+000 ! JRR 08/05 average 4.4, min 2.2 FWPCA (1968)
 2.00000 ! JRR 08/05 average 4.4, min 2.2 FWPCA (1968)
 ! INmax (mg N/mg Chla) : Maximum internal N concentration !
 45.0000 ! Istvanovics et al 1994, for C/Chla = 300 [Stage 1 = 12.5]
 4.00000 ! JRR 08/05 average 4.4, min 2.2 FWPCA (1968)
 4.00000 ! JRR 08/05 average 4.4, min 2.2 FWPCA (1968)
 7.000000E+000
 2.000000E+000
 4.700000E+000 ! JRR 08/05 average 4.4, min 2.2 FWPCA (1968)
 4.00000 ! JRR 08/05 average 4.4, min 2.2 FWPCA (1968)
 ! UNmax (mg N/mg Chla/day) : Maximum rate of Phytoplankton nitrogen uptake !
 6.3 ! [Stage 1 - 2.1]
 0.15000E+01
 0.15000E+01
 0.15000E+01
 0.15000E+01
 0.15000E+01

0.15000E+01
 ! IPmin (mg P/mg Chla) : Minimum internal P concentration !
 1.50000 ! Istvanovics et al 1994, for C/Chla = 300 [Stage 1 = 0.18]
 0.10000 ! JRR 08/05 average 0.32, min 0.1 FWPCA (1968)
 0.10000 ! JRR 08/05 average 0.32, min 0.1 FWPCA (1968)
 1.70000E-001
 1.20000E-001
 2.50000E-001 !(0.1<-- again not sure why that was beside) JRR 08/05 average 0.32, min 0.1
 FWPCA (1968)
 0.13000 !(0.1<-- was also beside number) JRR 08/05 average 0.32, min 0.1 FWPCA (1968)
 ! IPmax (mg P/mg Chla) : Maximum internal P concentration !
 21.0000 ! Istvanovics et al 1994, for C/Chla = 300 [Stage 1 = 0.68]
 1.00000 ! JRR 08/05 avg 0.32, min 0.1 FWPCA (1968) (RSmith 0.5 to 1)
 0.50000 ! JRR 08/05 avg 0.32, min 0.1 FWPCA (1968)
 5.00000E+000 (RSmith no change)
 =2)
 1.50000E+000 (RSmith 0.5 to 1)
 2.50000E+000 ! JRR 08/05 avg 0.32, min 0.1 FWPCA (1968) (RSmith 0.5 to 1.5)
 1.30000 ! JRR 08/05 avg 0.32, min 0.1 FWPCA (1968) (RSmith 0.5 to 1.5)
 ! UPmax (mg P/mg Chla/day) : Maximum rate of phosphorus uptake !
 0.45000E+00 [Stage 1 - 0.15]
 0.1000E+01 (RSmith Cyano 0.1 to 1.0)
 0.1000E+00
 0.20000E+01 (RSmith Chloro 0.3 to 3.0) (RSmith M)
 0.70000E+00 (RSmith Crypto 0.1 to 1.0) (RSmith M)
 0.40000E+00 (RSmith F_Diat 0.1 to 1.5)
 0.10000E+01 (RSmith F_Diat 0.1 to 1.5)
 ! ICmin (mg C/mg Chla) : Minimum internal C concentration !
 48.00000
 15.00000
 15.00000
 15.00000
 15.00000
 15.00000
 15.00000
 ! ICmax (mg C/mg Chla) : Maximum internal C concentration !
 136.00000
 80.00000
 80.00000
 80.00000
 80.00000
 80.00000
 80.00000
 ! UCmax (mg C/mg Chla/day) : Maximum rate of carbon uptake !
 20.00000
 50.00000
 50.00000
 50.00000
 50.00000
 50.00000
 50.00000
 ! IPcon (mg P/mg Chla) : Constant Internal P ratio if no int P is modelled !

```

0.30000  !(08/10/03 - was 0.3)
0.40000
0.40000
0.30000
0.30000
0.40000
0.40000
! INcon (mg N/mg Chla) : Constant Internal N ratio if no int N is modelled  !
3.00000
4.00000
4.00000
3.00000
3.00000
4.00000
4.00000
! NFixationRate (mg N/mg Chla /day): Maximum nitrogen fixation rate  !
2.00000
2.00000
2.00000
2.00000
2.00000
2.00000
2.00000
! gthRedNFix () : Growth rate reduction under maximal N fixation  !
1.00000
1.00000
1.00000
1.00000
1.00000
1.00000
1.00000
!-----!
! Temperature representation  !
! vT (no units) : Temperature multiplier  !
1.06000
1.09000  ! 1.025Sagehashi and Sakoda 2001 [Stage 1 - 1.1]{1.06}
1.07000
1.060000E+000
1.060000E+000
1.050000E+000
1.07500
! Tsta (Deg C) : Standard temperature  !
20.00000  ! [Stage 1 - 20]
24.00000  ! Robson et al 2001 [Stage 1 = 23]
20.00000
2.300000E+001  ! (RSmith 18 to 24)
1.600000E+001  ! (RSmith 20 to 19)
4.000000E+000  ! Orig 14 (2006_ScottMatt 18 to 8)
19.00000  ! Orig 14
! Topt (Deg C) : Optimum temperature  !
22.00000  ! Bruno and McLaughlin 1977
30.00000  ! Robson et al 2001 [Orig 34]

```

22.0000
 3.150000E+001 ! Orig 25 (RSmith 25 to 29)
 1.800000E+001 (RSmith 29 to 21)
 1.280000E+001 ! Orig 18 (2006_ScottMatt 22 to 12)
 23.00000 ! Orig 18 (RSmith was 22 to 22)
 ! Tmax (Deg C) : Maximum temperature !
 28.00000 ! Pollinger 1987 [Stage 1 - 31]
 39.00000 ! Robson etal 2001 [Stage 1 = 37] {35} (RSmith was 39 now 39)
 35.00000
 4.050000E+001 ! Orig 31 (RSmith -0.05 to 35)
 2.600000E+001 (RSmith 35 to 27.5)
 2.180000E+001 ! Orig 27 (2006_ScottMatt 31 to 20)
 31.00000 ! Orig 27 (RSmith was 31 now 31)
 !-----!
 ! Respiration mortality and excretion. !
 ! kr (/day) : Respiration rate coefficient !
 0.00000
 0.14250 ! Microcystis? (Robson etal 2001) [Stage 1-0.07] (RSmith 0.09 to 0.27) (RSmith M)
 0.00000 ! was 0.12 08/07/03 GROUP NOT MODELLED
 1.000000E-001 ! was 0.14 (RSmith 0.06 to 0.25) (RSmith M)
 8.000000E-002 ! high grazing from zoopl (Reynolds 1984) (RSmith 0.12 to 0.25) (RSmith M)
 8.000000E-002 ! was 0.12 (RSmith 0.11 to 0.25) (2006_ScottMatt back to 0.11) (RSmith M)
 0.12900 ! was 0.12 (RSmith 0.11 to 0.25) (2006_ScottMatt back to 0.11) (RSmith M)
 ! vR (no units) : Temperature multiplier (no units) !
 1.04000
 1.06000
 1.06000
 1.030000E+000
 1.060000E+000
 1.130000E+000
 1.03500
 ! Fraction of respiration relative to total metabolic loss rate !
 0.60000E+00 (DINOF)
 0.52600E+00 (CYANO) ! (RSmith 0.25 to 0.5) (EJ 0.5 to 0.526)
 0.25000E+00 (NODUL)
 5.200000E-001 (CHLOR) ! (RSmith 0.70 to 0.2) (EJ 0.2 to 0.333)
 6.500000E-001 (CRYPT) ! (RSmith 0.25 to 0.2) (EJ 0.2 to 0.333)
 2.800000E-001 (FDIAT) ! (RSmith 0.25 to 0.2) (2006_ScottMatt to 0.3) (EJ 0.3 to 0.349)
 0.34900E+00 (FDIAT) ! (RSmith 0.25 to 0.2) (2006_ScottMatt to 0.3) (EJ 0.3 to 0.349)
 ! Fraction of metabolic loss rate that goes to DOM (rest goes to POM) !
 0.10000E+00 (DINOF)
 0.70000E+00 (CYANO) ! (RSmith was 0.3 now 0.7)
 0.30000E+00 (NODUL)
 3.000000E-001 (CHLOR) ! (RSmith 1.0 to 0.2)
 5.000000E-001 (CRYPT) ! (RSmith 0.3 to 0.2)
 3.700000E-001 (FDIAT) ! (24/09/03 - was 0.2) (RSmith 0.3 to 0.2)(2006_ScottMatt to 0.3)
 0.40000E+00 (FDIAT) ! (24/09/03 - was 0.2) (RSmith 0.3 to 0.2)(2006_ScottMatt to 0.3)
 !-----!
 ! Salinity limitation !
 ! maxSP (psu) : Maximum potential salinity !
 36.00000 dinoflagellates
 36.00000 fwater cyanobacteria

36.00000 nodularia
 36.00000 chlorophytes
 36.00000 cryptophytes
 36.00000 marine diatoms
 36.00000 fwater diatoms
 ! phsal (no units) : Type of water environment (Angeline 23/08/2000) !
 0
 ! Sop (psu) : Minimum bound of salinity tolerance !
 18.00000
 3.00000
 28.00000
 14.00000
 20.00000
 1.00000
 1.00000
 ! Bep (no units) : Salinity limitation value at S=0 and S=maxSP !
 1.00000
 3.00000
 2.00000
 2.50000
 2.00000
 5.00000
 5.00000
 ! Aep (no units) : Salinity limitation value at S=Sop !
 1.00000
 1.00000
 1.00000
 1.00000
 1.00000
 1.00000
 1.00000
 !-----!
 ! Vertical migration and settling (0-stokes, 1-constant, 2-motile w/o photoinhibition 3-motile w/
 photoinhibition)
 ! phvel (no units) : Type of vertical migration algorithm !
 3
 1
 1
 1
 1
 1
 1
 1
 ! c1 (kgm⁻³min⁻¹) : Rate coefficient for density increase !
 0.90000 dinoflagellates
 0.124000 0.0427 Microcystis aeruginosa Wallace and Hamilton - 1999
 0.90000 nodularia
 0.90000 chlorophytes
 0.90000 cryptophytes
 0.90000 marine diatoms
 0.90000 fwater diatoms
 ! c3 (kgm⁻³min⁻¹) : Minimum rate of density decrease with time !
 0.04150 dinoflagellates

0.02300 !0.0000046 Wallace and Hamilton - 1999
 0.04150 nodularia
 0.04150 chlorophytes
 0.04150 cryptophytes
 0.04150 marine diatoms
 0.04150 fwater diatoms
 ! c4 (mhr⁻¹) : Rate for light dependent migration velocity !
 0.60000 Whittington et al 2000 [Stage 1 = 2.5?]
 0.30000 fwater cyanobacteria
 0.30000 nodularia
 0.30000 chlorophytes
 0.85000 cryptophytes
 0.85000 marine diatoms
 0.85000 fwater diatoms
 ! c5 (mhr⁻¹) : Rate for nutrient dependent migration velocity !
 0.60000 ! Whittington et al 2000 [Stage 1 = 0.2?]
 0.30000 fwater cyanobacteria
 0.65000 nodularia
 0.30000 chlorophytes
 0.65000 cryptophytes
 0.65000 marine diatoms
 0.65000 fwater diatoms
 ! IKm (uEm⁻²s⁻¹) : Half saturation constant for density increase !
 26.00000
 278.00000 Visser et al 1997
 25.00000
 25.00000
 25.00000
 25.00000
 25.00000
 ! min_pd (kg/m³) : Minimum phytoplankton density !
 980.00000 dinoflagellates
 990.00000 fwater cyanobacteria
 980.00000 nodularia
 980.00000 chlorophytes
 980.00000 cryptophytes
 980.00000 marine diatoms
 980.00000 fwater diatoms
 ! max_pd (kg/m³) : Maximum phytoplankton density !
 1050.00000 dinoflagellates
 1002.00000 fwater cyanobacteria
 1050.00000 nodularia
 1025.00000 chlorophytes
 1050.00000 cryptophytes
 1025.00000 marine diatoms
 1025.00000 fwater diatoms
 ! pw20 (kgm⁻³) : Density of water at 20 deg C !
 1000.00000
 ! dia (m) : Diameter of phytoplankton !
 0.50000E-04
 0.50000E-04
 0.50000E-04

```

0.80000E-05
0.10000E-04
0.10000E-04
0.10000E-04
! ws (ms^-1) : Constant settling velocity          !
0.00000E+00
-0.08500E-05  ! CYANO - 0.1 (-1.20) m/day change to 0.1 m/d
-0.08500E-05  ! CHLOR - 0.04 (-0.46) m/day change to 0.1 m/d
-0.23000E-06  ! NODUL - 0.03 (-0.35) m/day change to 0.02 m/d
-0.23000E-06  ! CRYPT - 0.02 (-0.23) m/day
-1.00000E-05  ! MDIAT - 0.8 (-9.30) m/day change to 0.2 m/d (Changed back to 0.8 - 2006 ScottMatt)
-1.00000E-05  ! FDIAT - 0.8 (-9.30) m/day change to 0.2 m/d (Changed back to 0.8 - 2006 ScottMatt)
! oth (mg O/L) : DO threshold which motile phytos will not migrate below  !
1.00000E+00
0.00000E+00
0.00000E+00
0.00000E+00
0.00000E+00
0.00000E+00
0.00000E+00
0.00000E+00
!-----!
! Resuspension          !
! tcpy (N/m^2) : Critical shear stress          !
0.02000          dinoflagellates
0.00100          fwater cyanobacteria
0.00100          nodularia
0.00100          chlorophytes
0.00100          cryptophytes
0.00100          marine diatoms
0.00100          fwater diatoms
! alpPy (mg Chla/m^2/s) : Resuspension rate constant          !
0.008
! KTPy (mg Chla/m^2) : Controls rate of resuspension          !
0.00000          dinoflagellates
0.00010          fwater cyanobacteria
0.00010          nodularia
0.01000          chlorophytes
0.00010          cryptophytes
0.00010          marine diatoms
0.00010          fwater diatoms
! DTphy (days) : Phytoplankton sediment survival time          !
2.00000
2.00000
2.00000
2.00000
2.00000
2.00000
2.00000
!-----!
! Algal toxin and metabolite dynamics          !
! IXmin (mg/L (mg Chla/L)^-1) : Internal metabolite conc when growth is zero  !
0.00000

```

```

0.20000
0.20000
0.00000
0.00000
0.00000
0.00000
! IXmax (mg/L (mg Chla/L)^-1) : Internal metabolite conc when growth is Pmax !
0.00000
2.00000
2.00000
0.00000
0.00000
0.00000
0.00000
! mX : Temperature decay constant for metabolites !
0.00000
0.01000
0.01000
0.00000
0.00000
0.00000
0.00000
!-----!
! JELLYFISH constants !
!-----!
<<<NOT MODELLED, SO THIS SECTION IS NOT INCLUDED IN THIS APPENDIX>>>
!-----!
! ZOOPLANKTON constants !
!-----!
! az (no units) : assimilation rate !
9.000000E-001 ! Cladocerans EJ starting with 1 !
9.000000E-001 ! Copepods EJ starting with 1 !
1.0000
1.0000
1.0000
!-----!
! Respiration mortality and excretion. !
! Unused (no units)
0.20000
! krz (/day) : Respiration rate coefficient !
1.200000E-001 !make cladocerans the same as zoop for first run !
6.000000E-002
0.04000
0.20000
0.20000
! kmz (/day) : Mortality rate coefficient !
1.000000E-002
1.000000E-002
0.04000
0.20000
0.20000
! kfz (-) : Fecal Pellet Fraction of Grazing !

```

```

5.000000E-002      ! EJ these may seem high since Az is 1 for this simulation  !
1.500000E-001
0.04000
0.20000
0.20000
! kez ( - ) : Excretion Fraction of Grazing      !
5.000000E-002      ! Also may seem high      !
1.500000E-001
0.04000
0.20000
0.20000
!-----
! INZcon
1.900000E-001
1.200000E-001
0.04000
0.20000
0.20000
! IPZcon
2.600000E-002
2.200000E-002
0.04000
0.20000
0.20000
!-----
! Salinity limitation      !
! Smxz (psu) : Maximum salinity, or optimum salinity for SIZE5      !
50.00000
50.00000
28.00000
28.00000
27.00000
! Smnz (psu) : Minimum salinity      !
0.00000
0.00000
6.00000
6.00000
6.00000
! Bez (no units) : Salinity intercept (for S=0)      !
0.00000
0.00000
2.00000
2.00000
2.00000
!-----
! Dissolved oxygen limitation      !
! DOmz (mg/L) : Minimum DO tolerance      !
0.200000  !
0.200000
0.00000
1.00000
1.00000

```



```

!-----!
! Temperature representation !
! vT (no units) : Temperature multiplier !
    1.100000E+000
    1.050000E+000
    1.08000
    1.08000
    1.08000
! Tsta (Deg C) : Standard temperature !
    1.600000E+001 !still basically have no idea what these should be... !
    1.300000E+001
    20.00000
    20.00000
    20.00000
! Topt (Deg C) : Optimum temperature !
    2.100000E+001
    1.300000E+001
    33.00000
    33.00000
    33.00000
! Tmax (Deg C) : Maximum temperature !
    3.400000E+001
    3.300000E+001
    39.00000
    39.00000
    39.00000
!-----!
! Grazing !
! ki (g phyto C/m^3)/(g zoo C/m^3)/day) : Grazing rate !
    2.400000E+000
    1.170000E+000
    0.72000
    0.20000
    0.20000
! vZ (no units) : Grazing temperature dependence !
    1.070000E+000
    1.040000E+000
    1.07000
    1.08000
    1.08000
! PzPHY (was Pij)(no units) : Preference of zooplankton for phytoplankton !
    0.00000 !EJ zoop 1 on phyto 1 (not modelled)
    0.00000 !EJ zoop 2 on phyto 1 (not modelled)
    0.00000 !EJ zoop 3 on phyto 1 (not modelled)
    0.00000 !EJ zoop 4 on phyto 1 (not modelled)
    0.00000 !EJ zoop 5 on phyto 1 (not modelled)
    0.05000 !EJ Cladoceran on cyanobacteria
    0.05000 !EJ Copepod on cyanobacteria
    0.00000 !EJ zoop 3 on cyano (not modelled)
    0.00000 !EJ zoop 4 on cyano (not modelled)
    0.00000 !EJ zoop 5 on cyano (not modelled)
    0.00000 !EJ Cladoceran on phyto 3 (not modelled)

```

0.00000	!EJ Copepod on phyto 3	(not modelled)
0.00000	!EJ zoop 3 on phyto 3	(not modelled)
0.00000	!EJ zoop 4 on phyto 3	(not modelled)
0.00000	!EJ zoop5 on phyto 3	(not modelled)
0.25000	!EJ Cladoceran on other	
0.25000	!EJ Copepod on other	
0.00000	!EJ Zoop 3 on other	(not modelled)
0.00000	!EJ Zoop 4 on other	(not modelled)
0.00000	!EJ Zoop 5 on other	(not modelled)
0.30000	!EJ Cladoceran on flagellates	
0.30000	!EJ Copepod on flagellates	
0.00000	!EJ Zoop 3 on flagellates	(not modelled)
0.00000	!EJ Zoop 4 on flagellates	(not modelled)
0.00000	!EJ Zoop 5 on flagellates	(not modelled)
0.20000	!EJ Cladoceran on early diatoms	
0.20000	!EJ Copepod on early diatoms	
0.00000	!EJ Zoop 3 on early diatoms	(not modelled)
0.00000	!EJ Zoop 4 on early diatoms	(not modelled)
0.00000	!EJ Zoop 5 on early diatoms	(not modelled)
0.20000	!EJ Cladoceran on late diatoms	
0.20000	!EJ Copepod on late diatoms	
0.00000	!EJ Zoop 3 on late diatoms	(not modelled)
0.00000	!EJ Zoop 4 on late diatoms	(not modelled)
0.00000	!EJ Zoop 5 on late diatoms	(not modelled)

! PzZOO (was Pzij) (no units) : Preference of zooplankton for zooplankton !
 <<<ABRIDGED: ALL ZEROES SINCE CARNIVOUROUS ZOOPLANKTON NOT MODELLED >>>

! PzPOC (no units) : Preference of zooplankton for detritus(POC)
 <<<ABRIDGED: ALL ZEROES; DETRITUS CONSUMPTION NOT MODELLED >>>

! PzBAC (no units) : Preference of zooplankton for bacterial
 <<<ABRIDGED: ALL ZEROES; BACTERIA NOT MODELLED >>>

! Kj (g C/m³) : Half saturation constant for grazing !
 3.200000E-001 !For Cladocerans
 2.700000E-001 !For Copepods
 0.00000
 0.00000
 0.00000

! HardorSoft (no units) : Faecal Pellet status (ie fraction that goes to sed)
 0.000 ! heterotrophic & mixotrophic microbial grazers
 0.95000 ! young copepods and rotifers EJ USED THE SAME AS THE MANUAL HERE
 0.00000 ! cladocera on Gladioferens
 0.00000 ! rotifers on Sulcanus
 0.00000 ! ciliates

! minres (mg/L) : Minimum grazing limit
 0.00000 ! on Phyto
 0.00000 on Zoop
 0.00000 on POM
 0.00000 on Bac
 0.00000 ! **this value is not used

!-----!

```

! FISH constants
!
<<<NOT MODELLED, SO THIS SECTION IS NOT INCLUDED IN THIS APPENDIX>>>
!-----!
! SEAGRASS constants
!
<<<NOT MODELLED, SO THIS SECTION IS NOT INCLUDED IN THIS APPENDIX>>>
!-----!
! MACROALGAE constants
!
<<<NOT MODELLED, SO THIS SECTION IS NOT INCLUDED IN THIS APPENDIX>>>
!-----!
! CLAM / MUSSEL constants
!
<<<NOT MODELLED, SO THIS SECTION IS NOT INCLUDED IN THIS APPENDIX>>>
!-----!
! MACROINVERTABRATE constants
!
<<<NOT MODELLED, SO THIS SECTION IS NOT INCLUDED IN THIS APPENDIX>>>
!-----!
! C, N & P CYCLE Constants
!-----!
! ORGANIC PARTICLES (POM) -----!
!
0.10      POC1max (/day) : Max transfer of POCL->DOCL      !
0.0050    POC2max (/day) : Max transfer of POCL->DOCL      !
6.000000E-002    POP1mx (/day) : Max transfer of POPL->DOPL (was0.0035)!
0.0050    POP2max (/day) : Max transfer of POPR->DOPR      !
1.000000E-002    PON1mx (/day) : Max transfer of PONL->DONL (was 0.002 24/09/03)!
0.0050    PON2max (/day) : Max transfer of PONR->DONR      !
! POM Diameter (m) : Diameter of POM particles
!
5.000000E-006    ! POM1 (eg. LABILE)(was 10um - adjusted to reflect dying algae)!
0.50000E-04     ! POM2 (eg. REFRACTORY)
! POM Density (kg/m^3) : Density of POM particles
!
1.020000E+003    ! POM1 (eg. LABILE)
0.10050E+04     ! POM2 (eg. REFRACTORY)
! TcPOM (N/m^2) : Critical shear stress for respn
!
3.000000E-003    ! POM1 (eg. LABILE)
0.0020         ! POM2 (eg. REFRACTORY)
! KePOC (mg/L/m) : Specific attenuation coefficient of POC
!
0.047         ! POC1 (eg. LABILE) JRR 08/05 Verduin 1982
0.04700E+00    ! POC2 (eg. REFRACTORY) JRR 08/05 Verduin 1982
!-----!
! DISSOLVED ORGANICS (DOM)
!
0.003        DOC1max (/day) : Max mineralisation of DOCL->DIC (was 0.005 02/10/03)!
0.001        DOC2max (/day) : Max mineralisation of DOCL->DIC
0.026        DOP1max (/day) : Max mineralisation of DOPL->PO4 0.006 08/10/03 (was 0.005 02/10/03)!
0.001        DOP2max (/day) : Max mineralisation of DOPR->PO4
0.006        DON1max (/day) : Max mineralisation of DONL->NH4 0.002 08/10/03 0.003 06/10/03 (was
0.005 02/10/03)!
0.001        DON2max (/day) : Max mineralisation of DONR->NH4
! KeDOC (mg/L/m) : Specific attenuation coefficient of DOC
!
0.0100E+00    ! DOC1 (eg. LABILE)
0.0100E+00    ! DOC2 (eg. REFRACTORY)
! Salinity bounds for DOCr flocculation
!
1.0000        Smindoc
10.000        Smaxdoc
! kfloc: flocculation rate constant
!

```

0.50000 !
 ! kSWNP: Rate of DOCr Photolytic Decay !
 0.00100 !
 !-----!
 ! DISSOLVED INORGANICS !
 ! Ionic Strength (required for DIC & pH calculation) !
 0.00150 Ionic Strength (g/m3) !
 ! Adsorption/Desorption !
 0.00000 Kadd1NH4 !
 0.00000 Kadd2NH4 !
 0.00000 Kadd1PO4 !
 0.00000 Kadd2PO4 !
 ! Nitrification/Denitrification !
 1.08000 vN2 (-) : Temp multiplier for denitrification !
 0.01000 koN2 (/day) : Denitrification rate coefficient (was 0.02 24/09/03)!
 0.50000 KN2 (mg/L) : Half sat const for denitrification !
 1.08000 vON (-) : Temp multiplier for nitrification !
 0.05000 koNH (/day) : Nitrification rate coefficient 0.08 06/10/03 (was 0.05 24/09/03), 0.04 01/10!
 2.00000 KOn (mg O/L) : Half sat constant for nitrification !
 3.42857 YNH (mg N/mg O) : Ratio of O2 to N for nitrification !
 !-----!
 ! SEDIMENT PARAMETERS
 ! NUTRIENT FLUXES !
 ! Theta(sed) : Temp multiplier of sediment fluxes !
 1.05 !
 ! PO4 sediment flux parameters !
 0.00260 SmpPO4 (g/m2/day) : Release rate of PO4 !
 0.50000 KDOS-PO4 (g/m^3) : Controls sed release of PO4 via O !
 1000000.0 KpHS-PO4 (-) : Controls sed release of PO4 via pH !
 ! NH4 sediment flux parameters !
 0.01900 SmpNH4 (g/m2/day) : Release rate of NH4 !
 0.50000 KDOS-NH4 (g/m^3) : Controls sed release of NH4 via O !
 1000000.0 KpHS-NH4 (-) : Controls sed release of NH4 via pH !
 ! NO3 sediment flux parameters !
 -0.0100 SmpNO3 (g/m2/day) : Release rate of NO3 !
 0.50000 KDOS-NO3 (g/m^3) : Controls sed release of NO3 via O !
 1000000.0 KpHS-NO3 (-) : Controls sed release of NO3 via pH !
 ! Si sediment flux parameters !
 0.30000 SmpSi (g/m2/day) : Release rate of Si (RSmith M) !
 4.00000 KDOS-Si (g/m^3) : Controls sed release of Si via O (RSmith M)!
 1000000.0 KpHS-Si (-) : Controls sed release of Si via pH !
 ! DOC sediment flux parameters !
 0.01000 SmpdocL (g/m2/day): Release rate of DOCL (was 0.092 JRR 8/8/05)!
 0.08200 SmpdocR (g/m2/day): Release rate of DOCR !
 0.50000 KDOS-doc (g/m^3) : Controls sed release of DOC via O !
 1000000.0 KpHS-doc (-) : Controls sed release of DOC via pH !
 ! DOP sediment flux parameters !
 0.00001 SmpdopL (g/m2/day): Release rate of DOPL (? - check against DOC?)!
 0.00001 SmpdopR (g/m2/day): Release rate of DOPR !
 0.50000 KDOS-dop (g/m^3) : Controls sed release of DOP via O !
 1000000.0 KpHS-dop (-) : Controls sed release of DOP via pH !
 ! DON sediment flux parameters !

```

0.00001      SmpdonL (g/m2/day): Release rate of DONL (? - check against DOC?)!
0.00001      SmpdonR (g/m2/day): Release rate of DONR      !
0.50000      KDOS-don (g/m^3) : Controls sed release of DON via O !
1000000.0    KpHS-don (-)   : Controls sed release of DON via pH !
!--- Sediment composition
! Fraction of sediment that is organics
0.15         sedOrganicFrac
! Sediment Porosity (i.e. porewater fraction)
0.10         sedPorosity
! Composite resuspension rate (g/m2/day)
0.020        resusRate
! Half sat conc for resus dependence on sed mass (g)
1.0E+08      resusKT - note it was just 1 in dycd 1sp example !
!-----!
! INORGANIC PARTICLE constants!
!-----!
! Density of suspended solid particles
3.091700E+03 deS (kg/m^3) : SSOL1
2650         deS (kg/m^3) : SSOL2
! Diameter of suspended solids groups
2.700000E-06 diaSS (m) : SSOL1 (RSmith M) !
0.000003     diaSS (m) : SSOL2
! Specific attenuation coefficient
0.04700E+00  KeSS (mg^-1Lm^-1) : SSOL1 JRR 08/05 Verduin (1982) !
0.04700E+00  KeSS (mg^-1Lm^-1) : SSOL2 JRR 08/05 Verduin (1982) !
!
! Critical shear stress
8.300000E-03 tcs (N/m2) : SSOL1
0.03         tcs (N/m2) : SSOL2
!-----!
!-----!
! METALS
<<<<NOT MODELLED, SO THIS SECTION IS NOT INCLUDED IN THIS APPENDIX>>>>
!-----!
! PATHOGEN and MICROBIAL INDICATOR ORGANISM constants
<<<<NOT MODELLED, SO THIS SECTION IS NOT INCLUDED IN THIS APPENDIX>>>>
!-----!

```